The Relationship of Adenoviruses to the DNA Damage Response Protein BLM

UNIVERSITY OF BIRMINGHAM

Submitted by Ellis Ryan

This project is submitted in partial fulfilment of the requirements for the award of the MRes

Supervisors: Dr Roger Grand & Dr Grant Stewart

Abstract

Adenoviruses (Ad) are able to interact with a number of proteins involved in the cellular response to DNA damage, in order to prevent concatamerisation of the viral genome and inhibition of viral replication. It is becoming increasingly apparent that the adenoviral E3 ligase complex (comprised of E1B-55K and E4 adenoviral proteins) is able to target a number of cellular DNA damage response proteins for proteasomal degradation. Here we show that the RecQ helicase, BLM, is degraded during infection with adenovirus serotypes 4, 5 and 12. In addition, we were able to show, through the use of mutant viruses, that the degradation of BLM is dependent on E1B-55K and E4 activity during Ad5 infection, a mechanism which is suggested to occur during both Ad4 and Ad12 infection. Using co-immunoprecipitation and GST pull-down assays, we were able to confirm E1B-55K and BLM interactions *in vivo* and *in vitro* during Ad5 and Ad12 infection, whilst additionally suggesting that E1B-55K binds to BLM via a region similar to the known E1B-55K binding site on p53. Finally, we found that the degradation of BLM during adenovirus infection was dependent on proteasome activity, establishing that a component of the E3 ligase complex, Cullin 4B, may be responsible for the degradation of BLM during adenovirus infection. These observations show that another component involved in DNA end resectioning, besides MRN, is a target for viral degradation by the adenovirus family.

Acknowledgements

I would firstly like to thank my supervisors, Dr Roger Grand and Dr Grant Stewart for all their help and guidance, both in the laboratory and in the writing of this project. In addition, I would like to thank all the other members of the DNA damage/Adenovirus group, past and present for their continual support including Natalie Forrester, Paul Minshall, Sarah Berhane, Rakesh Patel, Andrew Turnell and Shaun Wilson.

List of Contents

1. Introduction……...……1

1.1 Adenovirus……...…….2

1.2 The Adenovirus E1A and E1B-55K Proteins……...……3

1.3 The DNA Damage Response……...…….5

1.4 The DNA Damage Response and Adenovirus Infection……...…...7

1.5 Double-Stranded DNA Repair Pathways……..8

1.6 The RecQ Family of DNA Helicases……..……..9

1.7 Bloom Syndrome and the BLM Protein…….……10

1.8 BLM and Adenovirus Infection……..…12

1.9 Aims…….....13

2. Materials and Methods……...……14

2.1 Tissue Culture Techniques…….....15

2.1.1 Maintenance of Human Cell Lines…….....15

2.1.2 Human Cell Culture……..…...16

2.1.3 Viral Infections…….……...16

2.2 Cell Biology Techniques ……..…….17

2.2.1 Knock-down of Gene Expression using small-interfering RNAs (siRNAs)……..17

2.2.2 Exposure of Adherent Cell Lines to the Proteasome Inhibitor MG132…….18

2.3 Protein Chemistry Techniques……..……..19

2.3.1 Harvesting Human Adherent Cells……..19

2.3.2 Determination of Protein Concentration of Cell Lysates……...…..20

2.3.3 SDS-PAGE……..……20

2.3.4 Visualisation of Proteins Separated by SDS-PAGE……....21

2.3.5 Visualisation of Proteins on Nitrocellulose Membranes…….21

2.3.6 GST Pull-Down Assay……21

2.4 Immunological Techniques……23

2.4.1 Western Blotting……...23

2.4.2 Co-Immunoprecipitation…….....25

2.5 Molecular Biology Techniques……..25

2.5.1 GST-fusion Protein Production…….....25

2.5.2 GST-fusion Protein Purification……...26

3. Results……..28

3.1 BLM is Degraded Following Infection with Adenovirus Serotypes 4, 5 and 12…….……29

3.2 The Adenovirus E1B Protein is Required for the Degradation of BLM during Adenovirus Infection……32

3.3 Adenovirus Early Viral Protein E1B-55K Interacts with BLM *in vivo*……...32

3.4 The E1B-55K Protein Directly Interacts with BLM *in vitro*……...35

3.6 Degradation of BLM during Adenovirus Serotype 5 and 12 Infection is Proteasomal Dependent……...35

3.7 Cullin 4B is Partially Required For the Degradation of BLM during Adenovirus Infection……...39

4. Discussion……44

4.1 Limitations……..51

4.2 Future Work……51

5. References……..100

List of Figures and Tables

Table 1.1 Adenovirus Serotypes Classified to Date……...2

Figure 1.1 Adenovirus Genome Organisation……4

Figure 1.2 The DNA Damage Response Signalling Pathways……..6

Figure 1.3 Pro-recombinase and Anti-recombinase Roles of BLM During HRR……....11

Table 2.1 Human Cell Lines used in this Study……15

Table 2.2 Adenovirus Serotypes and Mutants used in this Study……17

Table 2.3 siRNAs used in this Study……18

Table 2.4 GST-Fusion Proteins used in this Study…….....22

Table 2.5 Primary Antibodies used in this Study…….24

Table 2.6 Secondary Antibodies used in this Study…….24

Table 2.7 Gene Expression Constructs for GST-Fusion Protein Production……27

Figure 3.1 Degradation of BLM Following Adenovirus Infection……...30

Figure 3.2 Degradation of BLM Following Mutant Adenovirus Infection……..33

Figure 3.3 BLM Interacts with E1B-55K *in vivo* in both Adenovirus 5 and 12 Transformed Cell Lines……34

Figure 3.4 Structure of BLM and Associated Domains……36

Figure 3.5 Assessment of the Protein Quality of the GST-BLM Fragments Produced in this Study……37

Figure 3.6 The E1B-55K Protein Directly Interacts with BLM *in vitro*……..38

Figure 3.7 Degradation of BLM during Adenovirus 5/12 Infection is Dependent on Proteasome Activity……40

Figure 3.8 The effect of Knock-down of Cullin Gene Expression on BLM Degradation during Adenovirus Infection …….....42

Figure 4.1 Comparison of the Amino Acid Sequences of BLM and p53 in the Proposed Binding Site for Ad5E1B-55K……49

Chapter One:

Introduction

1.1 Adenovirus

The adenovirus (Ad) family are a group of small DNA tumour viruses, with over 50 different serotypes (classified into groups A to G) identified to date (Table 1.1). The adenovirus family has been studied extensively and is frequently used to study mechanisms of viral replication and cellular transformation (Weitzman and Ornelles, 2005). Whilst adenovirus infection has not been linked with the development of any human cancers, infection with group A viruses, and particularly adenovirus serotype 12 (Ad12), has been associated with tumour development in new-born mice (Trentin et al., 1962). In addition, further evidence for the possible oncogenicity of adenoviruses comes from studies showing that most adenovirus serotypes are able to transform primary rodent cells *in vitro* (McBride et al., 1964; Freeman et al., 1967).

Table 1.1: Adenovirus Serotypes Classified to Date. The adenovirus serotypes identified to date are indicated, classified into groups A to G. Virus serotypes are considered to be most oncogenic the higher up in the table they appear (adenovirus serotypes in group A are considered to have the most oncogenic potential). Adenovirus serotypes used in this study are highlighted in red.

Group	Serotype
A	12, 18, 31
B1	3, 7, 16, 21, 50
B2	11, 14, 34, 35, 55
C	1, 2, 5, 6
D	8, 9, 10, 13, 15, 17, 19, 22-30, 32, 33, 36-39, 42-49, 51, 53, 54
E	4
F	40, 41
G	52

1.2 The Adenovirus E1A and E1B-55K Proteins

The adenovirus genome contains 6 different early genes (E1A, E1B, E2A, E2B, E3 and E4), and 5 late genes (L1, L2, L3, L4 and L5) (Figure 1.1) (Weitzman and Ornelles, 2005). Expression of E1A is necessary for the immortalisation of primary rodent cells *in vitro*, however, in order to completely transform these cells, expression of another oncogene, for example, E1B, is required (Van Den Elsen et al., 1983). E1A is the first viral protein to be expressed following infection and its expression is necessary for the activation of transcription of the other early viral genes. In addition to its function as a transcriptional activator, E1A also associates with a number of cellular proteins involved in gene expression and cell growth, with the aim to force cells into S-phase, in order to effectively replicate the viral genome. E1A interactions include association with the transcriptional co-activators p300/CREB-binding protein (CBP) and p300/CBP-associated factor (PCAF), the transcriptional co-repressor C-terminal binding protein (CtBP), and other proteins that regulate the cell-cycle such as p400, TRAF and TNF receptor-associated protein (TTRAP), the tumour suppressor retinoblastoma protein (pRB) and related proteins p107 and p130, dual-specificity Yak1-related kinases (DYRKs), and the cyclin-dependent kinase inhibitors (CKIs) p21 and p27 (Frisch and Mymryk., 2002; Pelka et al., 2008).

The E1B-55K protein is able to cooperate with E1A to stably transform cells. The E1B protein has early viral functions including the inhibition of the DNA damage response, and late viral functions such as the inhibition of cellular mRNA export and the promotion of viral mRNA export. The interaction between E1B-55K and the E4 open reading frame 6 (E4orf6) protein is thought to be essential for most of the functions of the E1B-55K protein. For

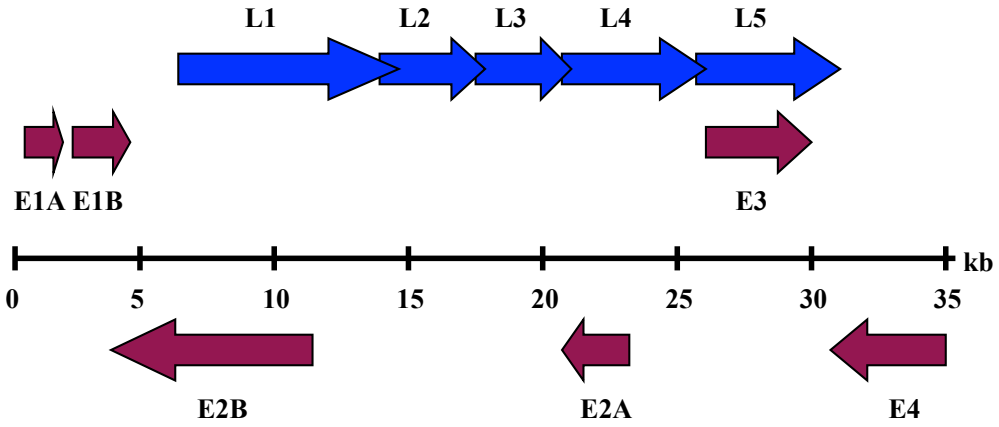

Figure 1.1: Adenovirus Genome Organisation. Schematic to outline the organisation of the adenovirus genome. Early adenovirus transcripts are indicated in red, late adenovirus transcripts are indicated in blue. Direction of the arrows represent the direction of transcription (modified from Russell, 2000).

example, the localisation of E1B-55K to the nucleus and viral replication centres appears to be dependent on E4orf6 association (Ornelles and Shenk, 1991; Dobbelstein et al, 1997). E1B-55K, together with E4orf6, is responsible for the degradation of proteins which act to inhibit viral replication. This is achieved, in the case of Ad5, by E1B-55K and E4orf6, along with Cullin 5 (Cul5), RING-box 1 (Rbx1) and elongins B and C, together forming an E3 ubiquitin ligase complex which is able to target p53, Mre11-Rad50-Nbs1 (MRN) and DNA ligase IV for degradation (Querido et al, 2001; Stracker et al, 2002; Baker et al, 2007). Late functions of the E1B-55K protein include the inhibition of cellular mRNA export and promotion of viral mRNA export from the nucleus, which may also be dependent on the degradation of cellular proteins (Dobbelstein et al, 1997; Woo and Berk, 2007).

1.3 The DNA Damage Response

Cells have complex mechanisms to sense and respond to various forms of DNA damage. The key regulators in the response to DNA damage are considered to the phosphatidylinositol 3 (PI3) kinase family members ataxia telangiectasia mutated (ATM) and ataxia telangiectasia and RAD3 related (ATR) kinases. The ATM kinase responds to double-strand breaks induced by ionising radiation (IR) and cellular stress, and the ATR kinase responds to single-stranded lesions induced by ultra-violet (UV) radiation and stalled replication forks (Khanna and Jackson, 2001).

In response to single-strand breaks induced by UV radiation and stalled replication forks, single-stranded DNA (ssDNA) is coated by replication protein A (RPA) to form a ssDNA-RPA complex. ATR interacting protein (ATRIP) is responsible for sensing the ssDNA-RPA complex and recruiting ATR to the site of the single-stranded lesion (Zou and Elledge, 2003).

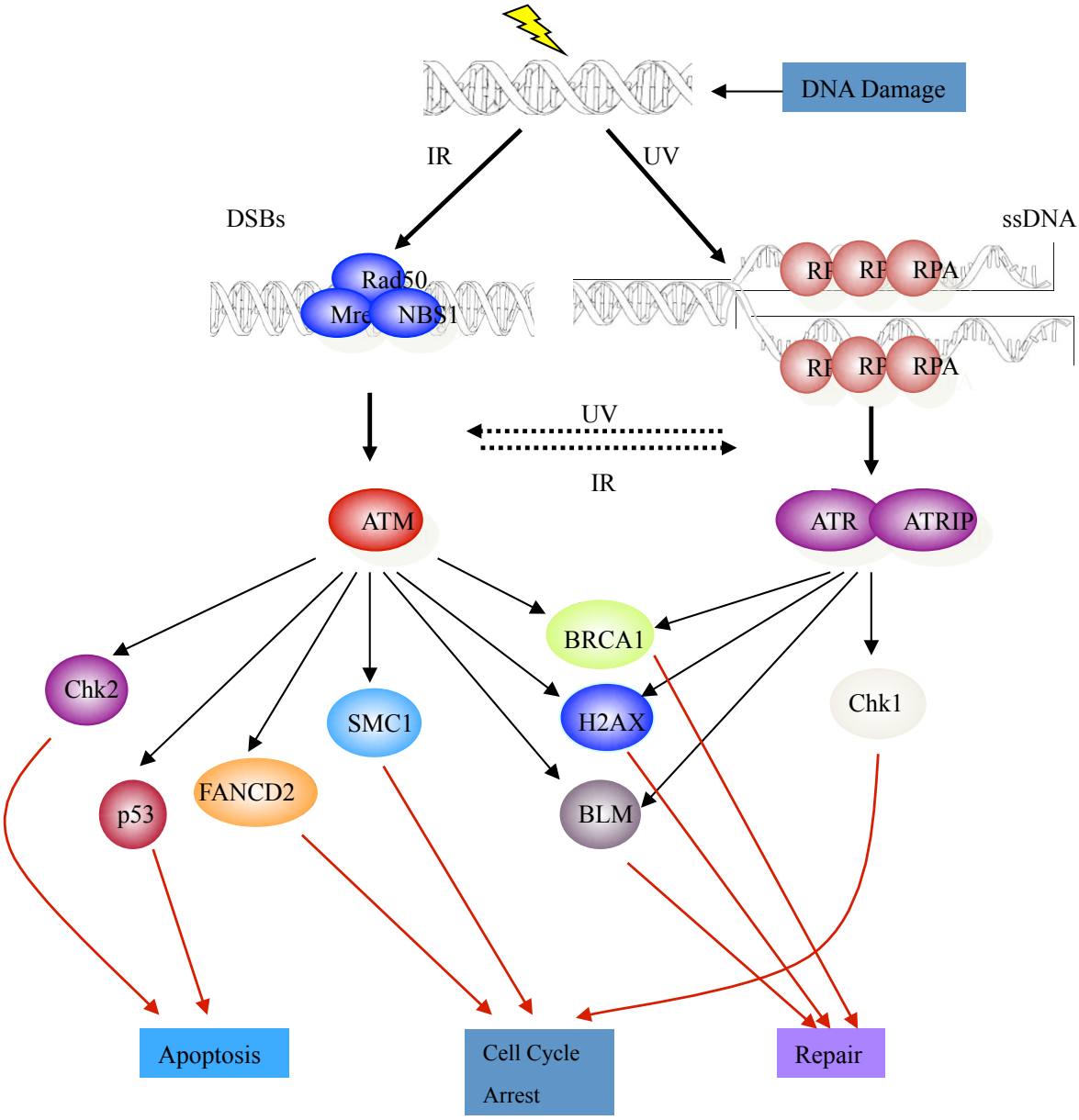

Figure 1.2: The DNA Damage Response Signalling Pathways. In response to single-strand breaks induced by IR (or collapsed replication forks), ssDNA is bound by RPA, which ultimately results in the association of ATRIP with ATR, leading to its activation. The activated ATR kinase is then able to phosphorylate and subsequently activate the DNA damage proteins indicated. The MRN complex is able to sense double-strand breaks induced by ionising radiation (or cellular stress). The MRN complex is then able to activate ATM, leading to the phosphorylation and subsequent activation of proteins involved in cell-cycle arrest, DNA repair and apoptosis (Zhou and Bartek, 2004).

The ssDNA-RPA complex also induces the binding of the RAD9-RAD1-HUS1 complex to the lesion via its association with RAD17-replication factor C 2 (RFC2) clamp loader complex (Yang and Zou, 2006). Association of the RAD9-RAD1-HUS1 complex with the single-stranded lesion causes topoisomerase II binding protein 1 (TOPBP1) recruitment and the subsequent activation of ATR (Kumagai et al., 2006). ATR is then able to phosphorylate downstream targets such as Chk1, BRCA1, H2AX and BLM, ultimately resulting in cell-cycle arrest and the stabilisation of stalled replication forks (Figure 1.2) (reviewed in Zhou and Bartek, 2004).

In response to double-strand breaks, the double-strand break sensor, the Mre11-Rad50-Nbs1 (MRN) complex, is recruited to the sites of damage where it binds to, and activates ATM, stimulating its autophosphorylation (Lee and Paul, 2005). ATM is then able to phosphorylate H2AX, which subsequently interacts with mediator of DNA damage checkpoint 1 (MDC1). H2AX and MDC1 recruit various DNA damage proteins to the site of the double-strand break. ATM then phosphorylates the recruited DNA damage proteins, including Chk2, p53, FANCD2, SMC1, BRCA1, H2AX, and BLM, ultimately leading to cell-cycle arrest and double-strand break repair (Figure 1.2) (Zhou and Bartek, 2004; Cimprich and Cortez, 2008).

1.4 The DNA Damage Response and Adenovirus Infection

During adenovirus infection, a relatively large amount of double-stranded viral DNA is produced which is probably recognised by the cell as damaged cellular DNA. Processing of this viral DNA by the cellular DNA damage response would be catastrophic for the virus, resulting in joining of DNA ends and the formation of viral concatemers (Weiden and Ginsberg, 1994). Mounting evidence now suggests that adenoviruses target components of the

DNA damage response in order to effectively replicate the viral genome (Lilley and Weitzman, 2007). In addition, adenoviruses are also able to inactivate critical components of cell-cycle checkpoint response such as p53, in order to avoid cell-cycle arrest or apoptosis in the host cell (Querido et al., 2001). Upon infection with adenovirus, ATM activation in response to linear double-stranded viral DNA is limited due to E1B-55K/E4orf6 degrading the double-strand break sensor, MRN (Carson et al., 2003; Stracker et al., 2002). In addition, the E4orf3 protein is able to relocalise the Mre11 to aggresomes and nuclear tracks, sequestering it so that ATM repair pathway cannot be activated (Evans and Hearing, 2005; Liu et al., 2005; Araujo et al., 2005). Non-homologous end joining (NHEJ) repair is prevented through its association and inhibition of DNA-dependent protein kinase catalytic subunit (DNA-PKcs) activity and through the degradation of DNA ligase IV by the E1B-55K/E4orf6 E3 ligase (Boyer et al., 1999; Baker et al., 2007). One study suggested that during adenovirus infection, ATR, RPA, ATRIP and TOPBP1 all localise to viral replication centres, however no ATR signalling response is observed throughout infection (Evans and Hearing, 2005). More recent evidence suggests that infection with adenovirus serotypes 5 and 12 have been shown to activate the ATR signalling pathways during late stages of infection in an E1B-55K-associated protein 5 (E1B-AP5)-dependent fashion (Blackford et al., 2008).

1.5 Double-Stranded DNA Repair Pathways

Double-strand break repair can be split into two categories; NHEJ and homologous recombination repair (HRR). Whether double-strand breaks are repaired by NHEJ and HRR is dependent on phase of the cell cycle and the DNA template available. NHEJ involves the Ku70/Ku80 protein hetero-dimer binding to the site of the double-strand break and recruiting DNA-PKcs. Binding of DNA-PKcs to the site of the double-strand break results in DNA

ligase IV, Artemis, XRCC4 and XRCC-like factor (XLF) recruitment to the sites of the double-strand break. Following auto-phosphorylation of DNA-PKcs, DNA-PKcs dissociates from the DNA and the double-strand break repair proteins are able to repair the double-strand break (Shrivastav et al., 2008). In contrast, HRR involves the resection of DNA ends by the MRN complex to expose ssDNA. ssDNA is then coated by RPA which subsequently recruits the recombinase Rad51. Rad51 forms a nucleoprotein filament with the ssDNA, and with the guidance of Rad54, invades the homologous region of the complementary sister strand, ultimately resulting in the formation of displacement-loops (D-loops) and Holliday junctions. DNA polymerase is then able to synthesise a new DNA strand and is ligated by DNA ligase to repair the double-strand break (Shrivastav et al., 2008).

1.6 The RecQ Family of DNA Helicases

Although HRR is a critical pathway in the maintenance of genome stability, it is also a requirement that excessive HRR is prevented, in order to avoid recombination events which could result in deleterious genome rearrangements. RecQ helicases are a family of DNA helicases which are thought to possess both pro-recombinase and anti-recombinase activities, the latter preventing excessive HRR and deleterious genome rearrangements (Chu and Hickson, 2009). RecQ helicases are able to translocate along ssDNA in the 3’ to 5’ direction, unwinding DNA via disruption of hydrogen bonds which are essential to hold duplex DNA together. In contrast to other helicases, RecQ helicases seem to have an affinity for recombination intermediates, including D-loops and both single and double Holliday junctions (Ouyang et al., 2008). In addition, RecQ helicases also seem to be able to bind to replication forks. In humans, the RecQ helicases include RecQL1, RecQL4, RecQL5, BLM and WRN, with mutations in RecQL4, BLM and WRN leading to the genetic instability

syndromes Rothmund-Thomson syndrome (RTS), Bloom syndrome (BS) and Werner syndrome (WS) respectively (Chu and Hickson, 2009).

1.7 Bloom Syndrome and the BLM Protein

BS is an extremely rare, autosomal recessive disease, with approximately only 240 cases identified worldwide. Characteristics of patients with BS include a short stature, hyper- or hypo-pigmentation, immune-deficiencies, sensitivity to the sun, fertility problems, defects in metabolism, and most significantly, predisposition to all types of cancer (Ouyang et al., 2008). Genomic instability is a characteristic of patients with BS, due to the loss of BLM and subsequent loss of anti-recombination activity. Deficiency in this anti-recombinase activity results in increased HRR and increased sister chromatid exchange by up to ten-fold compared to sister chromatid exchange in the normal population. Patients with BS have many abnormalities at the molecular and chromosome level, including excessive chromatid breaks, anaphase-bridges, chromosomal rearrangements and deletions, all of which resulting in a high incidence of genetic mutations and genetic instability (Payne and Hickson, 2009).

As far as is known, mutations in BLM in BS patients are limited to mutations leading to premature protein translation termination, or amino acid substitutions in the helicase domain of BLM which result in loss of helicase activity (Neff et al., 1999; German et al., 2007). In normal circumstances, BLM resides in the nucleus in structures known as promyelocytic leukemic (PML) nuclear bodies (N.B. These structures also contain other proteins involved in DNA repair including p53, the MRN complex and Topoisomerase 3α). In response to treatment with DNA damaging agents, BLM localises to DNA repair foci, where it co-localises with γH2AX, suggesting that BLM is involved in the early DNA damage response.

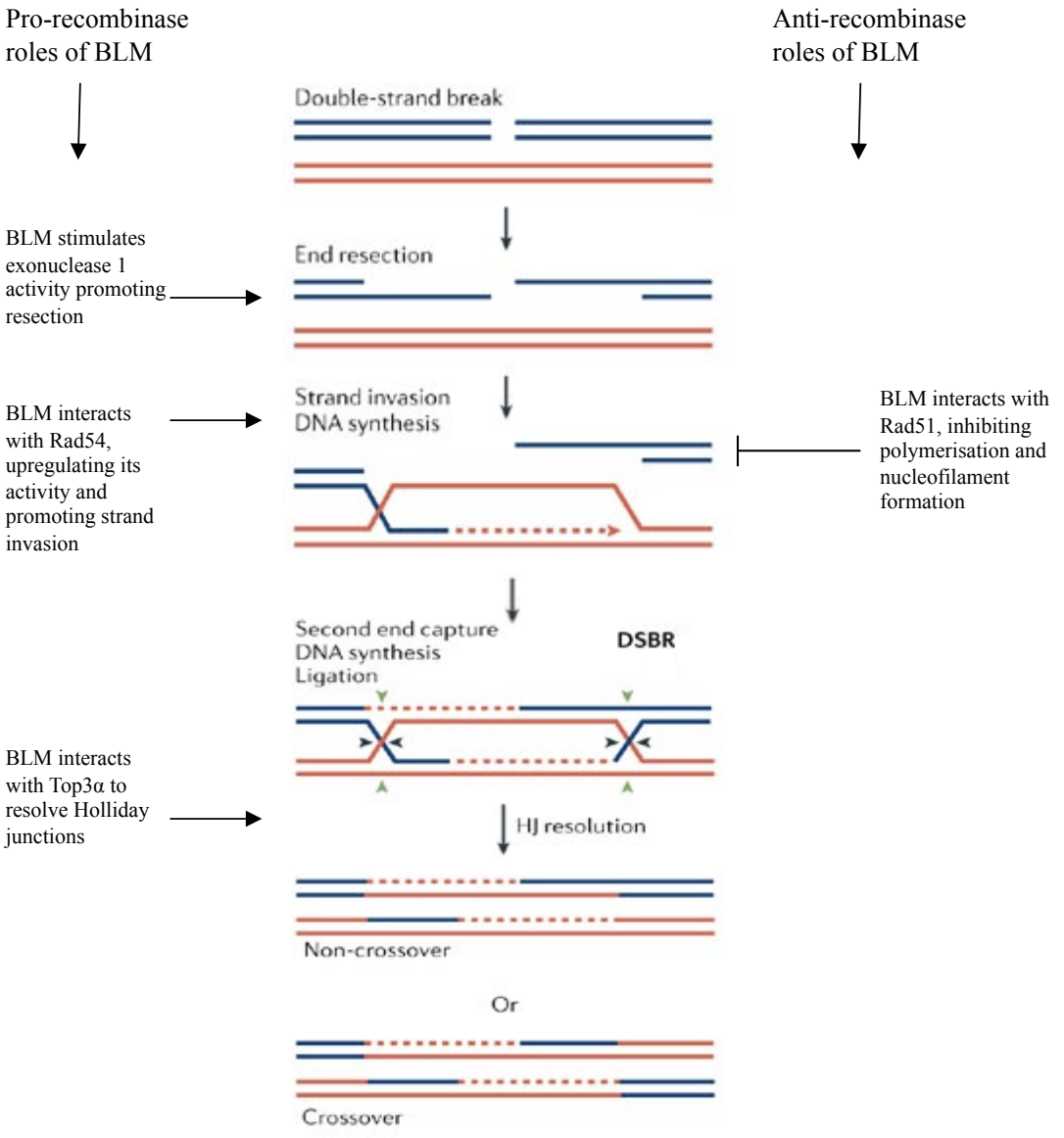

Figure 1.3 Pro-recombinase and Anti-recombinase Roles of BLM During HRR. The pro-recombinase roles of BLM during HRR are noted to the left-hand side of the diagram, whilst the anti-recombinase roles are noted to the right. Pro-recombinase roles of BLM include the stimulation of exonuclease 1 activity promoting resection of dsDNA to ssDNA, the upregulation of Rad54 activity to promote strand invasion and the interaction with Top3α to resolve Holliday junctions. Anti-recombinase roles of BLM include the inhibition of nucleofilament formation via BLM interactions with Rad51. HRR, homologous recombination repair; dsDNA, double-stranded DNA; ssDNA, single-stranded DNA; HJ, Holliday junctions; DSBR, double-strand break repair (modified from Sung and Klein, 2006).

Classically it is thought that BLM functions as an anti-recombination helicase, since mutations in BLM lead to an increase in sister chromatid exchanges and chromosomal abnormalities. Additional evidence for the anti-recombinase role of BLM includes evidence that BLM interacts with the recombinase Rad51, and subsequently inhibits Rad51 polymerisation, preventing nucleofilament formation and HRR (Figure 1.3) (Bugreev et al., 2007). Interestingly, recent evidence suggests that BLM has pro-recombinogenic roles (Figure 1.3). BLM is able to associate with Topoisomerase 3α, and this complex is recruited to double Holliday junctions by BLAP75/RMI1 where it is able to resolve them, promoting HRR (Wu et al., 2006; Raynard et al., 2006). This is advantageous since convergence of double Holliday junctions by BLM eliminates the crossing-over event of conventional Holliday junction resolution during HRR, limiting the extent of sister chromatid exchanges. However, this observation suggests that BLM is involved in later stages of HRR, and fails to explain why BLM colocalises with γH2AX at DNA damage foci, and so additional roles for BLM are likely. BLM has also been shown to interact with the pro-recombinase Rad54, up-regulating its activity and subsequently promoting HRR (Srivastava et al., 2009). In addition, BLM interacts with Exonuclease 1, stimulating its activity and the subsequent resection of DNA to form ssDNA (Nimonkar et al., 2008; Gravel et al., 2008). One study also suggests BLM processes stalled replication forks by stimulating fork regression, so that replication can be restarted (Ralf et al., 2006).

1.8 BLM and Adenovirus Infection

Mass spectrometric analysis of adenoviral E1B-55K interacting proteins revealed BLM as a potential interacting partner (Forrester, unpublished data 2010). Subsequent to this finding, our laboratory investigated, via Western blotting, BLM protein levels during adenovirus infection. Preliminary results from these investigations suggested that BLM was degraded in

response to adenovirus infection, suggesting a novel protein that adenovirus is able to degrade, along with p53, Mre11 and DNA ligase VI (Querido et al., 2001; Stracker et al., 2002; Baker et al., 2007) (Section 1.4).

1.9 Aims

Based on the preliminary data obtained from our laboratory, the principle aim of this study is to establish the relationship of adenoviruses to the DNA damage response protein BLM. In order to determine this, a number of objectives will be addressed:

1. To confirm preliminary findings that adenovirus serotypes are able to degrade the RecQ helicase, BLM
2. To determine which adenoviral proteins are responsible for the degradation of BLM
3. To confirm the importance of the identified viral protein(s) using:
    a) Co-immunoprecipitation assays to confirm *in-vivo* viral protein-BLM interactions
    b) GST pull-down assays to confirm *in-vitro* viral protein-BLM interactions
4. To determine the mechanism by which adenoviruses degrade BLM by:
    a) Using the proteasome inhibitor, MG132 to inhibit proteasome activity to establish whether the degradation of BLM is dependent on the proteasome
    b) Using small interfering RNAs (siRNAs) to knock-down Cullin gene-expression to establish the E3 ligase involved in BLM degradation.

Chapter Two:

Materials and Methods

2. Materials and Methods

2.1 Tissue Culture Techniques

2.1.1 Maintenance of Human Cell Lines

Cell lines used in this study were maintained in a 5% CO_2/95% O_2 incubator at 37°C (Table 2.1). All cell lines were sustained in Dulbecco's modified Eagle's medium (DMEM) (Sigma), containing 7% v/v foetal calf serum (FCS) (PAA Laboratories).

Table 2.1 Human Cell Lines used in this Study. The human cell lines used throughout the duration of this study are indicated, along with ATCC numbers and any additional information.

Cell line	ATCC number	Information
HeLa	CCL-2.2	Human cervival adenoma cell line expressing HPV-18 (Human Papilloma Virus) transforming genes
Ad5E1HEK293	CRL-1573	Human adenovirus type 5 transformed human embryo kidney cell line
Ad5E1HER911	N/A	Human adenovirus type 5 transformed human embryo retinoblast cell line
Ad12E1HER2	N/A	Human adenovirus type 12 transformed human embryo retinoblast cell line
Ad12E1HER10	N/A	Human adenovirus type 12 transformed human embryo retinoblast cell line

2.1.2 Human Cell Culture

In order to passage adherent cell lines, cells were washed twice with 0.15M saline (Sigma), trypsinised using 5mls of 0.05% trypsin-ethylenediaminetetraacetic acid (EDTA) (Invitrogen) and incubated at 37°C until cells had lost adherence to the tissue culture dish. After cells had come off the dish, 10mls of DMEM with 7% FCS was added to inactivate trypsin activity. Following inactivation, cells were centrifuged at 1,200 revolutions per minute (rpm) at room temperature for 4 minutes, resuspended in DMEM with 7% FCS to wash and centrifuged again. Following the wash, cells were resuspended in DMEM with 7% FCS and replated at the required density.

2.1.3 Viral Infections

HeLa cells, grown to 80% confluency on 6cm dishes, were infected with adenovirus serotypes (Table 2.2) diluted in approximately 200µl DMEM (no FCS), at an infectivity level of 20 particle forming units (pfu)/cell and left for 2 hours in a 37°C incubator. Following infection, adenovirus-containing medium was removed and 5mls of DMEM with 7% FCS added and incubated at 37°C until required.

Table 2.2 Adenovirus Serotypes and Mutants used in this Study. The adenovirus serotypes and mutants used throughout this study and their sources are indicated

Name	**Information**	**Source**
Ad3	Adenovirus serotype 3	Professor J. S. Mymryk
Ad4	Adenovirus serotype 4	Professor J. S. Mymryk
Ad5	Adenovirus serotype 5	Professor J. S. Mymryk
Ad7	Adenovirus serotype 7	Professor J. S. Mymryk
Ad9	Adenovirus serotype 9	Professor J. S. Mymryk
Ad11	Adenovirus serotype 11	Professor J. S. Mymryk
Ad12	Adenovirus serotype 12	Professor J. S. Mymryk
Ad5*dl*1520	Ad5E1B- mutant	Baker and Berk, 1987
Ad5*dl*355	Ad5E4orf6- mutant	Dr Keith Leppard
Ad12*dl*620	Ad12E1B- mutant	Byrd et al., 1987
h5pm4155	Ad5E4orf6- E4orf3- mutant	Professor Thomas Dobner

2.2 Cell Biology Techniques

2.2.1 Knock-down of Gene Expression using Small-Interfering RNAs (siRNAs)

24 hours prior to infection, expression of various genes was silenced using 7.5µl of 40mM of siRNA (Table 2.3) in 20µl of oligofectamine (Invitrogen), which was added to 1.5ml of optimem (Invitrogen) and left to incubate for 30 minutes at room temperature. Following incubation, siRNA mix was added to HeLa cells grown to a confluency of approximately 33% and left for 6 hours in a humidified incubator at 37°C. Following the 6 hour incubation period, siRNA mix was removed from the cells and replaced with DMEM with 7% FCS.

Table 2.3 siRNAs used in this Study. The siRNAs used to knock-down the expression of various genes in this study are shown. The target protein, siRNA type, sense sequence and source are indicated.

Target protein	**siRNA**	**Sense sequence**	**Source**
Non-silencing	AllStars	Proprietary	Qiagen
CUL2	SMARTpool	5' GGAAGUGCAUGGUAAAUUU 3' 5' CAUCCAAGUUCAUAUACUA 3' 5' GCAGAAAGACACACCACAA 3' 5' UGGUUUACCUCAUAUGAUU 3'	Dharmacon
CUL4A	s16045	5' GGUUUAUCCACGGUAAAGAtt 3'	Ambion
CUL4B	s16044	5' GAAGCUAUUCAGAAUAGUtt 3'	Ambion
CUL5	SMARTpool	5' GACACGACGUCUUAUAUUA 3' 5' GCAAAUAGAGUGGCUAAUA 3' 5' UAAACAAGCUUGCUAGAAU 3' 5' CGUCUAAUCUGUUAAAGAA 3'	Dharmacon
CUL7	s18991	5' CCACUUUUGAGCAUUAUUAtt 3'	Ambion

2.2.2 Exposure of Adherent Cell Lines to the Proteasome Inhibitor MG132

Infected HeLa's grown in 6cm dishes were treated with 10 μM of the proteasome inhibitor N-(benzyloxycarbonyl)leucinylleucinylleucinal (MG132) (Sigma) 2 hours post-infection in DMEM with 7% FCS and incubated at 37°C until required.

2.3 Protein Chemistry Techniques

2.3.1 Harvesting Human Adherent Cells

Cells were typically harvested by removing media, washing twice in cold 0.15M saline and scraping cells in 400µl of Urea-Tris-Bicine (UTB) lysis buffer (9M Urea (Sigma), 150mM β-mercaptoethanol (Sigma), 50mM Tris/hydrochloric acid (HCl) (pH 7.5) (Fisher Scientific)). Cell scrapings were then pooled into 1.5ml microfuge tubes, sonicated twice to disrupt cell membranes and DNA and centrifuged at 13,000 rpm for 15 minutes to clear the lysate. Following the spin, the supernatant was retained and the protein concentration of the lysate was determined (Section 2.3.2). Cell lysates were stored at -80°C until required.

For harvesting cells for use in Glutathione S-Transferase (GST) pull-down or co-immunoprecipitation assays, cell lines were harvested by washing twice in ice-cold 0.15M saline. In the second saline wash, cells were scraped, pooled into 15ml Falcon tubes and centrifuged at 2,000 rpm, 4°C for 5 minutes. Cells were then washed in 0.15M saline a further two times, centrifuging at 2,000 rpm, 4°C for 5 minutes each time. Following the final wash, cells were lysed in NETN (0.5% NP-40 (Sigma), 150mM NaCl (Sigma), 50mM Tris pH 7.5, 0.5mM EDTA (Sigma)) (typically 500µl of buffer per dish harvested). Cell lysates were then homogenised using a Wheaton-Dounce hand homogeniser and centrifuged at 3,000rpm, 4°C for 5 minutes, the supernatant was centrifuged again at 13,000 rpm, 4°C for 15 minutes. Finally, the supernatant was centrifuged once more at 45,000 rpm, 4°C for 30 minutes and the supernatant retained.

2.3.2 Determination of Protein Concentration of Cell Lysates

Protein concentrations of cell lysates were determined against a standard curve produced using known concentrations of bovine serum albumin (BSA) (Sigma) in 200µl of Bio-Rad Protein reagent (Bio-Rad Laboratories) which was diluted 1:5 with sterile water. 5µl of cell lysate was diluted in 45µl of sterile water, and 10µl of this diluted cell lysate was added to 200µl of Bio-Rad reagent diluted 1:5 with sterile water. Protein concentration determination of cell lysates was repeated four times to improve accuracy. Protein concentrations were read using a microplate reader (Bio-Rad model 680) at 595nm wavelength.

2.3.3 Sodium Dodecyl Sulphate-Polyacrylamide Gel Electrophoresis (SDS-PAGE)

In order to separate proteins based upon their molecular size, 6-12% polyacrylamide gels were made in a total volume of 50mls consisting of 30% w/v acrylamide (37:5:1 BIS-acrylamide) (Severn Biotech), 0.1% SDS (Severn Biotech), 0.1M Tris (Melford)/ 0.1M Bicine (pH 8.3) (Severn Biotech), 0.6% ammonium persulphate (APS) (Sigma) and 0.3% N, N, N', N'-Tetramethylethylenediamine (TEMED) (Severn Biotech). Gels were poured into pre-made gel chambers, and well-forming combs were immediately added and the gel was left to polymerise. After polymerisation, combs were removed and the polyacrylamide gel was washed twice in deionised water, wells were filled with running buffer (0.1M Tris/ 0.1M Bicine (pH 8.3) and 0.1% w/v SDS). Cell lysate, GST pull-down and co-immunoprecipitation samples were prepared for running on polyacrylamide gels by adding an equal amount of Laemmli sample buffer (25% v/v glycerol (BDH Laboratories), 5% β-mercaptoethanol, 2% w/v SDS, 0.01% w/v bromophenol blue (BDH Laboratories) and 65mM Tris (pH 6.8)). Once Laemmli sample buffer had been added, samples were heated to 80°C for 5 minutes,

centrifuged at 13,000 rpm for 1 minute, and loaded onto the polyacrylamide gels along with a molecular weight marker for reference at 10-15mA overnight.

2.3.4 Visualisation of Proteins Separated by SDS-PAGE

Proteins separated by SDS-PAGE were assessed for protein quality by staining the polyacrylamide gels for 30 minutes in 0.1% w/v Coomassie brilliant blue R-250 (Sigma) in 25% methanol (Sigma), 10% acetic acid (Fisher Scientific). After staining, polyacrylamide gels were destained in rapid Coomassie destain (acetic acid /methanol/ water (1:3:6 v/v)) overnight, and assessed after sufficient destaining.

2.3.5 Visualisation of Proteins on Nitrocellulose Membranes

Proteins transferred onto nitrocellulose membranes were visualised by staining with Ponceau-S Stain consisting of 0.1% Ponceau-S (Sigma) and 3% trichloroacetic acid (TCA) (BDH Laboratories) for 30 seconds. Nitrocellulose membranes were then washed three times with deionised water to visualise proteins, and washed in TBST Tris-Buffered Saline Tween-80 (TBST) (1% Tween-80 (Sigma), 0.15M NaCl (Sigma), 50mM Tris, HCl pH 7.4 (Fisher Scientific)) to remove the remaining stain.

2.3.6 GST Pull-Down Assay

To assess direct *in-vitro* protein-protein interactions, GST pull-down assays were performed. Ad5E1HEK293, Ad5E1HER911, Ad12E1HER2 and Ad12E1HER10 cell lysates (containing 10mg protein) were prepared as in Section 2.3.1 and incubated with 25µg GST-fusion proteins (Table 2.4) and left rotating at 4°C. After 3 hours, 25µl of packed glutathione-agarose beads (Sigma) were incubated for 1 hour at 4°C in order to isolate protein-protein

complexes. Following this incubation, samples were centrifuged at 3,000 rpm, 4°C for 1 minute and supernatant was discarded. Samples were then washed 4 times in NETN buffer, centrifuging at 3,000 rpm, 4°C for 1 minute between each wash. Finally, samples were washed with buffer B (2mM EDTA (Sigma) in PBS), any residual buffer was removed and 60µl of 25mM glutathione pH 8.2 (BDH Laboratories) was added and left to incubate for 1 hour at 4°C. Following this incubation, samples were centrifuged at 3,000 rpm, 4°C for 1 minute and the supernatant retained in a fresh microfuge tube. 30µl of glutathione was again added to the beads and incubated at 4°C for a further 30 minutes. After 30 minutes, samples were centrifuged at 3,000 rpm, 4°C for 1 minute and supernatant pooled with the previous supernatant. 25µl of Laemmli sample buffer was added to the samples, heated to 80°C for 5 minutes, centrifuged at 13,000 rpm for 1 minute and loaded onto 10% polyacrylamide gels along with 50µl of cell lysate as a control and resolved by SDS-PAGE (Section 2.3.3).

Table 2.4 GST-Fusion Proteins used in this Study. The GST-fusion proteins used in this study are indicated, along with the amino acids these fusion proteins incorporate and the source.

GST-fusion protein	**Incorporating**	**Source**
GST-BLM WT fragment	BLM wild-type fragment aa 1-1417	Produced in this study
GST-BLM fragment 1	BLM fragment aa 1-212	Produced in this study
GST-BLM fragment 2	BLM fragment aa 191-660	Produced in this study
GST-BLM fragment 3	BLM fragment aa 621-1041	Produced in this study
GST-BLM fragment 4	BLM fragment aa 1001-1417	Produced in this study

2.4 Immunological Techniques

2.4.1 Western Blotting

Following separation of proteins by SDS-PAGE, proteins were transferred onto nitrocellulose membrane using the following method. Transfer cassettes contained the following layers: a sponge, Whatman 3MM blotting paper, nitrocellulose membrane (Pall corporation), SDS-PAGE gel, Whatman blotting paper and a sponge (all equipment was pre-immersed in transfer buffer containing 20% v/v methanol, 0.19M glycine and 0.05M Tris). The transfer cassette was then placed in a transfer tank filled with transfer buffer for 6 hours at 280mA. Following the transfer, nitrocellulose membranes were stained to visualise proteins and subsequently destained in deionised water and TBST. Nitrocellulose membranes were kept in 5% skimmed dried milk (Marvel) in TBST for 30 minutes in order to block non-specific binding sites. Following blocking, primary antibodies (Table 2.4) were diluted in 5% skimmed dried milk in TBST and incubated with the nitrocellulose membrane overnight at 4°C on a rocking table. Following incubation with primary antibodies, nitrocellulose membranes were washed in TBST 6 times for 5 minutes each time. Nitrocellulose membranes were then incubated with secondary antibodies (Table 2.5) conjugated to horse-radish peroxidase (HRP) in 5% skimmed dried milk in TBST for 2 hours at room temperature. Following incubation, nitrocellulose membranes were again washed in TBST 6 times for 5 minutes each time. Proteins were then visualised by washing nitrocellulose membranes in enhanced chemi-luminescence (ECL) reagent (Millipore or GE Healthcare) for 1 minute, sealed in saran wrap and exposed to autoradiography film (Kodak) for the required amount of time.

Table 2.5 Primary Antibodies used in this Study. Indicated are the primary antibodies used in this study, the antigens they target, molecular weight, dilution, use, species and source N.B. WB- Western Blot; IP- Immunoprecipitation; GST- GST pull-down.

Antibody	Antigen	Dilution	Use	Species	Company/Source
2AG	Ad5 E1B	1 in 20	WB, IP, GST	Mouse	Professor Arnold Levine
β-Actin	β-Actin	1 in 10000	WB	Mouse	Sigma
BLM	BLM	1 in 1000	WB, IP	Rabbit	Bethyl
M73	Ad5 E1A	1 in 10	WB	Mouse	Harlow et al., 1985
5DO2	Ad12 E1A	1 in 10	WB	Mouse	In house
Mre11	Mre11	1 in 1000	WB	Mouse	Genetex
p53	p53	1 in 100	WB, IP	Mouse	Professor David Lane
TOPBP1	TOPBP1	1 in 1000	WB	Rabbit	Dr Grant Stewart
XPH9	Ad12 E1B	1 in 20	WB, IP, GST	Mouse	Merrick et al., 1991

Table 2.6 Secondary Antibodies used in this Study. Indicated are the secondary antibodies used in this study, the antigen they target, dilution, use, species and source.

Antibody	Antigen	Dilution	Use	Species	Company/Source
Mouse	Mouse	1 in 2000	WB, IP, GST pull-down	Goat	Dako Laboratories
Rabbit	Rabbit	1 in 3000	WB, IP, GST pull-down	Swine	Dako Laboratories

2.4.2 Co-Imunnoprecipitation

Cell lysate containing 5mg of protein as in Section 2.3.1 and was typically incubated with 10µl of primary antibody (Table 2.3), rotating at 4°C overnight. Following overnight rotation, cell lysates were centrifuged at 45,000 rpm at 4°C for 10 minutes and the pellet discarded. 40µl of Protein G-agarose beads (Sigma) were added to the cell lysates and rotated at 4°C for 1 hour. The samples were then centrifuged at 3,000 rpm for 1 minute at 4°C and supernatant discarded. Samples were then washed four times in 1ml of NETN buffer, centrifuging at 3,000 rpm at 4°C for 1 minute and discarding the supernatant each time. 50µl of Laemmli sample buffer was added to the samples, heated to 80°C for 5 minutes, centrifuged at 13,000 rpm for 1 minute and resolved by SDS-PAGE.

2.5 Molecular Biology Techniques

2.5.1 GST-Fusion Protein Production

10mls of Luria Bertani (LB)-broth (10g/L tryptone (Fisher Scientific), 10g/L NaCl and 5g/L yeast extract (Fisher Scientific)) supplemented with 100µg/ml ampicillin (Sigma) was inoculated with a colony of BL21 E. coli transformed with gene constructs (Table 2.7), and left in an orbital incubator at 37°C overnight. Following overnight incubation, 5mls of each LB-broth culture was added to 500mls of LB-broth supplemented with 100µg/ml of ampicillin, and grown at 220 rpm, 37°C until cultures reached an optical density of 0.6-0.7 absorbency units. 0.5mM isopropyl β-D-1-thiogalactopyranoside (IPTG) (Sigma) was then added to the cultures and grown for a further 3 hours at 30°C, 220 rpm. Following incubation, cultures were centrifuged at 6,000 rpm for 15 minutes, supernatants discarded and pellets frozen at -80°C until required.

2.5.2 GST-Fusion Protein Purification

Bacterial pellets were resuspended in 30mls of Buffer A (2mM EDTA, 1% Triton X100 (Sigma) in PBS) and sonicated twice for thirty seconds each time and centrifuged at 18,000 rpm for 5 minutes and pellet discarded. The bacterial cell lysate was centrifuged for a further 18,000rpm for 30 minutes and the pellet discarded. 2mls of 50:50 PBS: glutathione-agarose beads were added to the supernatant and rotated for 3 hours at 4°C. Samples were centrifuged at 2,000 rpm for 5 minutes, and to the supernatant 1ml of 50:50 PBS: glutathione-agarose beads were added and rotated at 4°C for a further hour. Meanwhile, pelleted beads were washed in 30mls of Buffer A three times, centrifuging at 2,000 rpm for 5 minutes at 4°C each time. Samples were then washed in 30mls of Buffer B, and centrifuged at 2,000 rpm, 4°C for minutes. To the beads, 2mls of 25mM glutathione (pH 8.2) was added and rotated at 4°C for 1 hour. Samples were then spun at 2,000 rpm for 5 minutes and supernatant retained. Glutathione was removed from the GST-fusion proteins by dialysis at 4°C overnight. Supernatants were transferred to dialysis tubing and dialysed overnight against in buffer containing 150mM NaCl, 25mM Tris (pH 7.5) and 1mM dithiothreitol (DTT) (Sigma).

Table 2.7 Gene Expression Constructs for GST-Fusion Protein Production. Indicated are the BLM gene fragments used in this study, the vectors they were ligated into and their source. BLM gene fragments were ligated into pGEX-4T-1 vectors (provided by Dr Sengupta) which contain an ITPG-inducible promoter, an ampicillin resistance gene and a GST gene. These gene expression constructs were used to produce the GST-BLM fusion proteins used in this study.

Gene	**Vector**	**Source**
BLM WT Fragment (aa 1-1417)	pGEX-4T-1	Dr Sengupta
BLM Fragment 1 (aa 1-212)	pGEX-4T-1	Dr Sengupta
BLM Fragment 2 (aa 191-660)	pGEX-4T-1	Dr Sengupta
BLM Fragment 3 (aa 621-1041)	pGEX-4T-1	Dr Sengupta
BLM Fragment 4 (aa 1001-1417)	pGEX-4T-1	Dr Sengupta

Chapter 3:

Results

3.1 BLM is Degraded Following Infection with Adenovirus Serotypes 4, 5 and 12

In order to confirm preliminary evidence from our laboratory that certain adenovirus serotypes are able to degrade BLM, HeLa cells infected with Ad3, 4, 5, 7, 9, 11 and 12 serotypes were harvested at 0, 24, 48, 72 and 96 hours post-infection and subjected to Western blotting (Figure 3.1). BLM was immuno-blotted, along with β-Actin as a loading control, and TOPBP1, Mre11 and p53 as controls which are known to be degraded during infection with various Ad serotypes. As expected, protein levels of TOPBP1 throughout the course of Ad3, 4, 5, 7, 9, 11 infection remained the same, whilst TOPBP1 was degraded 24 hours post-Ad12 infection. Protein levels of Mre11 during Ad3, 7, 9 and 11 infections remained unchanged throughout the course of infection, whilst Mre11 was degraded 48 hours post-Ad4, 5 and 12 infection. p53 protein expression is induced in cells infected with Adenovirus serotypes 3, 7, 9 and 11, whilst p53 was degraded during Ad 4, 5 and 12 infection as anticipated (Blackford et al, 2010; Forrester et al., 2011). Early adenoviral proteins E1A and E1B were also immuno-blotted to confirm infection with Ad 5 and 12 serotypes. Due to lack of appropriate antibodies, infection with Ad3, 4, 7, 9 and 11 serotypes was confirmed by Ponceau-S staining of nitrocellulose membranes to visualise viral structural proteins (data not shown). Protein levels of BLM after infection with Ad3, 7, 9 and 11 serotypes remained constant throughout the duration of infection. Infection with Ad4, 5 and 12 serotypes resulted in the degradation of BLM; after 24 hours during Ad5 and 12 infection, and 48 hours post-Ad4 infection (Figure 3.1).

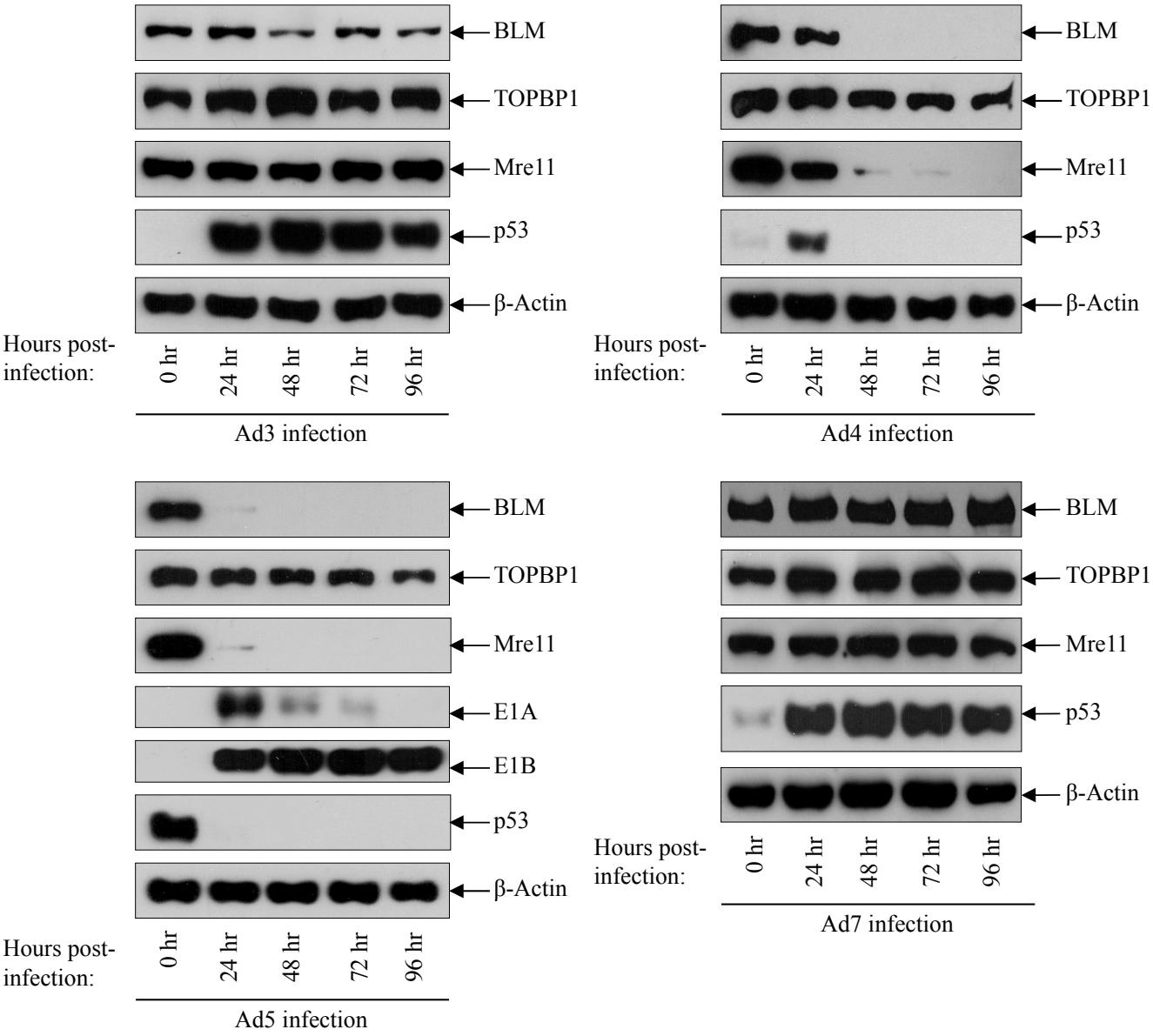

Figure 3.1: Degradation of BLM Following Adenovirus Infection. HeLa cells were infected with various adenovirus serotypes, harvested at 0, 24, 48, 72 and 96 hours post-infection and subjected to Western Blotting for BLM. In addition, β-Actin was immuno-blotted as a loading control, along with Mre11, p53 and TOPBP1 as controls which are known to be degraded during infection with certain adenovirus serotypes. These data are representative of one experiment performed three times independently.

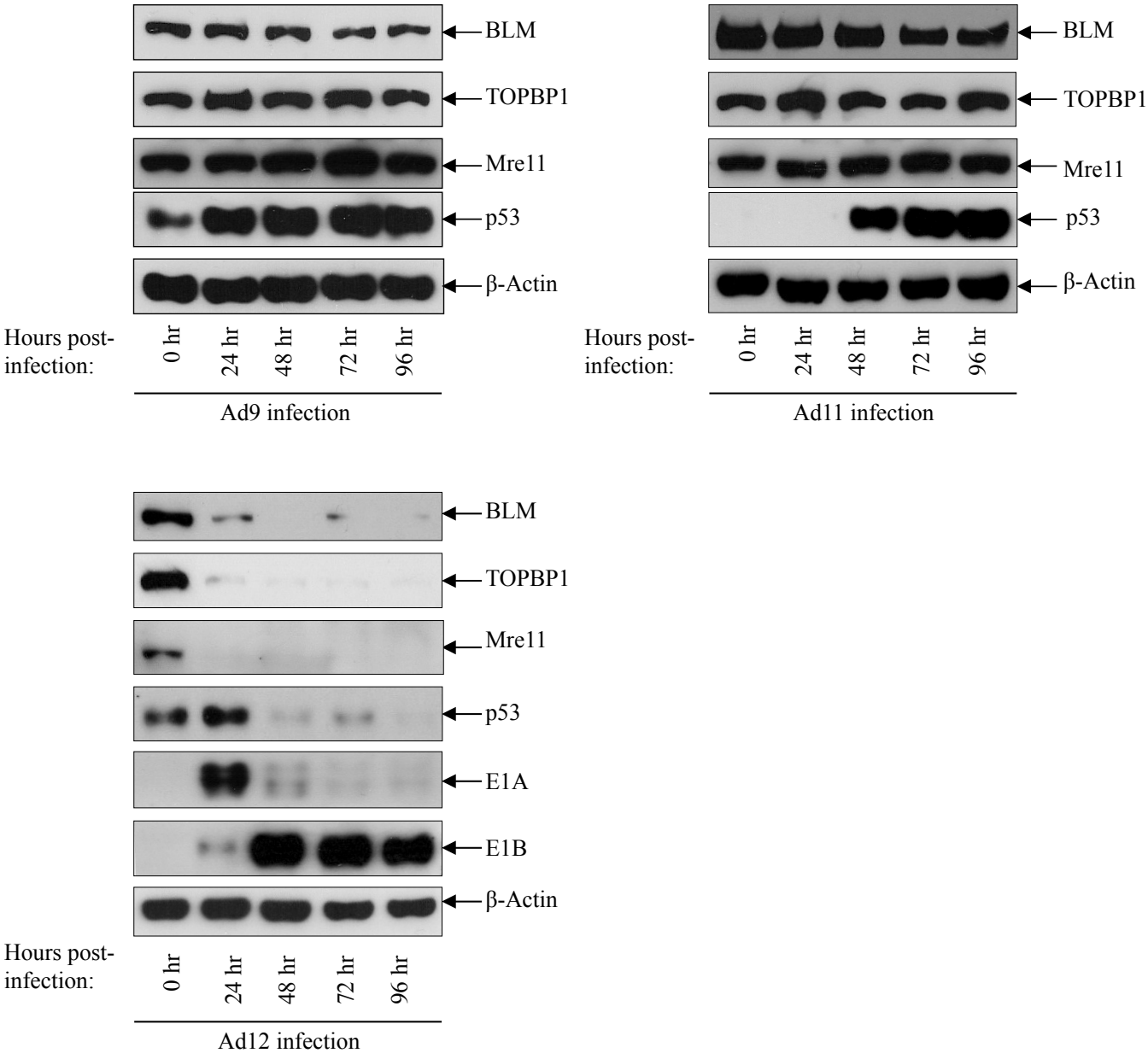

Figure 3.1 Continued: Degradation of BLM Following Adenovirus Infection. HeLa cells were infected with various adenovirus serotypes, harvested at 0, 24, 48, 72 and 96 hours post-infection and subjected to Western Blotting for BLM. In addition, β-Actin was immuno-blotted as a loading control, along with Mre11, p53 and TOPBP1 as controls which are known to be degraded during infection with certain adenovirus serotypes. These data are representative of one experiment performed three times independently.

3.2 The Adenovirus E1B Protein is Required for the Degradation of BLM during Adenovirus Infection.

In order to determine which adenoviral proteins are responsible for the degradation of BLM during adenovirus infection, HeLa cells infected with mutant Ad5*dl*1520 (Ad5 E1B- mutant), *Ad12dl620* (Ad12 E1B- mutant), Ad5*dl355* (Ad5 E4orf6- mutant) and h5pm4155 (Ad5 E4- mutant) viruses were harvested at 0, 24, 48, 72 and 96 hours post-infection and subjected to Western blotting for BLM (Figure 3.2). β-Actin was also immuno-blotted as a positive loading control, along with TOPBP1, Mre11, p53 as positive controls and Ad5 or 12 E1A and E1B-55K. In Ad5*dl*1520 and Ad12*dl*620 infected HeLa cells, levels of BLM remained constant throughout infection, suggesting that the degradation of BLM is E1B-dependent during both Ad5 and 12 infection. In Ad5*dl*355 and h5pm4155 infected HeLa cells, levels of BLM also remained constant throughout infection, suggesting that the degradation of BLM is E4-dependent during Ad5 infection (Figure 3.2).

3.3 Adenovirus Early Region E1B-55K Interacts with BLM *in Vivo*

In order to assess whether Ad E1B-55K interacts with BLM *in vivo*, co-immunoprecipitation assays were performed. Appropriate cell lysate was incubated with antibodies against BLM or E1B-55K and subsequent immuno-complexes were isolated from the cell lysates using Protein-G agarose beads and subjected to Western blotting for BLM or E1B-55K (Figure 3.3). Results from Figure 3.3A show that E1B-55K interacts with BLM *in vivo* in both Ad5E1HEK293 and Ad12E1HER2 cells. In a reciprocal experiment, immuno-precipitated BLM was immuno-blotted with antibodies against Ad5 and 12 E1B-55K proteins. Figure 3.3B confirms that E1B-55K from both Ad5 and 12 serotypes infection interacts with BLM *in vivo.*

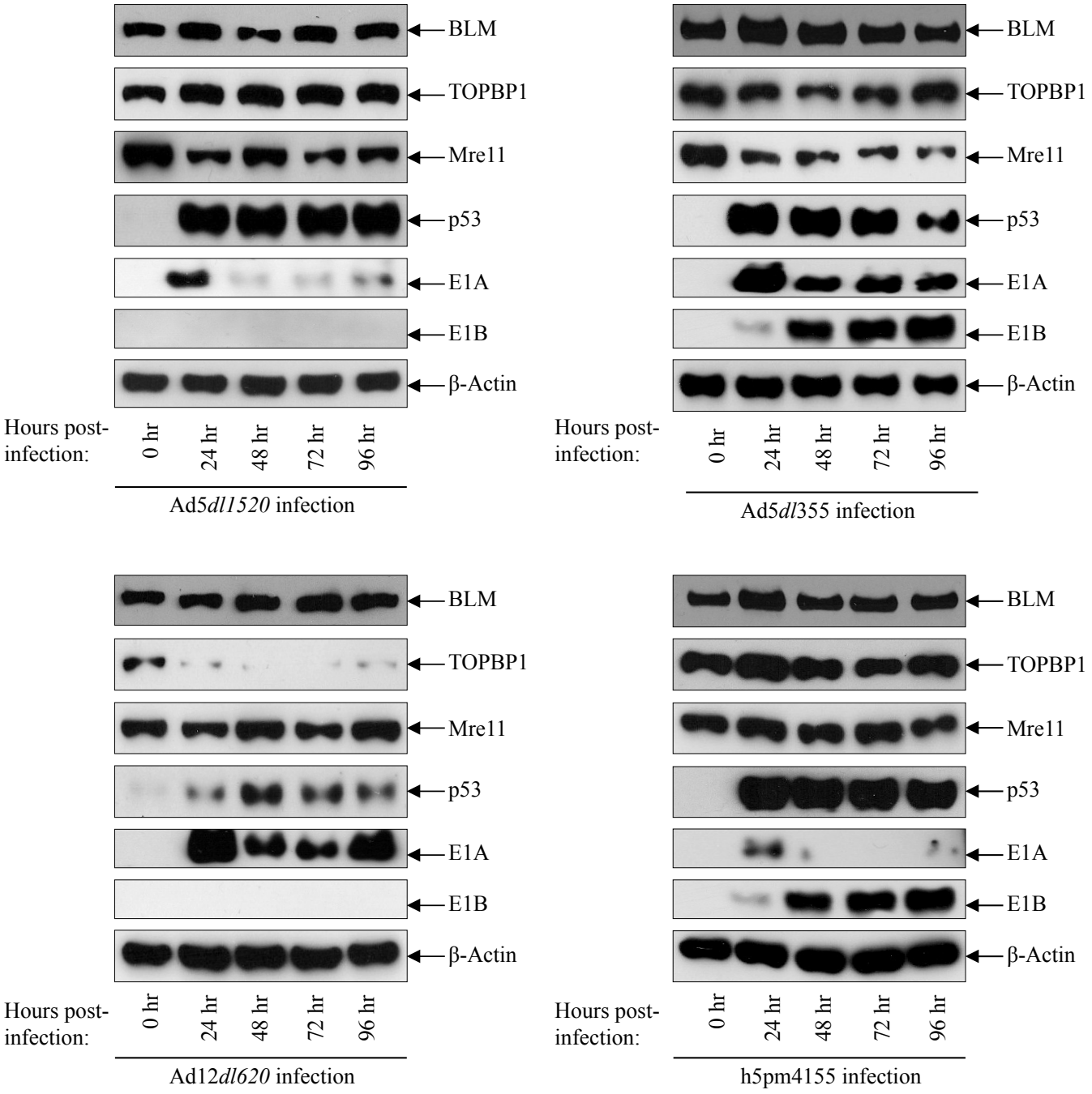

Figure 3.2: Degradation of BLM Following Mutant Adenovirus Infection. HeLa cells were infected with mutant adenoviruses, harvested at 0, 24, 48, 72 and 96 hours post-infection and subjected to Western blotting for BLM. β-Actin was also immuno-blotted as a loading control, along with p53, Mre11 and TOPBP1, also as controls, and E1A and E1B to assess for infection. These data are representative of one experiment performed twice.

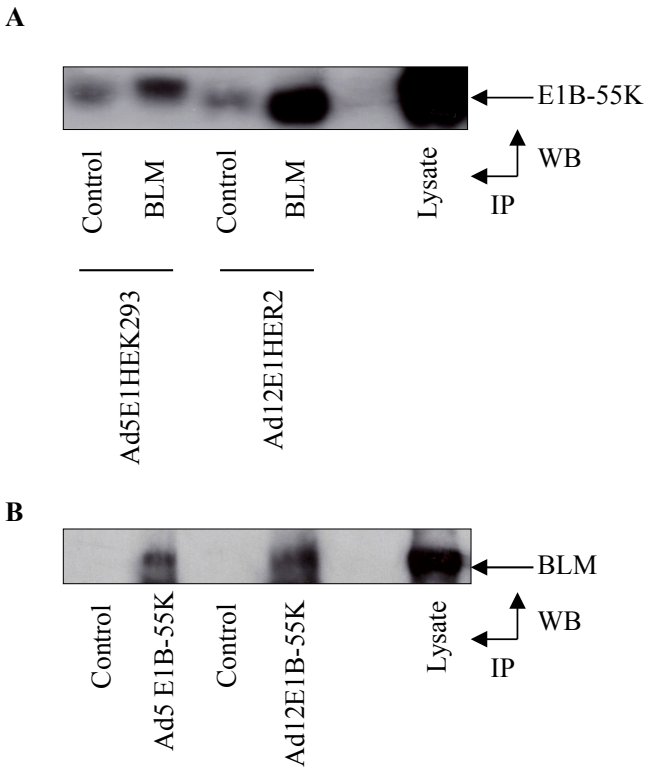

Figure 3.3: BLM Interacts with E1B-55K *in vivo* in both Adenovirus 5 and 12 Transformed Cell Lines. Appropriate cell lysate was incubated with antibodies against BLM or Ad5/Ad12 E1B-55K, protein-protein complexes were isolated using Protein-G beads and subjected to Western blotting for: **A.** E1B-55K or **B.** BLM. These data are representative of one experiment performed twice.

3.4 The Ad E1B-55K Protein Directly Interacts with BLM *in Vitro*

In order to assess whether the E1B-55K protein directly interacts with BLM *in vitro*, and to see which region of BLM E1B-55K binds, GST pull-down assays were performed. In order to perform these GST pull downs, various GST-BLM fragments were constructed (Table 2.4) (Figure 3.4). Purified GST-fusion proteins (Table 2.7) were resolved by SDS-PAGE and SDS-PAGE gels were Coomassie Blue stained to assess the purity of the GST-fusion proteins produced (Figure 3.5). Following assessment of the purity of the GST-fusion proteins produced, Ad5E1HER911, Ad5E1HEK293, Ad12E1HER10 and Ad12E1HER2 cell lysates were incubated with GST-fusion proteins and resulting protein complexes were isolated using glutathione-agarose beads. Protein complexes were subjected to Western blotting for Ad5 or Ad12 E1B-55K, depending on the cell lysate used, along with GST protein alone and cell lysate alone as non-specific binding and positive controls, respectively. Using Ad12 transformed cell lysates Ad12E1HER2 and Ad12E1HER10, protein complexes following GST pull-down were immuno-blotted for Ad12 E1B-55K, showing in both lysates, E1B-55K interacts with GST-BLM fragment 2 (191-660aa) *in vitro* (Figure 3.4 and 3.6). Using Ad5 transformed cell lysates Ad5E1HER293 and Ad5E1HEK911, protein complexes following GST pull-down were immuno-blotted for Ad5 E1B-55K, showing in both lysates, E1B-55K interacts with GST-BLM fragment 1 (aa 1-212) and fragment 2 (aa 191-660) *in vitro* (Figure 3.4 and 3.6).

3.5 Degradation of BLM during Adenovirus Serotype 5 and 12 Infection is Proteasome Dependent

In order to assess whether the degradation of BLM during infection with Ad 5 and 12 was dependent on the proteasome, HeLa cells were infected with Ad5 or 12 and treated with the

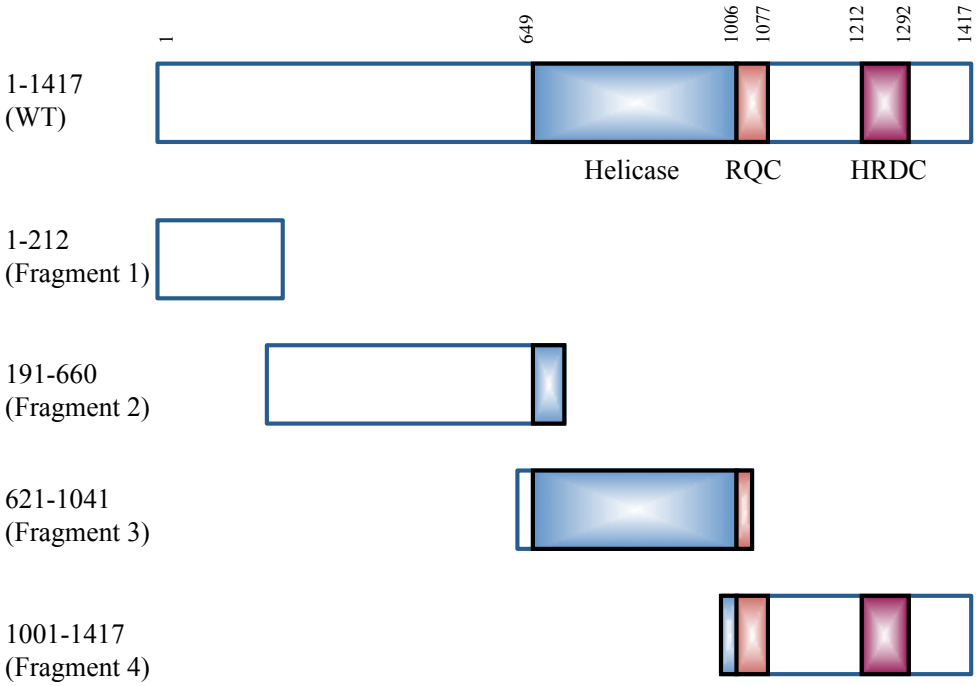

Figure 3.4 Structure of BLM and Associated Domains. Schematic representation of BLM and the GST-BLM fragments used in this study. Amino acid numbers are indicated above the full length BLM schematic. Various domains are indicated. RQC, RecQ carboxy-terminal; HRDC, Helicase and Rnase D C-terminal (modified from Srivastava et al., 2009).

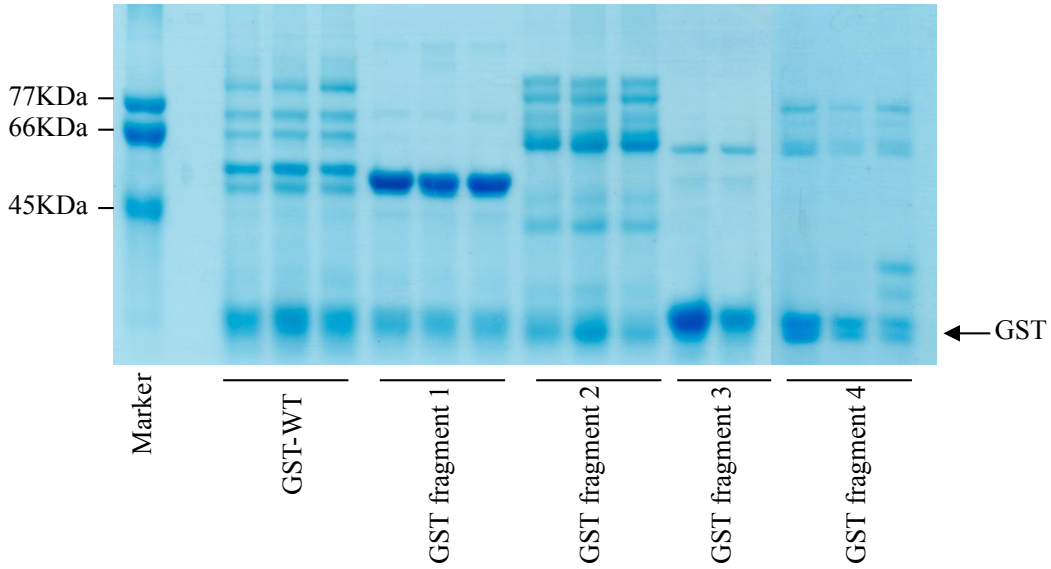

Figure 3.5: Assessment of the Protein Quality of the GST-BLM Fragments Produced in this Study. Plasmid DNA constructs were transformed into BL21 *E.Coli* in order to produce various GST-fusion proteins. GST-fusion proteins were purified, resolved by SDS-PAGE, Coomassie Blue stained and subsequently destained to assess protein purity.

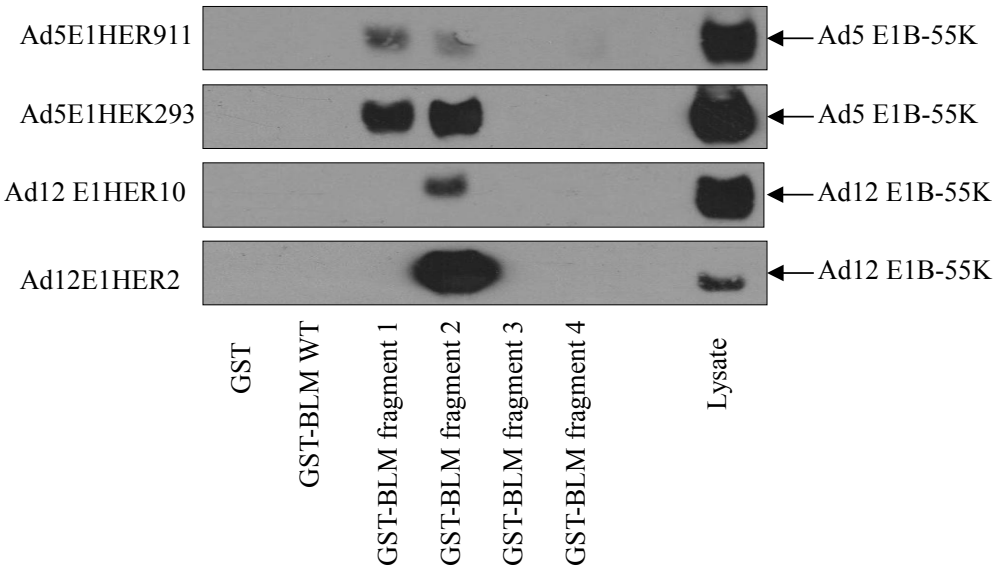

Figure 3.6: The E1B-55K Protein Directly Interacts with BLM *in Vitro*. Ad5E1HER911, Ad5E1HEK293, Ad12E1HER10 and Ad12E1HER2 cell lysates were incubated with various GST-BLM fusion proteins. Protein complexes were isolated with glutathione-agarose beads and subjected to Western blotting for Ad5 or 12 E1B-55K, depending on the cell lysate used. These data are representative of one experiment performed twice independently.

pan-proteasome inhibitor MG132. Cells infected with Ad5 and MG132 treated were harvested, with infected, untreated controls in parallel, at 0, 24hr and 48hr post-infection, whilst cells infected with Ad12 and MG132 treated were harvested, with infected, untreated controls in parallel, at 0, 12 and 24hrs post-infection. Both were subjected to Western blotting for β-Actin (loading control), Mre11 (positive control) and BLM (Figure 3.7). BLM was partially degraded by 24 hours post-Ad5 infection in untreated HeLa cells, in cells treated with the proteasome inhibitor, BLM was degraded by 48 hours post-Ad5 infection. In untreated cells infected with Ad12, BLM was degraded 24 hours post-Ad12 infection, whilst in cells treated with MG132, BLM was only partially degraded 24 hours post-Ad12 infection. These data suggest that the degradation of BLM during Ad5 and 12 infection is, at least, partially dependent upon the proteasome (Figure 3.7).

3.6 Cullin 4B is Partially Required for the Degradation of BLM during Adenovirus Infection

Ad5 and Ad12 infected HeLa cell lysates which had been previously treated with siRNAs to silence expression of various Cullins including CUL2, CUL4A, CUL4B, CUL5 and CUL7 for Ad5 infection, and CUL2, CUL5 and CUL7 for Ad12 infection were harvested at 0, 24 and 48 hours post-infected and subjected to Western blot analysis (Figure 3.8). In Ad5 infected HeLa cells, silencing of Cul2, Cul5, Cul4A and Cul7 resulted in the degradation of BLM similar to that of the non-silencing control, suggesting that these Cullins are not responsible for degradation of BLM. However, in Ad5 infected HeLa cells treated with Cul4B siRNA, BLM still appeared to be partially present 48 hours post-infection, suggesting that silencing of Cul4B expression partially stabilises BLM degradation. In Ad12 infected HeLa cells,

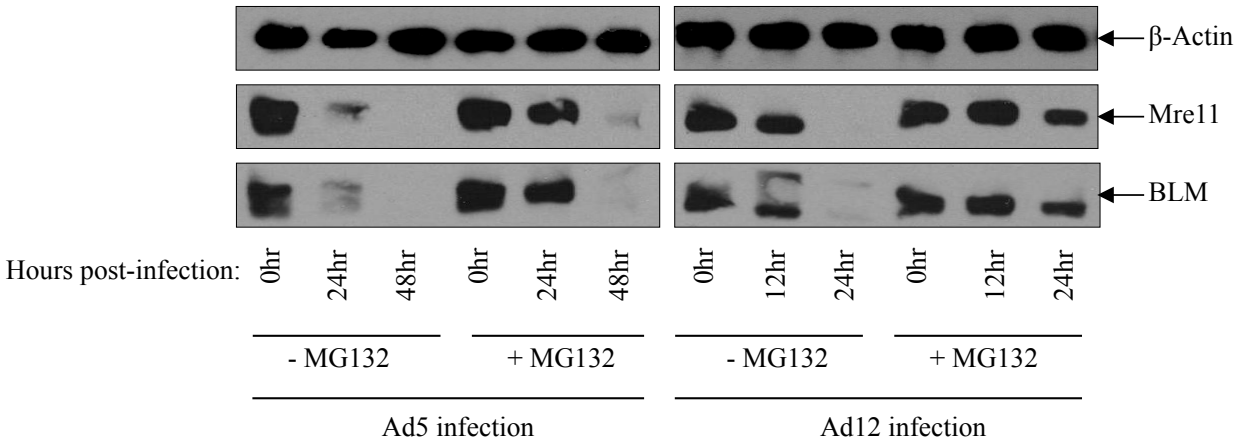

Figure 3.7: Degradation of BLM During Adenovirus 5/12 Infection is Dependent on Proteasome Activity. HeLa cells were infected with Ad5 or 12, were treated with the proteasome inhibitor MG132 and harvested at 0, 24 and 48 hour time points for Ad5 infected cells, and 0, 12 and 24 hour time points for Ad12 infected cells. Lysates were subjected to Western blotting for β-Actin as a loading control, Mre11 as a positive control and BLM. These data are representative of one experiment performed two times independently.

silencing of Cul2, Cul5 and Cul7 resulted in the degradation of BLM similar to that of the non-silencing control, suggesting that these Cullins are not responsible for the degradation of BLM. Unfortunately there was not sufficient Cul4B siRNA available to determine the effect during Ad 12 infection (Figure 3.8).

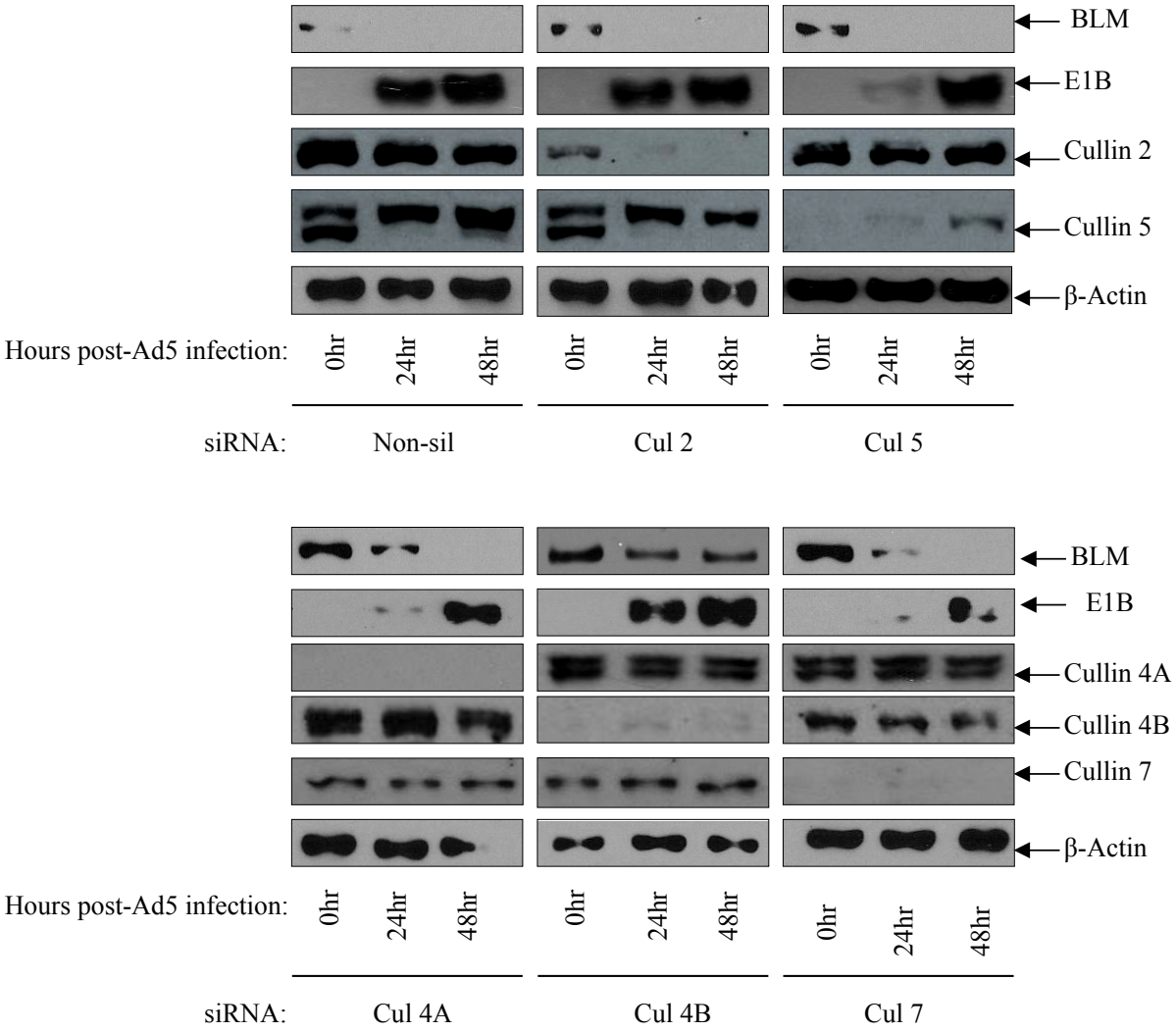

Figure 3.8: The Effect of Cullin knock-downs on BLM degradation. HeLa cell lysate from cells infected with Ad5 and treated with siRNAs against various Cullins, were harvested after 0, 24 and 48 hours post-infection and subjected to Western blotting for β-Actin as a loading control, various Cullins to assess silencing efficiency, E1B-55K as an infection control and BLM. These data are representative of one experiment performed twice.

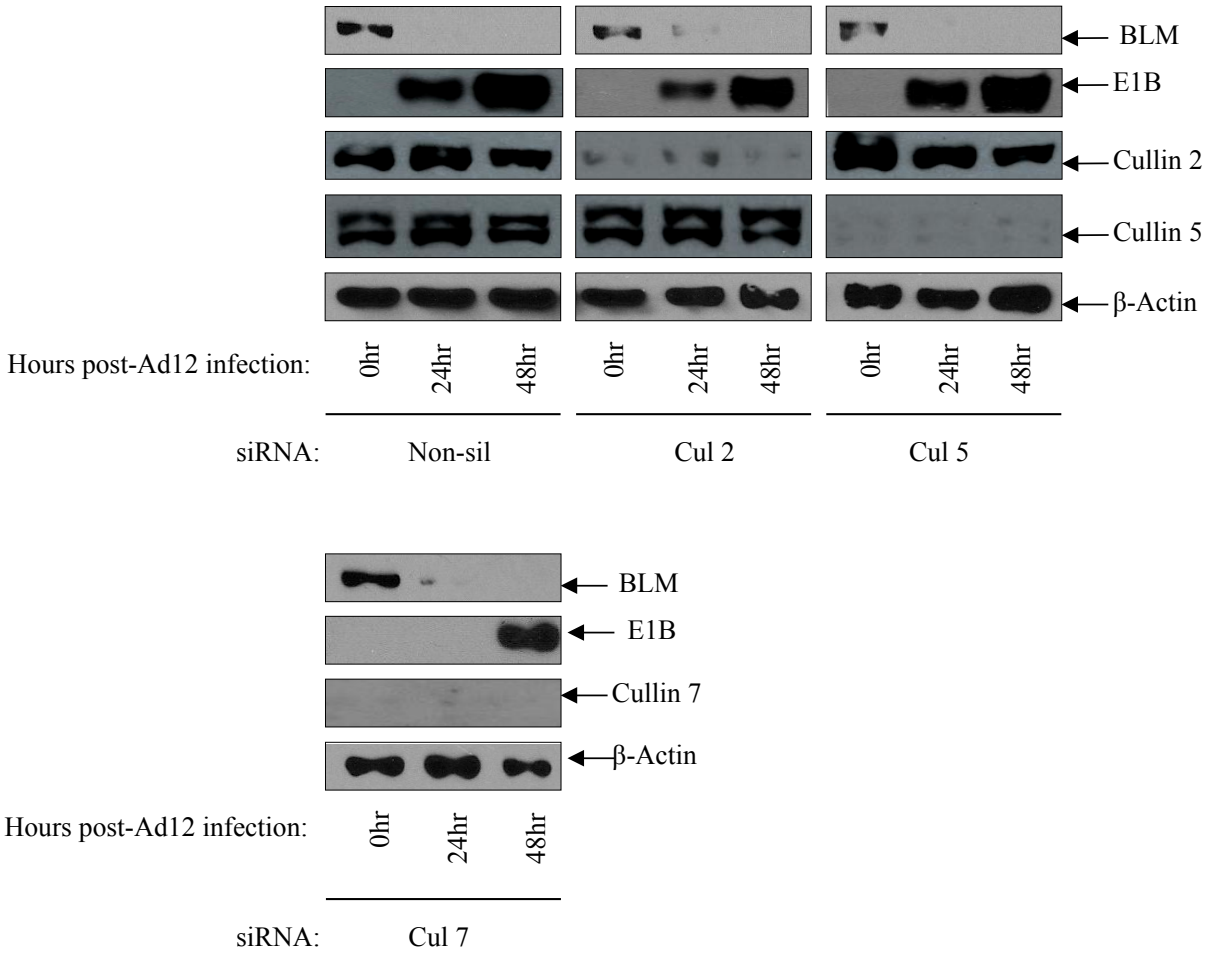

Figure 3.8 Continued: The Effect of Cullin knock-downs on BLM Degradation. HeLa cell lysate from cells infected with Ad12 and treated with siRNAs against various Cullins, were harvested after 0, 24 and 48 hours post-infection and subjected to Western blotting for β-Actin as a loading control, various Cullins to assess silencing efficiency, E1B-55K as an infection control and BLM. These data are representative of one experiment performed twice.

Chapter Four:

Discussion

4. Discussion

Our laboratory first suggested an association between BLM and adenovirus after mass spectrometric analysis of adenovirus E1B-55K binding partners showed that BLM associated with E1B-55K *in vivo* (Forrester, unpublished data 2010). Following this, our laboratory investigated this interaction further by looking at BLM protein levels during the course of adenovirus infection. Preliminary data suggested that BLM is degraded throughout infection with various adenovirus serotypes. To our knowledge there was no other evidence to suggest an association between adenovirus and BLM at the beginning of this study. However, during this project a paper was published suggesting that Ad5 is responsible for the degradation of BLM, mirroring the work that was on going in our laboratory (Orazio et al., 2011).

The first objective of this study was to confirm the preliminary observations that certain adenovirus serotypes are able to degrade the RecQ helicase BLM (Objective 1, Section 1.9). The work presented in this study confirmed that BLM is degraded during Ad4, 5 and 12 infection. During infection with Ad5 and Ad12, BLM was degraded by 24 hours post-infection, and during Ad4 infection, BLM was degraded 48 hours post-infection (Figure 3.1). This confirms the preliminary evidence in our laboratory and in addition, confirms the findings from the recent study by Orazio et al. demonstrating that BLM is degraded during Ad5 infection (Orazio et al., 2011). In addition to confirming these findings, we have also identified two novel adenovirus serotypes, 4 and 12, which also degrade BLM during infection.

To date, there has been no assigned role for the degradation of BLM during adenovirus infection. We suggest a number of reasons why adenoviruses could target BLM. It is already

known that adenoviruses target components of the HRR pathway (e.g. MRN), in order to prevent DNA damage repair and in turn prevent processing and ligation of viral DNA ends (Carson et al., 2003; Stracker et al., 2002). Recent evidence suggests that BLM has important pro-recombinase roles in HRR both during DNA end resectioning and resolving of recombination intermediates (Section 1.7). Evidence that BLM has important roles in DNA end resectioning comes from studies that have shown that BLM is able to associate with Exonuclease 1, and stimulate its nuclease activity to resect dsDNA to ssDNA (Nimonkar et al, 2008; Gravel et al, 2008). In addition, BLM can also interact with Rad54 and stimulate its activity, also promoting HRR (Srivastava et al, 2009). These events occur early in the HRR pathway and may explain why BLM is degraded in the early stages of infection. Degradation of BLM and the subsequent inhibition of the HRR pathway may be advantageous during adenovirus infection as to inhibit the recombinase activity of BLM, so that BLM cannot interfere with adenovirus replication by resolving ends of viral genomes. There is considerable evidence to indicate that Ad5 targets multiple components of pathways they need to deregulate or disrupt (Section 1.4). BLM has also been shown to have roles in the later stages of the HRR pathway, converging double Holliday junctions through its interaction with Topoisomerase 3α (Wu et al, 2006; Raynard et al, 2006). The implications of this function of BLM in the context of adenovirus infection are unclear at present. On the other hand, some evidence suggests that BLM has anti-recombinase activities, therefore inhibiting HRR. Indeed, Bloom's syndrome patients with mutated BLM have excessive HRR and subsequent genomic instability, suggesting that BLM predominantly acts as an anti-recombinase. In addition, BLM is able to interact with Rad51, inhibiting polymerisation and nucleofilament formation, and therefore inhibiting HRR (Bugreev et al., 2007). Intriguingly, other adenovirus serotypes which do not degrade BLM replicate normally (adenovirus

serotypes 3, 7, 9 and 11), suggesting that the degradation of BLM is not essential for viral replication. However these viruses also fail to degrade p53, Mre11 and TOPBP1 and so they obviously employ other strategies for inhibiting DNA break repair, possibly through the degradation of DNA ligase IV (Baker et al., 2007). These intriguing inconsistencies will hopefully be resolved by future investigation.

The next objective of this study was to determine which viral proteins are responsible for the degradation of BLM during adenovirus infection (Objective 2, Section 1.9). Using mutant viruses, data obtained in this study demonstrated that E1B-55K and E4orf6 are essential for BLM degradation during Ad5 infection, confirming the result also obtained by Orazio et al (Figure 3.2) (Orazio et al., 2011). In addition to these findings, we were also able to show that the degradation of BLM during Ad12 infection is dependent on E1B-55K, but unfortunately no Ad12 virus mutant in E4 was available to determine if BLM degradation is E4 dependent, although this seems highly likely (Figure 3.2). In addition, no mutant Ad4 viruses were available to investigate whether BLM degradation was also E1B-55K and E4 dependent. However, overall these findings suggest that the E1B55K/E4orf6 linked E3 ubiquitin ligase complex is responsible for the degradation of BLM during Ad5 and 12 infection.

A further objective of this study was to validate a role for the E1B-55K protein during the degradation of BLM (Objective 3a, Section 1.9). Co-immunoprecipitation assays showed that E1B-55K interacts with BLM during infection with both Ad5 and 12 (Figure 3.3). Unfortunately no Ad4 E1B-55K antibody was available to assess BLM interactions during Ad4 infection. These results further validate a role for E1B-55K in the degradation of BLM, probably acting as a link between the substrate and E4orf6 and the E3 ligase.

Following confirmation of E1B-55K interactions with BLM *in vivo,* the next objective of this study was to determine with which region of BLM E1B-55K interacts (Objective 3b, Section 1.9). Our results showed that Ad5 E1B-55K associates with GST-BLM fragment 1 (incorporating amino acids 1-212) and GST-BLM fragment 2 (incorporating amino acids 191-660) (containing part of the helicase domain) *in vitro.* Interestingly, Ad12 E1B-55K associates with GST-BLM fragment 2 only, suggesting that different Adenovirus serotypes may have evolved different binding sites (Figure 3.6). Although the binding site for Ad5E1B-55K on p53 has been determined (Lin et al., 1994), no site of interaction for any other proteins degraded during Ad5 infection has been mapped. Comparison of the amino acid sequences of BLM and the proposed E1B-55K binding site on p53 shows a region of homology around amino acids 425-430. Tryptophan 23 and proline 27 in p53 have been suggested to be of particular importance for interaction with Ad5E1B55K and these are conserved in BLM. Significantly, this suggested binding site is present in GST-BLM fragment 2 which interacts with Ad5 and Ad12 E1B-55K proteins (Figure 4.1). Interestingly, a comparible site is present in Mre11 although the homology is not so marked (Hartl et al., 2008).

The next objective of this study was to further elucidate a role for the interaction between E1B-55K and BLM (Objective 4a, Section 1.9). As previously discussed, using mutant viruses we were able to show that BLM degradation is dependent on E1B-55K and E4orf6 during Ad5 infection, and although Ad12 E4 and Ad4 mutant viruses were unavailable, this does suggest that the E1B-55K/E4orf6 ligase complex may be responsible for the of BLM. Our results showed that degradation of BLM during Ad5 and 12 infection were dependent on

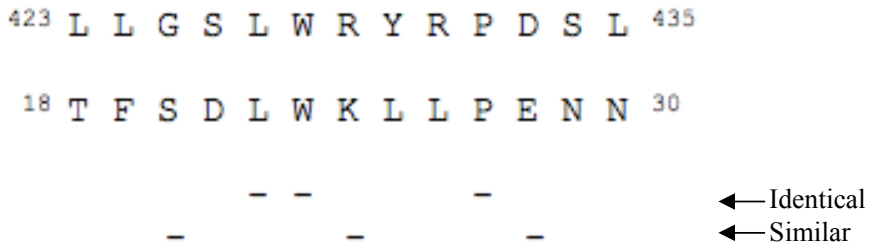

Figure 4.1: Comparison of the Amino Acid Sequences of BLM and p53 in the Proposed Binding Site for Ad5E1B-55K. Comparison of Ad5E1B-55K's binding site to p53 and BLM's amino acid sequence reveals a region of homology between amino acids 425 and 43. Significantly, this region of homology is present within the GST-BLM fragment 2 which has been shown to interact with both Ad5 and Ad12 E1B-55K proteins in this study (Lin et al., 1994).

the proteasome, suggesting that E1B-55K/E4orf6 complex targets BLM for proteasomal degradation (Figure 3.7).

The study from Orazio et al suggested that Cul5 is a component of the E1B-55k/E4orf6 E3 ubiquitin ligase complex which is responsible for the degradation of BLM during Ad5 infection. In order to show this, a Cul5 dominant negative gene, comprising the N-terminal domain of Cul5, which is unable to ubiquitinate substrates, was transfected into cells. It was found that BLM was no longer degraded in these cells, suggesting that Cul5 is essential for the degradation of BLM (Orazio et al, 2011). However, it has been suggested that the use of this dominant negative Cul5 construct also inactivates other Cul E3 ubiquitin ligases, and so the inhibition of BLM degradation may not be due to inactivation of Cul5, but due to inactivation of all of the Cullins. In order to investigate this more fully, we reduced the expression of various Cul's using siRNA to examine the effect on BLM degradation (Objective 4b, Section 1.9). Silencing of Cul5 did not affect BLM degradation during Ad5 infection, and in addition did not affect BLM degradation during Ad12 infection (Figure 3.7). In addition, silencing of Cul2, 4A and 7 in Ad5 infection did not affect BLM degradation. Interestingly, reduction of Cul4B expression seemed to partially stabilise BLM degradation during Ad5 infection, suggesting that Cul4B may be involved in the E1B-55K/E4orf6 complex that is involved in BLM degradation. Silencing of Cul2 and Cul7 during Ad12 infection did not affect BLM degradation. Unfortunately, sufficient Cul4A and Cul4B siRNA was not available to determine their possible role during Ad12 infection.

4.1 Limitations

One issue during this study was the lack of mutant viruses available to determine which viral proteins were responsible for the degradation of BLM. We were able to confirm that the degradation of BLM during Ad5 infection was dependent on both E1B and E4, probably working together as an E3 ligase to degrade BLM (Figure 3.2). In addition, we were able to determine that degradation of BLM during Ad12 infection was dependent on E1B activity. However, no mutant Ad12 E4 virus was available to determine if degradation of BLM is additionally dependent on E4 activity during Ad12 infection. In addition, no mutant Ad4 viruses were available to determine if the degradation of BLM was dependent on E1B/E4 activity. Access to such mutant viruses would have provided us with a complete set of data, helping us to further elucidate the interaction between BLM and adenovirus. We were unable to obtain to any Ad4 serotype antibodies throughout the duration of this study, meaning we were unable to confirm the potential interaction between BLM and E1B-55K both *in vitro* and *in vivo* during Ad4 infection (Figure 3.3 and 3.5). Due to limited availability of siRNAs, unfortunately we were unable to knock-down gene expression of Cul4A and 4B during Ad12 infection. Therefore, we were unable to determine whether knock-down of Cul4A partially stabilised BLM degradation, as in Ad5 infection (Figure 3.7). In addition, we were unable to knock-down gene expression of any Cullins during Ad4 infection, due to the lack of siRNA available in our laboratory.

4.2 Future Work

In order to circumvent the limitations in this study, it would be beneficial to obtain mutant Ad12 E4 virus, and also a mutant Ad4 E1B-55K and E4 virus. This would allow us to determine whether different adenovirus serotypes adopt the same mechanism of BLM

degradation as in Ad5 infection. It would also be beneficial to assess the effect of BLM degradation after knock-down of Cul4A and 4B gene expression during Ad12 infection, to determine whether the degradation of BLM is partially stabilised after knock-down of Cul4B gene expression, as in Ad5 infection (Figure 3.7). Access to additional Cul2, 4A, 4B, 5 and 7 siRNAs would also be useful to assess whether knock-down of Cul4B gene expression also stabilises BLM degradation during Ad4 infection.

In addition to circumventing the limitations associated with this study, a number of other experiments would further elucidate the relationship between the adenoviruses and BLM. Immunofluorescence microscopy could be undertaken to observe the localisation of BLM during adenovirus infection. It would be interesting to determine if BLM localises to viral replication centres during adenovirus infection. In addition, it may be interesting to repeat these immunofluorescence assays using mutant viruses which do not degrade BLM (Figure 3.2), to compare differences in BLM localisation.

Understanding the Modulation of DNA Repair Pathways by the Human Oncogenic Virus KSHV

UNIVERSITY OF BIRMINGHAM

Submitted by Ellis Ryan

This project is submitted in partial fulfilment of the requirements for the award of the MRes

Supervisors: Professor David Blackbourn & Dr Roger Grand

Abstract

Kaposi's sarcoma associated herpesvirus (KSHV) is a double-stranded DNA virus belonging to the herpesvirus subfamily. Complex cellular defence mechanisms limit the potential for viruses, including KSHV, to replicate in the host. Such defences include the interferon response that can restrict virus replication and contain spread. It is becoming increasingly apparent that in addition to these immune defences, the cellular response to DNA damage also functions as an important anti-viral mechanism. Here we present the first report showing that *de novo* KSHV infection can activate components of the cellular DNA damage response; namely phosphorylation of ataxia-telangiectasia mutated (ATM), NBS1, Chk1, replication protein A (RPA) and H2AX. In addition, we show that KSHV reactivation to evoke lytic replication also activates components of the DNA damage response; namely phosphorylation of ATM, Chk2, RPA and H2AX. The inhibition of the ATM/ataxia-telangiectasia mutated and RAD3-related (ATR) signalling pathways may be important for KSHV infection efficiency, since abrogation of these signalling pathways improves KSHV infectivity. Curiously, abrogation of the ATM/ATR signalling pathways during KSHV reactivation impeded reactivation, suggesting a complex relationship between KSHV and the cellular DNA damage response. Finally, we have shown that KSHV is able to both inhibit, and induce the cellular DNA damage response, depending on the context, in response to DNA damaging agents, bringing another level of complexity to the relationship. Taken together, these data reveal a complex interaction between KSHV and the DNA damage response that requires further study to delineate the mechanism and understand the consequences for pathogenesis.

Acknowledgements

I would firstly like to thank my supervisors, Dr Roger Grand and Professor David Blackbourn for all of their help throughout the duration of this project. In addition, I would like to thank all the other members of the DNA damage and KSHV groups, for their support including Shaun Wilson, Paul Minshall, Laura Quinn, Simon Chanas, Rachel Wheat and Hannah Jeffery.

List of Contents

1. Introduction……..……53

1.1 Kaposi's Sarcoma-Associated Herpes Virus…….....54

1.2 Contribution of KSHV Viral Proteins to Oncogenesis…….……..54

1.3 The DNA Damage Response…….…….57

1.4 KSHV and the DNA Damage Response…….……60

1.5 Other Herpesviruses and the DNA Damage Response…….……..60

1.6 Aims…….……...63

2. Materials and Methods…….……..64

2.1 Tissue Culture Techniques…….…….65

2.1.1 Maintenance of Cell Lines…….…….65

2.1.2 Cell Culture…….66

2.1.3 Reactivation of VK219 Cell Line to Induce Lytic Replication/ Expansion Of VK219 Cells for KSHV Production……..66

2.1.4 Harvesting the Recombinant KSHV from VK219 Cells……67

2.1.5 Determination of KSHV Titre……67

2.1.6 KSHV Viral Infections……...……68

2.2 Cell Biology Techniques……...……68

2.2.1 Exposure of Adherent Cell Lines to UV radiation…….68

2.2.2 Exposure of Adherent Cell Lines to Irradiation…….. ……..68

2.2.3 Exposure of Adherent Cell Lines to Caffeine…….. ……..69

2.2.4 Flow Cytometry……..69

2.2.5 Fluorescence Microscopy…….....69

2.3 Protein Chemistry Techniques……...…….70

2.3.1 Harvesting Adherent Cells from Culture Dishes……70

2.3.2 Protein Determination of Cell Lysates…….....70

2.3.3 SDS-PAGE…….....71

2.3.4 Staining of Proteins on Nitrocellulose Membranes…….....71

2.4 Immunological Techniques…….....72

2.4.1 Western Blotting……...…….72

2.5 Statistical Techniques…….....73

2.5.1 Paired, Two-sided T-Test…….....73

3. Results…….....76

3.1 *De novo* KSHV Infection Activates Components of the DNA Damage Response……77

3.2 KSHV Reactivation of KSHV Lytic Replication Activates Components of the ATM and ATR DNA Damage Signalling Pathways……..80

3.3 Inhibition of ATM/ATR DNA Damage Signalling Pathways by Caffeine Treatment Increases KSHV Infectivity of Ad5E1HEK293 Cells……...82

3.4 Inhibition of the ATM/ATR DNA Damage Signalling Pathways by Caffeine Treatment Inhibits Reactivation of KSHV in Latently Infected Vero Cells……..86

3.5 Lytic KSHV Replication Inhibits the DNA Damage Response in Response to Ultra-Violet Radiation……...……89

3.6 Latent KSHV Infection Induces the DNA Damage Response in Response to Ionising Radiation…..…….....91

4. Discussion……93

4.1 Limitations……....……99

4.2 Future Work……...……99

5. References…….……100

List of Figures and Tables

Figure 1.1 The KSHV Episome…….....56

Figure 1.2 The DNA Damage Response Signalling Pathways…….……...59

Figure 1.3 Conserved Proteins in Both MHV68 and KSHV; an Indication that KSHV may be Involved with the DNA Damage Response…….……62

Table 2.1 Cell Lines Used in this Study……..65

Table 2.2 Primary Antibodies Used in this Study……...74

Table 2.3 Secondary Antibodies Used in this Study……...75

Figure 3.1 Validation of KSHV Infectivity in Ad5E1HEK293 Cells……..78

Figure 3.2 *De Novo* KSHV Infection Activates Components of the DNA Damage Response…….....….....79

Figure 3.3 KSHV Reactivation of Lytic Replication Activates Components of the DNA Damage Response……..……81

Figure 3.4 Inhibition of ATM/ATR DNA Damage Signalling Pathways by Caffeine Treatment Increases KSHV Infectivity in Ad5E1HEK293 Cells……84

Figure 3.5 Inhibition of the ATM.ATR DNA Damage Signalling Pathways By Caffeine Treatment Inhibits Reactivation of KSHV in VK219 Cells……...…….87

Figure 3.6 Lytic KSHV Replication Inhibits the DNA Damage Response in Response to Ultra-Violet Radiation……..……..90

Figure 3.7 Latent KSHV Infection Induces the DNA Damage Response in Response to Ionising Radiation……..92

Chapter One:

Introduction

1. Introduction

1.1 Kaposi's Sarcoma-Associated Herpesvirus

Kaposi's sarcoma-associated herpesvirus (KSHV), or human herpesvirus-8 (HHV-8), is a large double-stranded DNA rhadinovirus belonging to the gamma-herpesvirus subfamily (Mesri et al., 2010). Similarly to other herpesviruses, individuals infected with KSHV are life-long carriers, a result of KSHV's ability to successfully evade the host immune response (Coscoy, 2007). Thus, KSHV exists in one of two replicative phases, the first, known as latency, is a programme whereby viral gene expression is limited to a small number of genes and the production of infectious virions is prohibited. It is in this latent phase that the virus is effectively invisible to the host immune system. In response to certain stimuli, KSHV can become 'reactivated', or lytic, whereby a range of KSHV genes associated with viral replication are expressed, enabling the production of infectious virus particles. This process of reactivation is executed by the expression of the viral lytic switch gene, replication transactivation activator (RTA) (Miller et al., 1997). Like other members of the herpesvirus subfamily, the KSHV genome exists independently of the host genome in the infected cell in an episomal form (reviewed in Mesri et al., 2010). Originally identified in Kaposi's sarcoma (KS) lesions in 1994, KSHV is recognised as the aetiological agent of both KS and primary effusion lymphoma (PEL) (Cesarman et al., 1996; Chang et al., 2004; Bouvard et al., 2009). In addition, KSHV infection is also associated with the development of Multicentric Castleman's disease (Soulier et al., 1995).

1.2 Contribution of KSHV Proteins to Oncogenesis

A body of evidence suggests that expression of both latent and lytic KSHV proteins contributes to the oncogenic transformation of Kaposi's sarcoma cells during KSHV

infection. Latency-associated nuclear antigen (LANA), vCyclin, vFLIP, viral micro-RNAs and Kaposins A and B are expressed during the latent phase of KSHV infection, the expression of these genes is thought to contribute to the malignant phenotype of KS (Mesri et al., 2010) (Figure 1.1). Besides its role of maintaining the KSHV viral episome, LANA has a number of functions which are thought to contribute to the oncogenicity of KSHV, including the inhibition of p53, pRB-E2F and Wnt signalling pathways, subsequently interfering with apoptotic, transcriptional and proliferative programmes, respectively (Radkov et al., 2000; Fujimuro et al., 2003; Shin et al., 2005). In addition, LANA has been shown to target the anti-angiogenic protein VHL for proteasomal degradation and stimulate the expression of telomerase reverse transcriptase (TERT) (Verma et al., 2004; Cai et al., 2006). The expression of the KSHV latent viral protein vCyclin is thought to promote cell proliferation and, consequently, viral replication through its ability to activate cyclin-dependent kinase 6 (CDK6) (Godden-Kent et al., 1997). Expression of the latent viral protein vFLIP contributes to oncogenesis through interaction with, and activation of, nuclear factor-kappaB (NF-κB) (Liu et al., 2002). Activation of NF-κB leads to a number of downstream effects including the activation of cytokines and chemokines, whilst additionally having important roles in the control of apoptosis, such as the activation of the anti-apoptotic proteins B-cell lymphoma 2 (Bcl-2) and B-cell lymphoma extra large (Bcl-XL) (Guasparri et al., 2004; Sakakibara et al., 2009). Expression of the latent viral protein Kaposin A has been shown to have transforming capabilities in rodent cell lines, whilst the expression of Kaposin B indirectly increases levels of pro-inflammatory cytokines through its ability to activate MK2, a MAPK-associated protein which inhibits the degradation of mRNA which is rich in AU regions and to which a number of cytokines belong (Muralidhar et al., 1998; McCormick and Ganem., 2005).

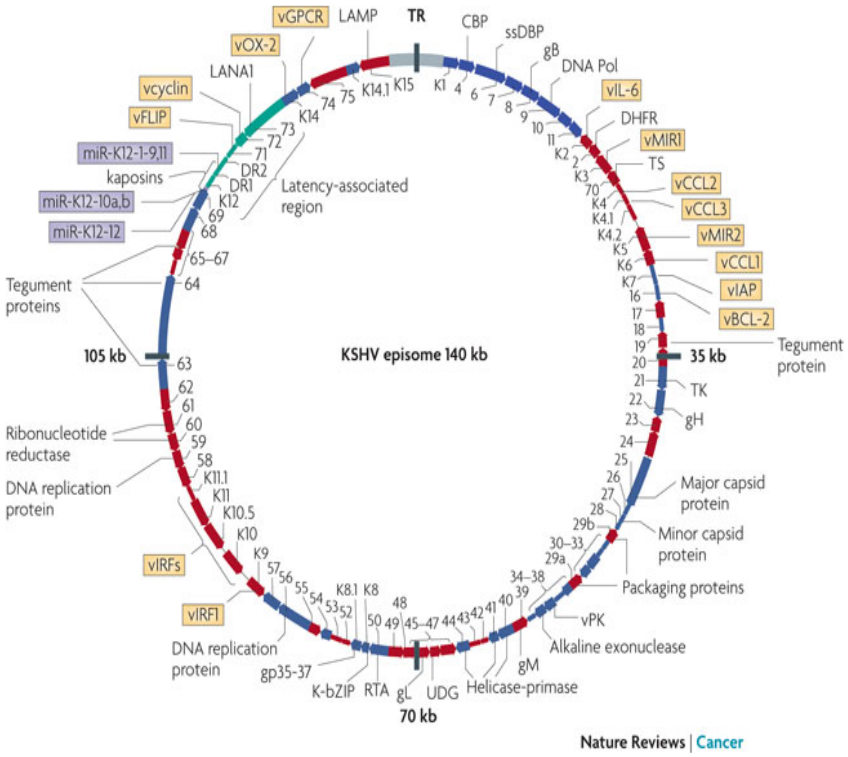

Figure 1.1: The KSHV Episome. Schematic showing the 140kb KSHV genome. The KSHV genome contains 87 open reading frames (ORFs) and approximately 17 microRNAs. Identified ORFs and the proteins they encode are indicated on the schematic, cellular orthologues are indicated in yellow, microRNAs are indicated in purple and latency-associated ORFs are indicated in green (reproduced from Mesri et al., 2010)

During lytic infection, a number of viral proteins are expressed which are thought to contribute to the oncogenicity of KSHV. These include vG-protein coupled receptor (vGPCR), vinterleukin-6 (vIL-6), vCC chemokine ligand (vCCL), vBcl-2, vinterferon regulatory factor (vIRFs) and K1 (Figure 1.1). vGPCR is able to induce a number of signalling cascades including the MAP kinase signalling pathway and the AKT/mTOR pathway. This results in the activation of multiple transcription factors including hypoxia-inducible factor-1α (HIF1α), NF-kB amongst others which in turn are able to induce the expression of pro-inflammatory cytokines and chemokines, and pro-angiogenic factors (reviewed in Jham and Montaner., 2010). The expression of the viral orthologs vIL-6 and vCCL promote angiogenesis in experimental systems, their expression is also thought to promote cell proliferation and survival (Boshoff et al., 1997; Aoki et al., 1999; Stine et al., 2000). Expression of vBCL-2 during KSHV infection leads to the inhibition of pro-apoptotic proteins and subsequently results in the inhibition of apoptosis. vIRF1 is able to inhibit apoptosis by inhibiting activation of p53 by ATM in response to DNA damage (Shin et al., 2005). Expression of the lytic viral K1 protein contributes to transformation through its ability to activate the Akt anti-apoptotic pathway and inhibit the Fas-mediated apoptotic pathway (Tomlinson and Damania., 2004; Berkova et al., 2009).

1.3 The DNA Damage Response

During the early stages of tumourigenesis, DNA damage pathways are frequently inactivated, circumventing apoptosis and inhibiting cellular proliferation. It is becoming increasingly apparent that, in order for viruses to effectively replicate their genomes, they must inactivate components of the DNA damage response pathway, probably contributing to oncogenic transformation by these viruses (Lilley et al., 2007). The two primary ‘sensors’ of the DNA

damage response are the ataxia-telangiectasia mutated (ATM) and ataxia telangiectasia and Rad3-related (ATR) kinases. ATM responds to double-stranded DNA breaks often occuring as a result of ionising radiation (IR) exposure and cellular stress, whilst ATR primarily responds to single-stranded lesions and collapsed replication forks (Khanna and Jackson., 2001).

In single-stranded lesions, ssDNA is bound by replication protein A (RPA) and this complex recruits ATR via ATR-interacting protein (ATRIP), to the site of damage (Zou and Elledge., 2003). The ssDNA-RPA complex recruits and subsequently activates the Rad17-replication factor C 2 (RFC2) clamp loader complex which causes the Rad9-Rad1-Hus1 complex to bind DNA (Yang and Zou., 2006). Topoisomerase II binding protein 1 (TOPBP1) then binds to ATRIP and the Rad9 component of the Rad9-Rad1-Hus1 complex which results in the activation of ATR (Kumagai et al., 2006). ATR is then able to phosphorylate a number of proteins involved in cell-cycle arrest and DNA repair including BRCA1, H2AX, BLM, Chk1 and p53 (Figure 1.2) (Zhou and Bartek., 2004).

Double-strand breaks are sensed by the Mre11-Rad50-Nbs1 (MRN) complex, which is able to activate ATM (Lee and Paul, 2005). ATM then phosphorylates H2AX, which recruits mediator of DNA damage checkpoint 1 (MDC1) to the site of DNA damage, resulting in the amplification of H2AX phosphorylation (Rogakou et al., 1998). Together, MDC1 and H2AX are able to recruit various DNA damage proteins to the site of the double-strand break including Chk2, BRCA1 and p53, which are subsequently phosphorylated by ATM, leading to cell-cycle arrest and DNA repair or, if the level of damage is too great, apoptosis (Figure 1.2) (Stucki and Jackson., 2006; reviewed in Cimprich and Cortez, 2008).

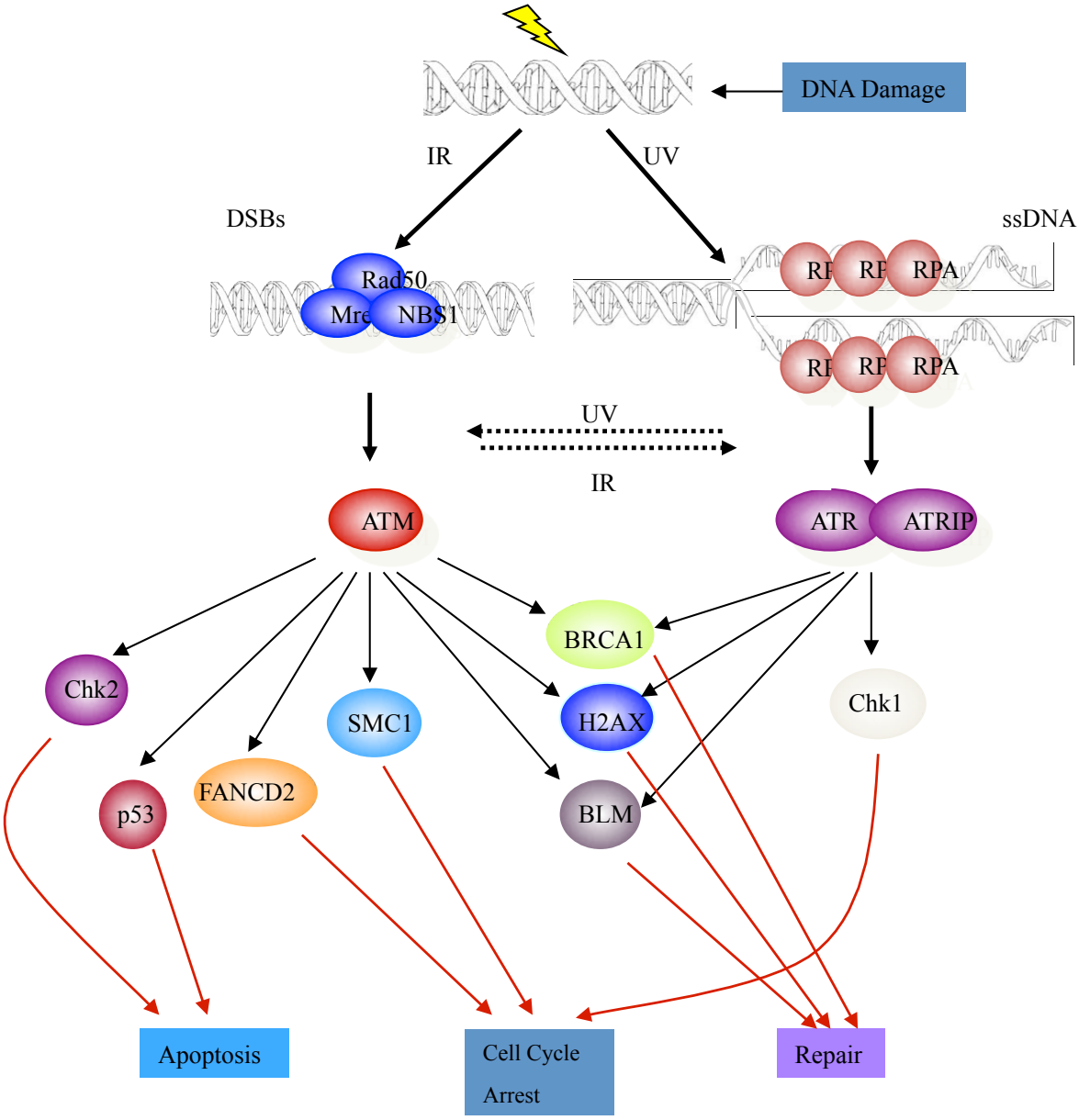

Figure 1.2: The DNA Damage Response Signalling Pathways. In response to single-strand breaks induced by IR (or collapsed replication forks), ssDNA is bound by RPA, which ultimately results in the association of ATRIP with ATR, leading to its activation. The activated ATR kinase is then able to phosphorylate and subsequently activate the DNA damage proteins indicated. The MRN complex is able to sense double-strand breaks induced by ionising radiation (or cellular stress). The MRN complex is then able to activate ATM, leading to the phosphorylation and subsequent activation of proteins involved in cell-cycle arrest, DNA repair and apoptosis. IR, ionising radiation; UV, ultra-violet radiation; DSBs, double-strand breaks; ssDNA, single-stranded DNA (Zhou and Bartek, 2004).

1.4 KSHV and the DNA Damage Response

Complex defence mechanisms limit the potential for oncogenic viruses to replicate effectively in the host; such mechanisms include the host interferon response and activation of host-cell apoptotic pathways (Weitzman et al., 2010). It is becoming increasingly apparent that, in addition to evading these defences, many viruses exploit, circumvent or 'hijack' components of the DNA damage repair pathway in order to effectively replicate their genomes. In the context of KSHV infection, little is understood regarding KSHV's involvement with the DNA damage response. A recent study from Shin et al demonstrated that carboxyl-terminal transactivation domain of KSHV vIRF is able to bind to, and inhibit, ATM activation. This study also showed that vIRF1 can inhibit the transcriptional activation activity of p53 by targeting p53 for proteasomal degradation. Taken together, vIRF1 is shown to inhibit the ATM/p53 signalling pathway, in order to avoid activation of the DNA damage pathway and subsequently promote viral replication (Shin et al., 2006). In another study, the immortalised endothelial cell line hTERT-HDMEC was transduced with a vCyclin retrovirus and the effect on the DNA damage proteins ATM, H2AX and Chk2 was examined. Interestingly, expression of vCyclin activated ATM, H2AX and Chk2, providing the first evidence to suggest that a KSHV viral protein is able to activate components of the DNA damage signalling pathway (Koopal et al., 2007).

1.5 Other Herpesviruses and the DNA Damage Response

γ-herpesvirus68 (MHV68) is a murine herpesvirus which is related to KSHV, encoding a number of conserved proteins such as vBcl-2, vCyclin, LANA and vGPCR (Figure 1.3) (reviewed in Barton et al., 2011). Interestingly, a number of studies demonstrate the involvement of the DNA damage response during MHV68 infection. MHV68 is able to

activate phosphorylation of H2AX via the expression of the viral protein, orf36, thereby activating the DNA damage response. Phosphorylation of H2AX appears to promote viral replication, since infection with mutant orf36 attenuated virus replication (mutated by transposon insertion in the kinase domain) (Tarakanova et al., 2007). These data are consistent with other reports that suggest the induction of the DNA damage response by MHV68 infection is important for effective viral replication. For example, treatment with the DNA damaging drug etoposide was shown to enhance MHV68 replication in B-cell lines (Forrest and Speck, 2008). Other members of the herpesvirus subfamily have also been associated with the cellular DNA damage response including herpes simplex virus 1 (HSV1), cytomegalovirus (CMV) and Epstein-Barr virus (EBV). HSV1 is able to activate the cellular DNA damage response; inducing the phosphorylation of RPA, NBS1, Chk2 and p53 (Wilkinson and Weller, 2004; Shirata et al., 2005). In addition, HSV1 proteins have been associated with the redistribution of DNA damage proteins including ATRIP away from viral replication centres. Conflicting with previous data suggesting RPA is activated in response to HSV1 infection, some data suggests that RPA is also redistributed away from viral replication centres (Wilkinson and Weller, 2006). CMV infection also activates the cellular DNA damage response; ATM, Chk2, p53 and H2AX become phosphorylated during CMV infection. In addition, during CMV infection some DNA damage proteins, including ATM, Chk2 and a number of proteins involved double-strand break repair are mislocalised away from viral replication centres (Gaspar and Shenk, 2005; Luo et al., 2007). Activation of DNA damage proteins has also been observed during EBV infection. One study demonstrated that EBV lytic replication activates components of the DNA damage pathway, namely ATM, Chk2, H2AX and p53 (Kudoh et al., 2005). Another recent publication demonstrated that, during initial infection of primary B-cells with EBV, H2AX and ATM become phosphorylated,

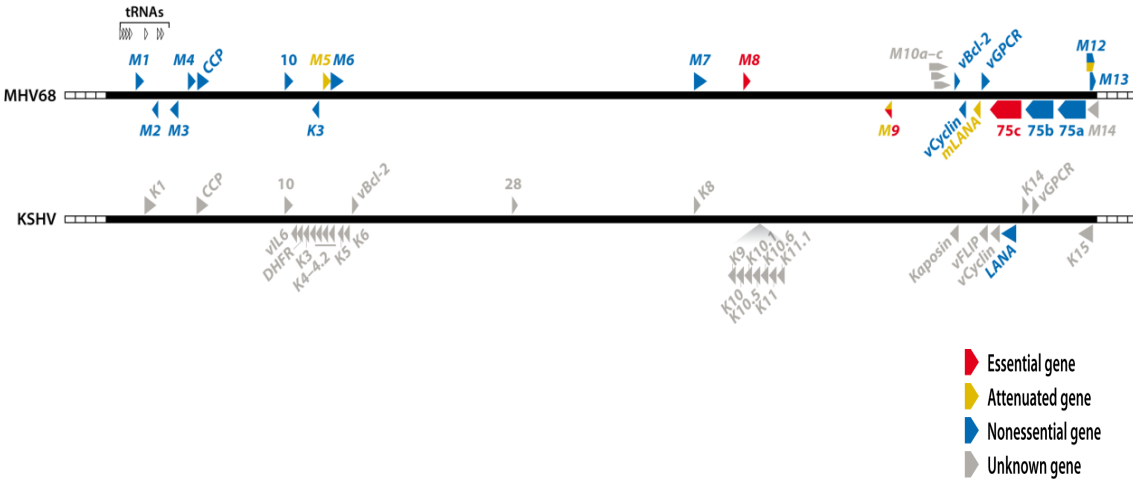

Figure 1.3: Conserved Proteins in both MHV68 and KSHV; an Indication that KSHV may be Involved with the DNA Damage Response. Schematic showing the genomes of KSHV and the closely related murine herpesvirus, MHV68. Note the conserved proteins, LANA, vCyclin, vGPCR and vBcl2, between the two viruses (modified from Barton et al., 2011).

whilst 53BP1 located to sites of DNA damage (Nikitin et al., 2010). The implications of these studies are discussed in Chapter 4.

1.6 Aims

It has become apparent that a number of herpesviruses, including KSHV, are able to interact with components of the cellular DNA damage response. At least in the context of KSHV, the details and consequences of these interactions are incompletely understood. Therefore, the principle aim of this study is to elucidate the relationship between KSHV infection and the cellular DNA damage response. In order to investigate this aim, the following objectives will be addressed:

1. Determine the effects of *de novo* KSHV infection on components of the cellular DNA damage response
2. Determine the effects of reactivation of KSHV lytic replication on components of the cellular DNA damage response
3. Determine whether KSHV uses the cellular DNA damage response during infection by examining the effect of abrogation of ATM/ATR DNA damage signalling pathways during
    a) *De novo* KSHV infection
    b) Reactivation of KSHV lytic replication
4. Determine the capacity of KSHV to modulate the DNA damage response to mutagenic treatments.

Chapter Two:

Materials and Methods

2. Materials and Methods

2.1 Tissue Culture Techniques

2.1.1 Maintenance of Cell Lines

Ad5E1HEK293 cells (Table 2.1) were maintained in Dulbecco's modified Eagle's medium (DMEM) (Sigma) supplemented with 10% foetal calf serum (FCS) (PAA Laboratories), 1.1% Penicillin-Streptomycin (Invitrogen) and 1.1% non-essential amino acids (NEAA) (Invitrogen). Both uninfected and infected Vero cells (Table 2.1) were maintained in MEM AQ medium (Sigma) containing 11.1% FCS, 1.1% NEAA, 0.002% Penicillin-Streptomycin and 5ug/ul puromycin (Sigma) (medium supplemented with puromycin for use with latently infected KSHV cells only). All cells lines were kept in a humidified 5% CO_2, 37°C incubator.

Table 2.1 Cell lines used in this study. The mammalian cell lines used throughout the duration of this project are indicated, as well as ATCC number and any additional information.

Cell Line	ATCC number	Information
Vero	CCL-81	Cell line from the kidney epithelial cells of the African green monkey
VK219	N/A	Vero cell line from the kidney epithelial cells of the African green monkey latently infected with a recombinant KSHV Virus (vKSHV.219) (Vieira and O'Hearn, 2004)
Ad5E1HEK293	CRL-1573	Human adenovirus serotype 5 transformed human embryo kidney cell line

2.1.2 Cell Culture

To passage cells, adherent cells were washed twice in 0.15M saline (Sigma) (pre-warmed to 37°C), subcultured using 5mls of 0.05% trypsin- ethylenediaminetetraacetic acid (EDTA) (Invitrogen) and stored in a 37°C incubator until all cells had lifted off of the dish/flask. Trypsin was then quenched by the addition of appropriate cell medium, which was then pooled into universal tubes and the cells pelleted by centrifugation at 1,200 revolutions per minute (rpm) for 5 minutes at room temperature. Cells were then resuspended in appropriate cell media to wash, and spun again at 1,200 rpm, for 5 minutes at room temperature. Pelleted cells were then resuspended in the appropriate cell medium and replated onto dishes/flasks at the required density.

2.1.3 Reactivation of VK219 Cell Line to Induce Lytic Replication / Expansion of VK219 Cells for KSHV Production

Prior to reactivation the following day, VK219 cells (Table 2.1) (a gift from J.Vieira) which constitutively expresses green fluorescence protein (GFP) under the control of elongation factor-1a (EF-1a) promoter and red fluorescence protein (RFP) under the control of a lytic PAN promoter (Vieira and O'Hearn, 2004), were plated at a density of 3 x 10^6 cells/flask in 10 T175 flasks in MEM AQ media (supplemented with 5µg/ml of puromycin) and incubated overnight. Cells were washed in 0.15M saline and stimulated with 2.27mls of reactivation mix containing 12.4mls of recombinant Baculovirus (Back50) (also a gift from J. Vieira), 12.4mls of MEM AQ medium supplemented with 10% FCS, 5.5% NEAA, 0.002% Penicillin-Streptomycin (no puromycin) and 309ul of 1M sodium butyrate (Sigma), in order to promote KSHV lytic replication. Cells were incubated at 37°C for 48 hours before harvesting KSHV, or alternatively as required.

2.1.4 Harvesting the Recombinant KSHV from VK219 cells

Following 48 hour incubation, supernatants were collected from the T175 flasks and centrifuged at 2,000 rpm, 4°C for 15 minutes. The supernatant was decanted into Beckman tubes and spun at 13,500 rpm at 4°C for 4 hours. Supernatant was then discarded, 50µl of EBM-2 medium (no supplements) (Clonetics) was added to the pellets, tubes were sealed with nescofilm and left at 4°C overnight. The next day, medium containing the virus was pooled into a 1.5ml microfuge tube and centrifuged at 4,000 rpm for 4 minutes at room temperature. Supernatant was transferred to a new microfuge tube and stored at 4°C until required.

2.1.5 Determination of KSHV Titre

The day before titration, Ad5E1HEK293 cells were seeded onto a 96-well plate at a density of 2 x 10^4 cells per well in Ad5E1HEK293 medium. Prior to infection, serial dilutions of recombinant KSHV were prepared, diluted in EBM-2 medium (no supplements) at 1/100, 1/500, 1/1000, 1/5000, 1/10000, 1/20000, 1/40000, 1/80000. Ad5E1HEK293 cells were infected with each dilution of virus in duplicate and spun at 1,200 rpm for 30 minutes. Following the spin, cells were incubated at 37°C for 90 minutes. After 90 minutes, inoculums were removed, cells were washed once in Ad5E1HEK293 medium and incubated at 37°C for 48hrs in Ad5E1HEK293 medium. After 48 hours, infected cells were counted, in duplicate, at a range of dilutions by visualisation of GFP expression by fluorescence microscopy. Following the cell counts, average infectious units (IU) per ml were calculated using the following formula:

Virus titre (IU/ml): average number of GFP-positive cells x dilution factor x 10

2.1.6 KSHV Viral Infections

The day before infection, Ad5E1HEK293 cells were seeded into 6-well plates at a density of 6 x 10^5 cells per well. On the day of infection, culture medium was removed and the cells were washed in 0.15M saline. Cells were infected with recombinant KSHV (vKSHV.219) virus at an multiplicity of infection (MOI) of 1, diluted in EBM-2 media (no supplements). Following addition of inoculums to the cells, cells were centrifuged at 1,200 rpm for 30 minutes at room temperature. Following the spin, cells were incubated for 90 minutes at 37°C. Inoculums were then removed and replaced with culture medium, and cells were incubated at 37°C until required.

2.2 Cell Biology Techniques

2.2.1 Exposure of Adherent Cell Lines to ultra-violet (UV) radiation

Adherent cell lines were removed of cell medium which was left to incubate at 37°C whilst the cells were being treated. Cells grown in 6cm dishes were exposed to $20JM^{-2}$ of UV radiation to induce single-strand DNA breaks (lids of the tissue culture dishes were removed before exposure), medium heated to 37°C was returned and cells were left to incubate at 37°C in a humidified incubator until required.

2.2.2 Exposure of Adherent Cell Lines to Ionising Radiation (IR)

In order to induce double-stranded DNA breaks, adherent cell lines were exposed to 5 Grays of IR using a CS-137 irradiator (model CIS IBL 437). Following IR, cells were incubated at 37°C in a humidified incubator until required.

2.2.3 Exposure of Adherent Cell Lines to Caffeine

In order to inhibit the ATM/ATR kinases, 5mM of caffeine (Cal Biochem) was added to cell medium in sterile conditions and exposed cells were left to incubate at 37°C in a humidified incubator until required.

2.2.4 Flow Cytometry

Ad5E1HEK293 cells infected with vKSHV.219 were assessed for infectivity levels by measuring the percentage GFP expression using flow cytometry. Adherent Ad5E1HEK293 cells were treated with 0.05% trypsin-EDTA for 3 minutes in a 37°C incubator or alternatively until all cells had come off the plate. Trypsin was then quenched by adding Ad5E1HEK293 medium to the cells. Cells were then centrifuged at 1,200 rpm for 5 minutes at room temperature. Following the spin, cells were resuspended in phospho-buffered saline (PBS) (Oxoid) and centrifuged once more. Following centrifugation, cells were fixed in 1% paraformaldehyde (PFA) (Fisher Scientific) in PBS, and GFP expression was quantified using a Coulter XL-MCL flow cytometer (Beckman-Coulter).

2.2.5 Fluorescence Microscopy

Visualisation of GFP and red RFP expression of VK219 and Ad5E1HEK293 infected cells was achieved using a Nikon eclipse E600 microscope and images processed using image-pro express software.

2.3 Protein Chemistry Techniques

2.3.1 Harvesting Adherent Cells from Culture Dishes

Adherent cells grown on tissue culture flasks/dishes were harvested by one of two methods. Firstly, adherent cells were washed twice in 0.15M ice-cold saline, in the second wash, cells were removed from the tissue culture flask/dish with a cell scraper and pelleted at 1,200 rpm, 4ºC for 5 minutes. Cells were resuspended in ice-cold 0.15M saline, pelleted again, any residual saline was removed and cells were resuspended in 400µl of Urea-Tris-β-mercaptoethanol (UTB) lysis buffer containing 9M urea (Sigma), 150mM β-mercaptoethanol (Sigma) and 50mM Tris (Melford)/HCl pH 7.5 (Fisher Scientific), and pooled into 1.5ml microfuge tubes. Cell lysates were then sonicated twice for 10 seconds each time, centrifuged at 13,000rpm for 15 minutes to clear the lysate and the protein concentrations determined (Section 2.3.2).

Alternatively, adherent cells were harvested by trypsinising with 0.05% trypsin-EDTA for 3 minutes in a 37ºC incubator. After cells had lifted off the tissue culture dish/flask, trypsin was inactivated by the addition of appropriate cell media. Cells were pelleted at 1,200 rpm for 5 minutes, resuspended in 0.15M saline to wash and centrifuged again at 1,200 rpm for 5 minutes. Supernatant was removed and cells were resuspended in 400µl of UTB and transferred to 1.5ml microfuge tubes. Cells were sonicated and cleared as before.

2.3.2 Protein Determination of Cell Lysates

Protein concentrations of cell lysates were determined against a standard curve produced using known concentrations of bovine serum albumin (BSA) (Sigma). 5µl of cell lysate was diluted in 45µl of sterile distilled water, and 10µl of diluted cell lysate was added to one well

of a 96-well plate, repeated in quadruplet. 200µl of Bio-Rad Protein Reagent (Bio-Rad Laboratories) diluted 1:5 in sterile distilled water was added to each well and protein concentrations were read on a microplate reader (Bio-Rad model 680) at 595nm wavelength.

2.3.3 Sodium Dodecyl Sulphate-Polyacrylamide Gel Electrophoresis (SDS-PAGE)

20-50µl of cell lysate diluted in an equal volume of Laemmli sample buffer (25% v/v glycerol (BDH Laboratories), 5% β-mercaptoethanol, 2% w/v SDS (Severn Biotech), 0.01% w/v bromophenol blue (BDH Laboratories) and 65mM Tris (pH 6.8)). Samples were boiled at 80ºC for 5 minutes, spun at 13,000 rpm for 1 minute and loaded, along with a molecular weight marker onto 6-12% polyacrylamide gels (30% w/v acrylamide (37:5:1 BIS-acrylamide) (Severn Biotech), 0.1% SDS, 0.1M Tris/ 0.1M Bicine (Melford) (pH 8.3), 0.6% ammonium persulphate (APS) (Sigma) and 0.3% N,N,N',N',-Tetramethylethylthylenediamine (TEMED) (Severn Biotech)). SDS-PAGE gels were run between 10-25mA, either overnight or through the day.

2.3.4 Staining of Proteins on Nitrocellulose Membranes

In order to visualise proteins transferred onto nitrocellulose membranes, membranes were stained with Ponceau-S stain containing 3% trichloroacetic acid (TCA) (BDH Laboratories) and 0.1% Ponceau-S (Sigma) for 30 seconds. Membranes were then washed in distilled water to remove residual Ponceau-S stain. Following visualisation of proteins, nitrocellulose membranes were washed in Tris-Buffered Saline Tween-80 (TBST) containing 0.15M NaCl (Sigma), 50mM Tris, 1% Tween-80 (Sigma) and HCl pH 7.4), until all Ponceau-S stain was removed from the membrane.

2.4 Immunological Techniques

2.4.1 Western Blotting

Proteins separated by SDS-PAGE were transferred onto nitrocellulose membranes using the following method. SDS-PAGE gels were inserted into a transfer cassette containing a sponge, one piece of Whatmann blotting paper, nitrocellulose membrane (Pall corporation), the SDS-PAGE gel, another piece of Whatmann blotting paper and another sponge (all components within the transfer cassette were pre-immersed in transfer buffer). Transfer cassettes were placed in a transfer tank filled with pre-chilled transfer buffer (20% v/v methanol (Sigma), 0.19M glycine (Melford) and 0.05M Tris), and left transferring at 200mA overnight (18 hours). Following the transfer, nitrocellulose membranes were stained in Ponceau-S stain to visualise transferred proteins and assess for equal loading amongst the samples (Section 2.3.4). Nitrocellulose membranes were then washed in TBST to remove the Ponceau-S stain and subsequently incubated in 5% w/v skimmed milk (Marvel) diluted in TBST or 5% w/v BSA (Sigma) in TBST for 30 minutes to block non-specific antibody binding to the nitrocellulose membrane. Primary antibodies (Table 2.2) were incubated with the nitrocellulose membrane by heat sealing in polythene bags, and left on a rocker at 4ºC overnight. Following overnight incubation, nitrocellulose membranes were washed in TBST 6 times for 5 minutes each time. Nitrocellulose membranes were then incubated with the appropriate secondary antibody (Table 2.3) diluted in 5% w/v dried skimmed milk or 5% w/v BSA, and left on a rocker at room temperature for 2 hours. After 2 hours, nitrocellulose membranes were washed again in TBST, 6 times for 5 minutes each time. Nitrocellulose membranes were then incubated in enhanced chemiluminescence (ECL) (Millipore) for 1 minute, sealed in saran wrap and exposed to autoradiography film (Kodak) to allow

visualisation of appropriate proteins. Typical exposure times varied from 10 seconds to 2 hours.

2.5 Statistical Techniques

2.5.1 Paired, Two-Sided T-Test

Two-sided, paired T-tests were conducted in order to determine whether the mean difference between two groups (typically treated against control samples) were statistically significant. All t-tests were performed at the 95% confidence interval, i.e. a p-value of 0.05 using GraphPad Prism software.

Table 2.2: Primary antibodies used throughout the duration of this study. The primary antibodies used throughout the duration of this study are indicated, as well as the antigen they target, dilution used, molecular weight, application, species and source.

Antibody	Antigen	Dilution	Size (kDa)	Use	Species	Company/Source
ATM	ATM	1 in 500	350	WB	Mouse	Oncogene Research Products
β-Actin	β-Actin	1 in 10000	45	WB	Mouse	Sigma
Chk1	Chk1	1 in 1000	56	WB	Mouse	Santa Cruz
Chk2	Chk2	1 in 5000	62	WB	Rabbit	Professor Steve Elledge
Histone H3 (H2AX)	H2AX	1 in 1000	15	WB	Rabbit	Cell Signaling
KCP	KCP	1 in 1000	60	WB	Mouse	In house
LANA1	LANA1	1 in 500	222	WB	Mouse	Novacastra
LANA1	LANA1	1 in 1000	222	WB	Rat	Advanced Biotechnologies
NBS1	NBS1	1 in 1000	95	WB	Mouse	Abcam
p-ATM	Phospho-ATM	1 in 1000	350	WB	Rabbit	R&D Systems
p-Chk1	Phospho-Chk1	1 in 1000	56	WB	Rabbit	Bethyl
γH2AX	γH2AX	1 in 1000	15	WB	Mouse	Millipore
p-NBS1	Phospho-NBS1	1 in 500	95	WB	Rabbit	SAB
p-RPA32	Phospho-RPA32	1 in 1000	32	WB	Rabbit	Bethyl
p53	p53	1 in 100	53	WB	Mouse	Professor David Lane
RPA32	RPA32	1 in 1000	32	WB	Rabbit	Abcam

Table 2.3: Secondary antibodies used in this study. The secondary antibodies used in this study are indicated, as well as the antigen they target, dilution used, species and source.

Antibody	**Antigen**	**Dilution**	**Use**	**Species**	**Company/Source**
Mouse	Mouse	1 in 2000	WB	Goat	Dako Laboratories
Rabbit	Rabbit	1 in 3000	WB	Swine	Dako Laboratories
Rat	Rat	1 in 1000	WB	Rabbit	Dako Laboratories

Chapter Three:

Results

3.1 *De novo* KSHV Infection Activates Components of the DNA Damage Response

In order to determine the effects of *de novo* KSHV infection on components of the DNA damage response, Ad5E1HEK293 cells were infected with a recombinant KSHV, vKSHV.219, which constitutively expresses GFP under the control of a EF-1a promoter and RFP under the control of a lytic PAN promoter (Vieira and O'Hearn, 2004). Ad5E1HEK293 cells were infected with vKSHV.219 and since infected and lytically replicating cells express GFP and RFP respectively, infection and reactivation was confirmed by fluorescence microscopy. Ad5E1HEK293 cells were analysed for GFP and RFP expression by fluorescence microscopy at 0, 8, 24, 48, 72 and 96 hours post-infection, with uninfected control Ad5E1HEK293 cells in parallel. Microscopy images showed Ad5E1HEK293 cells were latently infected with vKSHV.219 as early as 8 hours post-infection, with a small number of infected cells undergoing lytic replication by 24 hours post-infection (Figure 3.1A).

In addition to visualisation of KSHV infection by fluorescence microscopy, the percentage of infected Ad5E1HEK293 cells was quantified by flow cytometry. Approximately 100,000 cells were harvested, fixed and analysed for GFP expression. Figure 3.1B shows a typical GFP expression pattern following recombinant KSHV infection. At 8 hours post-infection, approximately 37% of live Ad5E1HEK293 cells were latently infected with KSHV, by 24 hours post-infection, approximately 81% of live Ad5E1HEK293 cells were latently infected with vKSHV.219 virus. Following 48, 72 and 96 hours post-infection, the percentage of Ad5E1HEK293 cells latently infected with KSHV gradually decreased to 49%, 39% and

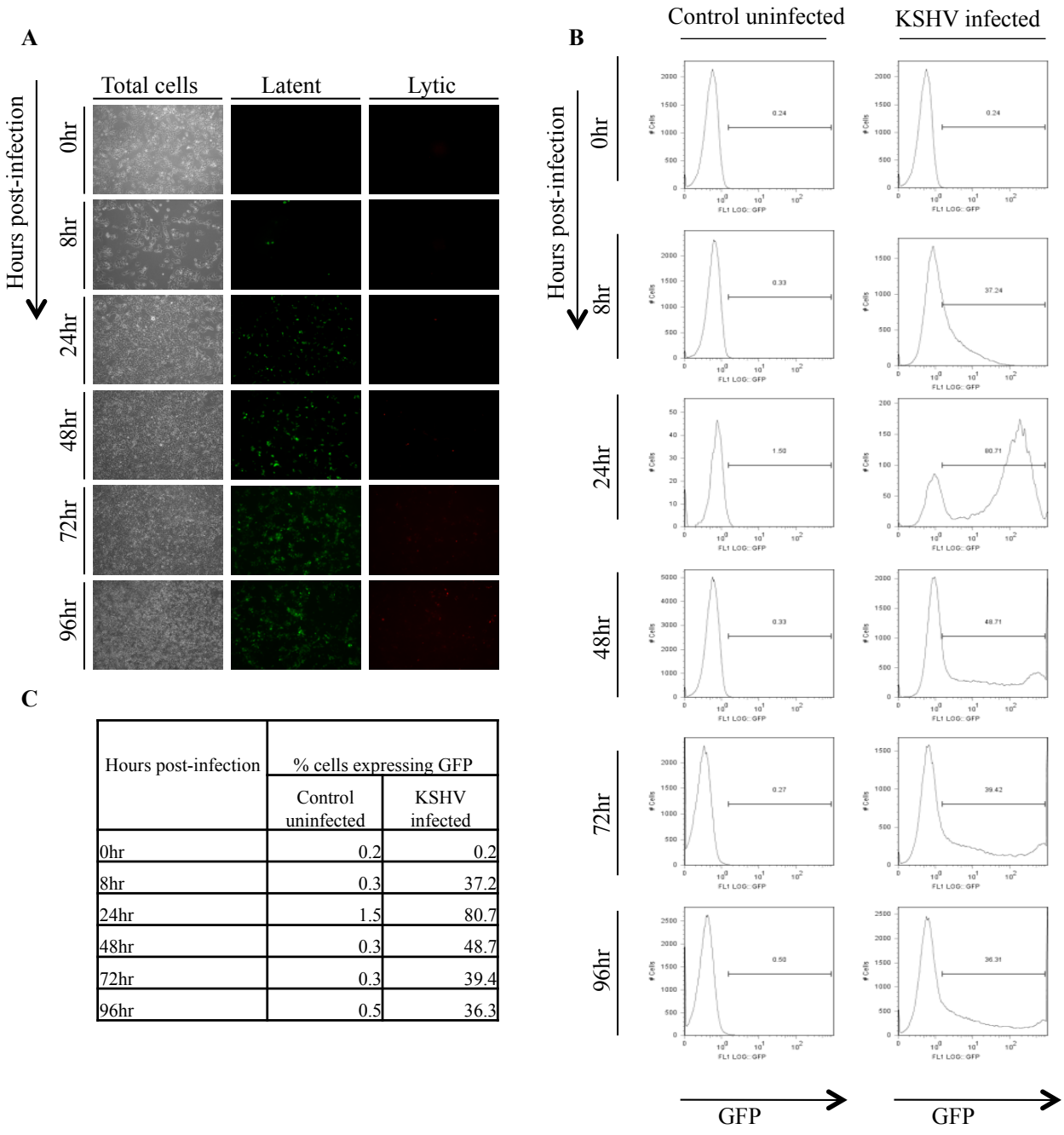

C

Hours post-infection	% cells expressing GFP	
	Control uninfected	KSHV infected
0hr	0.2	0.2
8hr	0.3	37.2
24hr	1.5	80.7
48hr	0.3	48.7
72hr	0.3	39.4
96hr	0.5	36.3

Figure 3.1: Validation of KSHV Infectivity in Ad5E1HEK293 Cells. Ad5E1HEK293 cells were infected with a recombinant KSHV (vKSHV.219) that expresses GFP under the control of a constitutively active promoter, and RFP under the control of a KSHV lytic promoter. **A.** Following 0, 8, 24, 48, 72 and 96 hours post-KSHV infection, cells were examined by fluorescence microscopy to confirm both latent (GFP) and lytic (RFP) infection. **B.** Quantification of KSHV infectivity was achieved by flow cytometry to measure the percentage of cells expressing GFP in infected Ad5E1HEK293 cells against uninfected controls. **C.** The percentage of infected Ad5E1HEK293 cells expressing GFP against uninfected controls are indicated. These data are representative of one experiment performed twice.

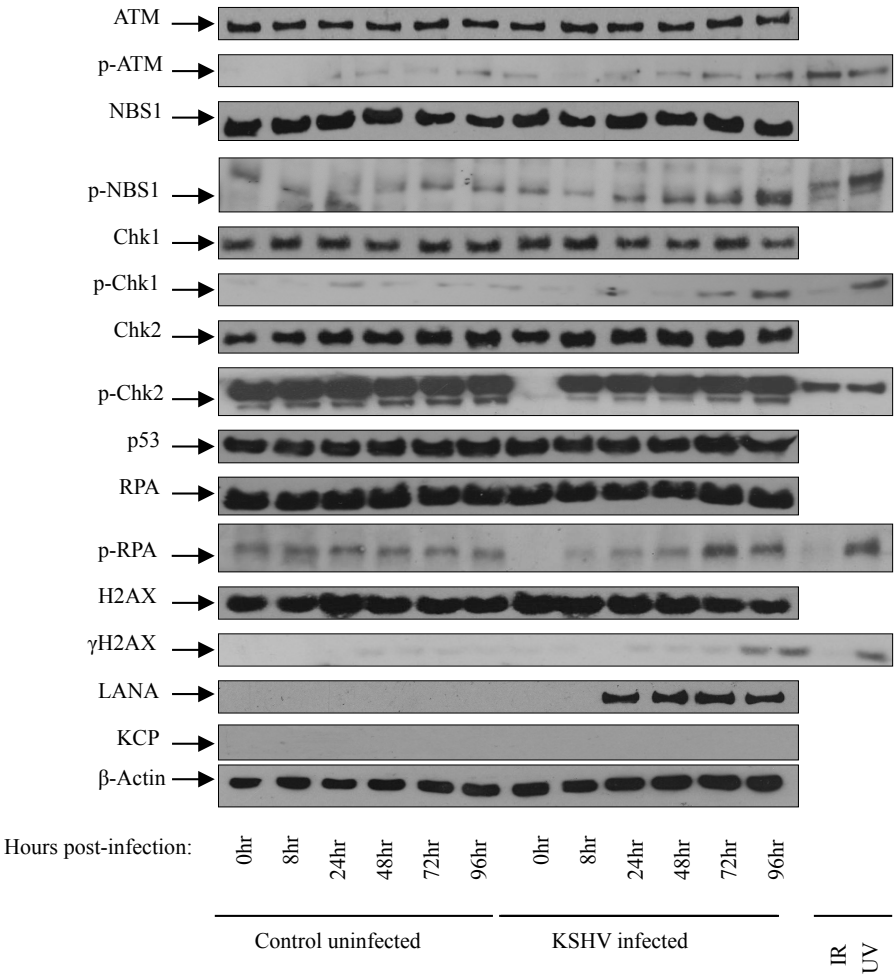

Figure 3.2: *De novo* KSHV Infection Activates Components of the DNA Damage Response. Ad5E1HEK293 cells were infected with a recombinant KSHV (vKSHV.219) and harvested at 0, 8, 24, 48, 72 and 96 hours post-infection with uninfected control cells in parallel. Lysates were subjected to Western blotting for a number of representative DNA damage response proteins, KSHV latent (LANA) and lytic (KCP) proteins as controls, and β-Actin used as a loading control. UV and IR treated samples were included as a control to verify phospho-antibodies were working. These data are representative of one experiment performed twice.

36%, respectively, probably due to the proliferation of uninfected cells (Figure 3.1B and 3.1C).

Infected Ad5E1HEK293 cells, along with uninfected controls, were harvested at 0, 8, 24, 48, 72 and 96 hours post-infection and lysates were subjected to Western blotting for a number of representative DNA damage response proteins. In addition, KSHV latent (LANA) and lytic (KCP) proteins were immuno-blotted as controls, and β-Actin used as a loading control. IR and UV samples were loaded to verify that the phospho-antibodies were working. The latent KSHV protein LANA was detected at 24 hours post-infection, confirming previous microscopy and flow cytometry data demonstrating successful infection (Figure 3.1). The lytic KSHV protein KCP remained undetected throughout the course of KSHV infection (Figure 3.2), probably owing to the fact that only a small number of infected cells were undergoing lytic replication (Figure 3.1A). Total protein levels of the DNA damage proteins ATM, NBS1, Chk1, Chk2, p53, RPA, H2AX remained unchanged throughout the course of KSHV infection when compared to uninfected controls (Figure 3.2). Phosphorylation of Chk2 remained unchanged when compared to uninfected control samples. Phosphorylation of ATM, NBS1, Chk1, RPA and H2AX increased in the later stages of KSHV infection, suggesting the infected cells respond to KSHV infection by activation of the DNA damage response (Figure 3.2).

3.2 KSHV Reactivation of Lytic KSHV Replication Activates Components of the ATM and ATR DNA Damage Signalling Pathways

In order to assess the effect of reactivation of KSHV lytic replication on components of the DNA damage response, we used the VK219 cell line, latently infected with vKSHV.219

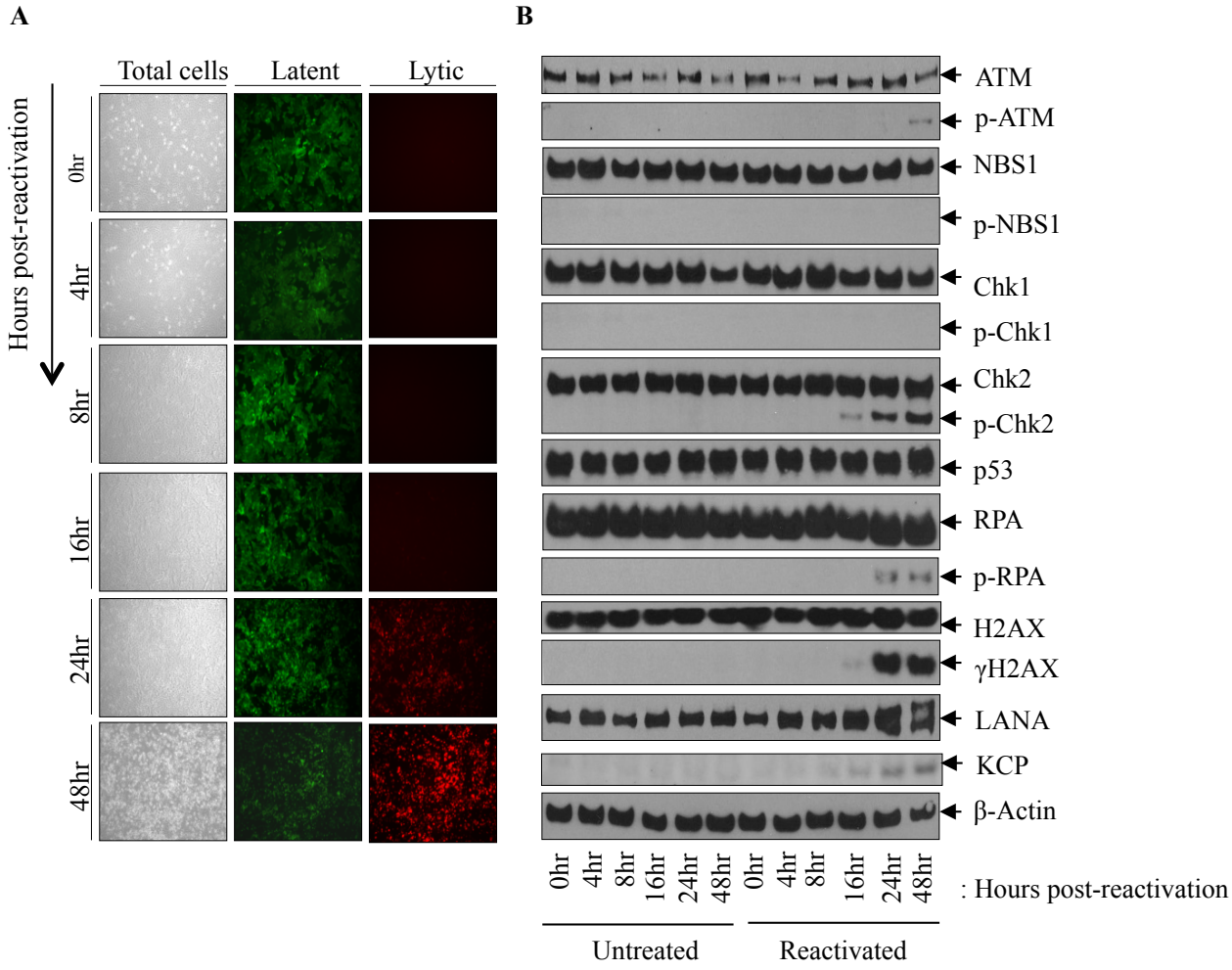

Figure 3.3 KSHV Reactivation of Lytic Replication Activates Components of the DNA Damage Response. VK219 cells latently infected with vKSHV.219 virus were reactivated using a baculovirus which expresses the KSHV lytic switch protein RTA. **A.** Reactivated cells, and unreactivated controls were analysed by fluorescence microscopy at 0, 4, 8, 16, 24 and 48 hours post-reactivation to assess levels of reactivation. **B.** Both reactivated and unreactivated control cells were harvested at 0, 4, 8, 16, 24 and 48 hours post-reactivation and analysed by Western blotting for a panel of representative DNA damage response proteins, KSHV latent (LANA) and lytic (KCP) proteins as controls, and β-Actin used as a loading control. These data are representative of one experiment repeated 3 times independently.

virus. Using Back50 which expresses the lytic switch protein RTA under the control of a HCMV promoter, we induced lytic KSHV replication in these cells, which was assessed by observing RFP expression by fluorescence microscopy. A small number of infected cells were lytically replicating after approximately 16 hours post-reactivation, and, by 48 hours, approximately 100% of infected cells had become lytic (Figure 3.3A). Reactivated cells, with untreated controls in parallel, were harvested at 0, 4, 8, 16, 24 and 48 hours post-reactivation and subjected to Western blotting for a panel of DNA damage proteins along with KSHV latent (LANA) and lytic (KCP) proteins as controls, and β-Actin as a loading control. LANA was detected in all untreated and reactivated samples, confirming the cells were latently infected with KSHV. Protein levels of KCP increased at approximately 16 hours post-reactivation, showing successful reactivation of latently infected Vero cells. Total protein levels of the DNA damage response proteins ATM, NBS1, Chk1, Chk2, p53, RPA and H2AX remained unchanged during reactivation into the lytic KSHV phase. No phosphorylated NBS1 or Chk1 was detected throughout the course of infection (immuno-blotted at the same time as results obtained in Figure 3.2 so antibodies were confirmed as working). Levels of p-ATM, p-Chk2, p-RPA and γH2AX increased during reactivation, suggesting that the lytic phase causes host cells to activate components of both the ATM and ATR DNA damage signalling pathways (Figure 3.3B).

3.3 Inhibition of ATM/ATR DNA Damage Signalling Pathways by Caffeine Treatment Increases KSHV Infectivity of Ad5E1HEK293 Cells.

In order to assess whether the ATM/ATR DNA damage signalling pathways are required for KSHV infectivity, Ad5E1HEK293 cells were infected vKSHV.219 virus and inoculated Ad5E1HEK293 cells were treated with caffeine, a broad-range ATM/ATR kinase inhibitor

(Sarkaria et al., 1999). Infection was confirmed by visualisation of GFP by fluorescence microscopy (data not shown), and the extent of infection was quantified by measuring GFP expression by flow cytometry. Cells were analysed at 0, 8, 24, 48, 72 and 96 hours post-infection, with inoculated, untreated Ad5E1HEK293 cells as controls in parallel. At 0 hours post-infection, 0.3% of infected control cells (not treated with caffeine) expressed GFP, and 0.4% of infected caffeine-treated cells were expressing GFP, which was accepted as background fluorescence. At 8 hours post-infection, infected cells treated with caffeine were 28.6% GFP positive, compared with 20.8% in infected, untreated controls. At 24 hours post-infection, 62.0% of caffeine-treated infected cells were GFP positive, compared to 51.2% GFP positive in untreated control cells. A comparable difference in GFP expression was observed at 48, 72 and 96 hours post-infection (Figure 3.4A, B and C).

In addition, caffeine-treated KSHV infected cells, along with untreated, infected controls were harvested 0, 8, 24, 48, 72 and 96 hours post-infection/treatment and subjected to Western blotting for γH2AX to assess efficiency of ATM/ATR inhibition, and β-Actin as a loading control. A decrease in γH2AX was observed 96 hours post-infection in cells treated with caffeine when compared to untreated controls, suggesting ATM/ATR pathways had been compromised (Figure 3.4D). To assess whether these results were reproducible, and whether the percentage difference in GFP expression observed between caffeine treated and untreated infected cells were statistically significant, the experiment was repeated twice more, results pooled and two-sided paired t-tests conducted. Similar percentage changes in GFP expression were observed between 8, 24, 48, 72 and 96 hours post-infection/treatment, with those cells treated with caffeine having approximately 10% or more GFP expression was observed compared to untreated controls. Statistically significant differences at the 95% confidence

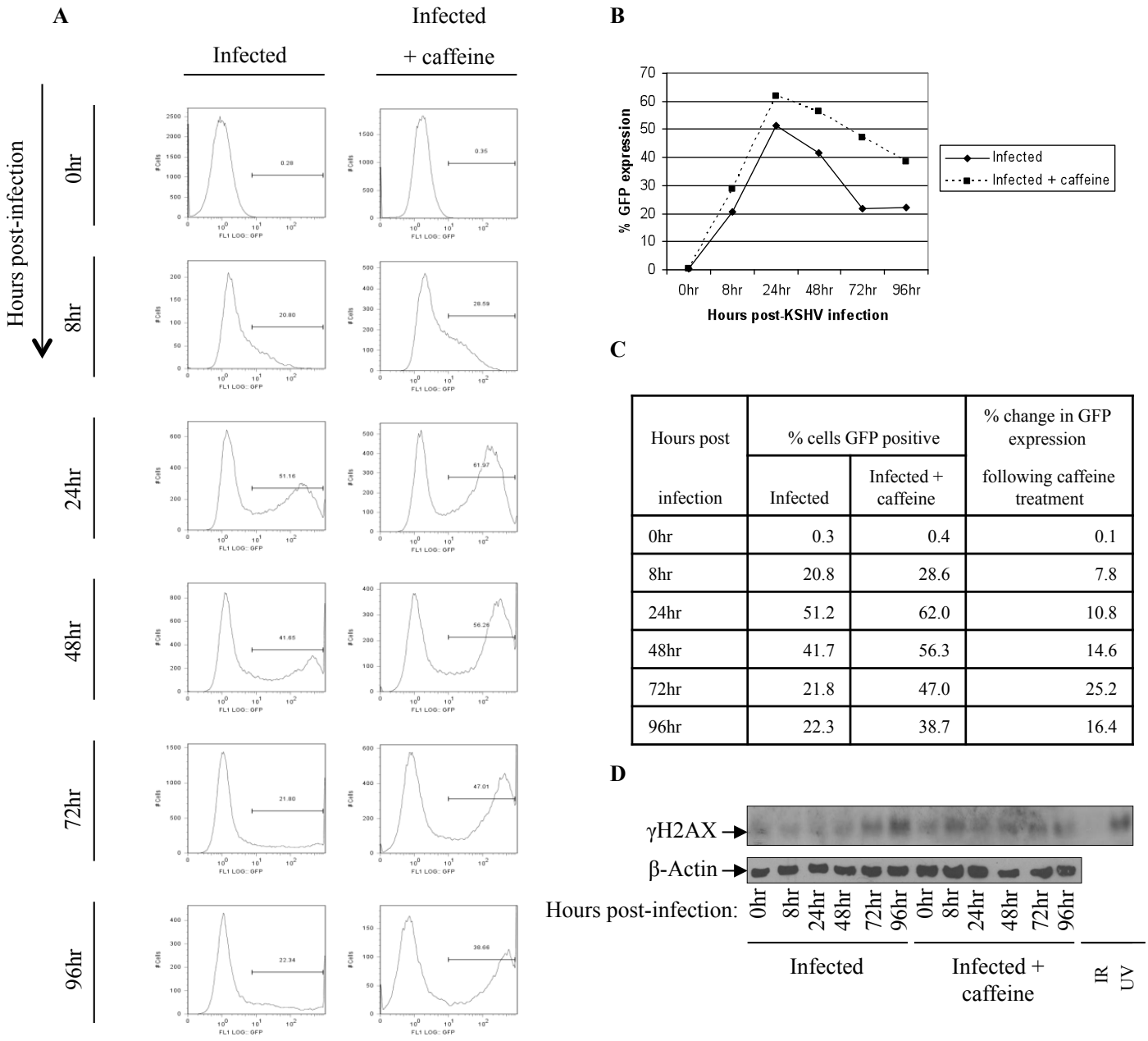

Hours post infection	% cells GFP positive		% change in GFP expression following caffeine treatment
	Infected	Infected + caffeine	
0hr	0.3	0.4	0.1
8hr	20.8	28.6	7.8
24hr	51.2	62.0	10.8
48hr	41.7	56.3	14.6
72hr	21.8	47.0	25.2
96hr	22.3	38.7	16.4

Figure 3.4: Inhibition of ATM/ATR DNA Damage Signalling Pathways by Caffeine Treatment Increases KSHV Infectivity in Ad5E1HEK293 Cells. Ad5E1HEK293 cells were infected with vKSHV.291 virus and treated with the ATM/ATR inhibitor caffeine. **A.** At 0, 8, 24, 48, 72 and 96 hours post-infection/treatment, cells were harvested and subjected to flow cytometric analysis to determine the percentage of GFP expressing (i.e. percentage of KSHV infected) cells. **B.** The percentage of caffeine-treated, infected cells expressing GFP compared to untreated, infected controls. **C.** The percentage change in GFP expression of caffeine-treated, infected cells expressing GFP against untreated, infected controls. **D.** Caffeine-treated, infected cells were harvested, along with untreated infected cells at 0, 8, 24, 48, 72 and 96 hours post-infection and analysed by Western blotting for γH2AX to assess efficiency of ATM/ATR inhibition and β-actin as a loading control. These data represent one experiment repeated twice.

E

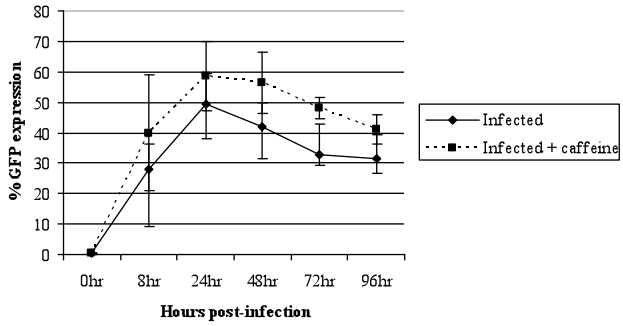

F

Hours post-infection	Caffeine	Mean % GFP expression	SD	SEM	df	P value	t value	Statistical significance?
0hr	-	0.3	0.0	0.0				
	+	0.4	0.1	0.1	2	0.2403	1.6521	No
8hr	-	28.1	8.3	4.8				
	+	40.0	18.9	10.9	2	0.2106	1.8183	No
24hr	-	49.5	10.0	5.7				
	+	58.4	11.3	6.5	2	0.0156	7.9044	Yes
48hr	-	41.8	7.8	4.5				
	+	56.4	10.2	5.9	2	0.0085	10.808	Yes
72hr	-	33.0	9.7	5.6				
	+	48.1	3.6	2.1	2	0.1046	2.8435	No
96hr	-	31.5	7.9	4.6				
	+	41.1	4.9	2.8	2	0.1401	2.3828	No

Figure 3.4 Continued: Inhibition of ATM/ATR DNA Damage Signalling Pathways by Caffeine Treatment Increases KSHV Infectivity in Ad5E1HEK293 Cells. Ad5E1HEK293 cells were infected vKSHV.219 virus and treated with the ATM/ATR inhibitor caffeine. At 0, 8, 24, 48, 72 and 96 hours post-infection, cells were harvested and subjected to flow cytometric analysis to determine the percentage of GFP expressing, i.e. percentage of KSHV infected cells. **E.** The experiment was repeated three times to confirm the results shown were reproducible. Error bars shown represent standard deviation. **F.** Statistical analysis of the change in percentage GFP expression between KSHV-infected cells treated with caffeine against untreated controls.

interval were observed at 24 hours and 48 hours post-infection/treatment (Figure 3.4E and 3.4F).

3.4 Inhibition of the ATM/ATR DNA Damage Signalling Pathways by Caffeine Treatment Inhibits Reactivation of KSHV in Latently Infected Vero Cells.

In order to determine whether the ATM/ATR DNA damage signalling pathways are important during reactivation of KSHV lytic replication, VK219 cells were reactivated by treating with Back50. Following treatment with Back50, cells were treated with caffeine to inhibit the ATM/ATR kinases. Caffeine-treated KSHV infected cells, with untreated, reactivated controls in parallel, were harvested at 0, 4, 8, 16, 24 and 48 hours post-reactivation/treatment and subjected to Western blotting for γH2AX to assess efficiency of ATM/ATR inhibition, and β-Actin as a loading control. A decrease in γH2AX was observed from 16 hours post-reactivation in cells treated with caffeine when compared to untreated controls, suggesting ATM/ATR pathways have been compromised (Figure 3.5A).

Following reactivation and caffeine treatment, infected Vero cells were analysed for evidence of lytic KSHV replication, with reactivated, untreated control cells in parallel, by observing RFP expression by fluorescence microscopy. Analysis of microscopy images showed cells that were treated with caffeine exhibited less RFP expression, suggesting lower levels of reactivation (Figure 3.5B). In order to confirm this observation quantitatively, 10 fields of cells were counted at 0, 4, 8, 16, 24 and 48 hours post-reactivation and caffeine treatment, with untreated, reactivated infected cells in parallel as controls. The number of GFP and RFP positive cells in each field was counted and the percentage of reactivated cells calculated. No reactivated cells were observed at 0, 4 and 8 hours post-reactivation, in either the control or

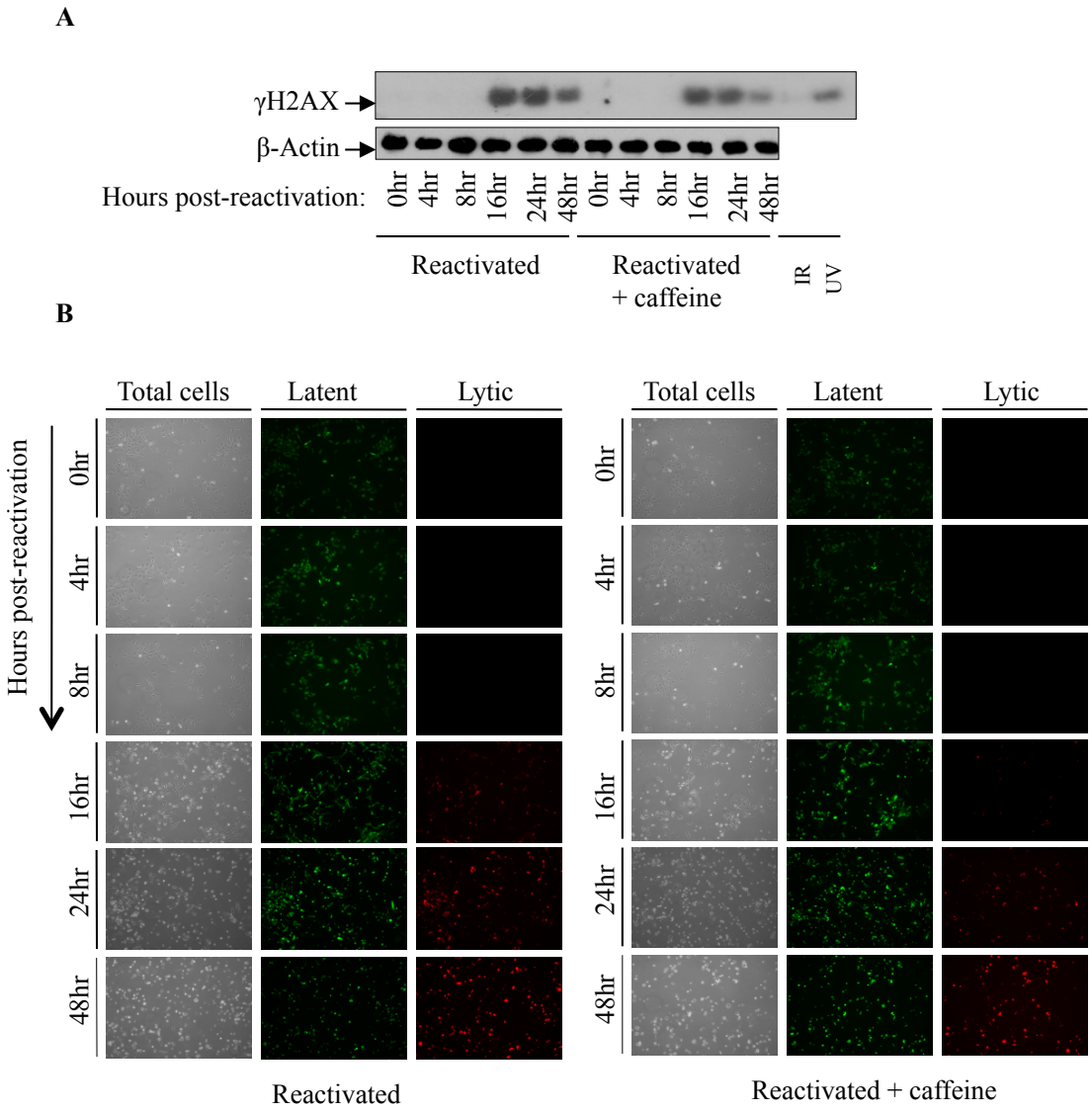

Figure 3.5: Inhibition of the ATM/ATR DNA Damage Signalling Pathways by Caffeine Treatment Inhibits Reactivation of KSHV in VK219 Cells. VK219 cells latently infected with vKSHV.219 virus were reactivated using a baculovirus with expresses the KSHV lytic switch protein RTA. Reactivated cells were treated with caffeine, with untreated, reactivated VK219 cells as controls. **A.** Caffeine-treated, reactivated cells were harvested, with untreated reactivated VK219 cells at 0, 4, 8, 16, 24 and 48 hours post-reactivation and analysed by Western blotting. **B.** Following treatment, reactivated, VK219 cells were examined by fluorescence microscopy to assess for reactivation against untreated, reactivated controls. These data are representative of one experiment performed twice.

C

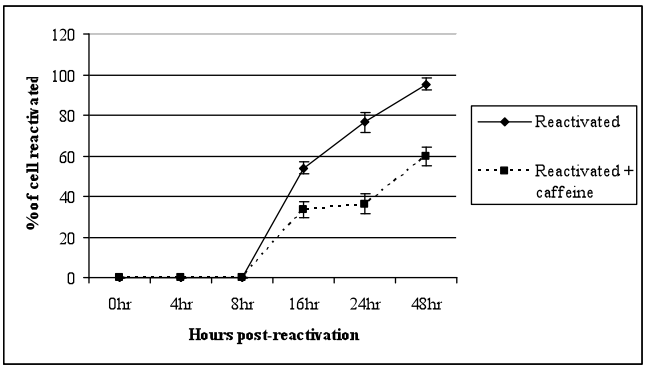

D

Hours post-reactivation	Caffeine	Mean % RFP expression	SD	SEM	df	P value	t value	Statistical significance
0hr	-	0	N/A	N/A				
	+	0	N/A	N/A	N/A	N/A	N/A	N/A
4hr	-	0	N/A	N/A				
	+	0	N/A	N/A	N/A	N/A	N/A	N/A
8hr	-	0	N/A	N/A				
	+	0	N/A	N/A	N/A	N/A	N/A	N/A
16hr	-	53.8	2.9	0.9				
	+	33.6	4.1	1.3	9	0.0001	21.7541	Yes
24hr	-	76.4	4.9	1.5				
	+	36.3	5.0	1.6	9	0.0001	17.2668	Yes
48hr	-	95.4	3.2	1.0				
	+	59.5	4.7	1.5	9	0.0001	32.8964	Yes

Figure 3.5 Continued: Inhibition of the ATM/ATR DNA Damage Signalling Pathways by Caffeine Treatment Inhibits Reactivation of KSHV in VK219 Cells. VK219 cells latently infected with vKSHV.219 virus were reactivated using a baculovirus which expresses the KSHV lytic switch protein RTA. Reactivated cells were treated with caffeine, with untreated, reactivated VK219 cells as controls. In addition to assessing reactivation levels using fluorescence microscopy, following treatment, reactivated, VK219 cells were examined by counting the number of GFP and RFP positive cells in ten fields at 0, 4, 8, 16, 24 and 48 hours post-reactivation, and from this working out the percentage of reactivated cells. **C.** Collated results from ten counted fields are shown, with error bars denoting standard deviation. **D.** t tests were conducted to determine whether the differences in percentage reactivation between treated and non treated reactivated cells were statistically significant. t tests were conducted at the 95% confidence interval. These data are representative of one experiment performed twice.

the caffeine treated samples. On average, at 16 hours post-reactivation, 33.6% of cells latently infected with recombinant KSHV had become lytic in those cells treated with caffeine, compared with 53.8% of cells becoming lytic in control cells. Following 24 hours reactivation, 36.3% of latently infected Vero cells had become lytic when treated with caffeine, compared to 76.4% lytic cells in the controls. At 48 hours post-reactivation, 59.5% of caffeine treated, latently infected Vero cells were lytic, whilst 95.4% of latently infected Vero cells were lytic in the untreated controls. The percentage differences in reactivation between caffeine treated and untreated latently infected cells at 16, 24 and 48 hours post-reactivation were all considered to be statistically significant at the 95% confidence interval (Figure 3.5C and D).

3.5 Lytic KSHV Replication Inhibits the DNA Damage Response in Response to Ultra-Violet Radiation

To establish whether cells infected with KSHV respond differently to DNA damage compared to uninfected controls, uninfected Vero cells, VK219 cells (latently infected with KSHV) and VK219 cells which had been reactivated to induce lytic KSHV replication 24 hours previously, were exposed to $20JM^{-2}$ of UV radiation to induce ssDNA breaks. Cells were harvested at 0, 1, 2, 4, 8, and 24 hours following UV radiation and subjected to Western blotting for p53, LANA (infection control), KCP (lytic infection control) and β-Actin (loading control). In response to UV radiation, VK219 cells (latently infected with KSHV) induced p53 expression in a similar manner to control uninfected Vero cells. However, in reactivated VK219 cells, the induction of p53 was repressed (Figure 3.6).

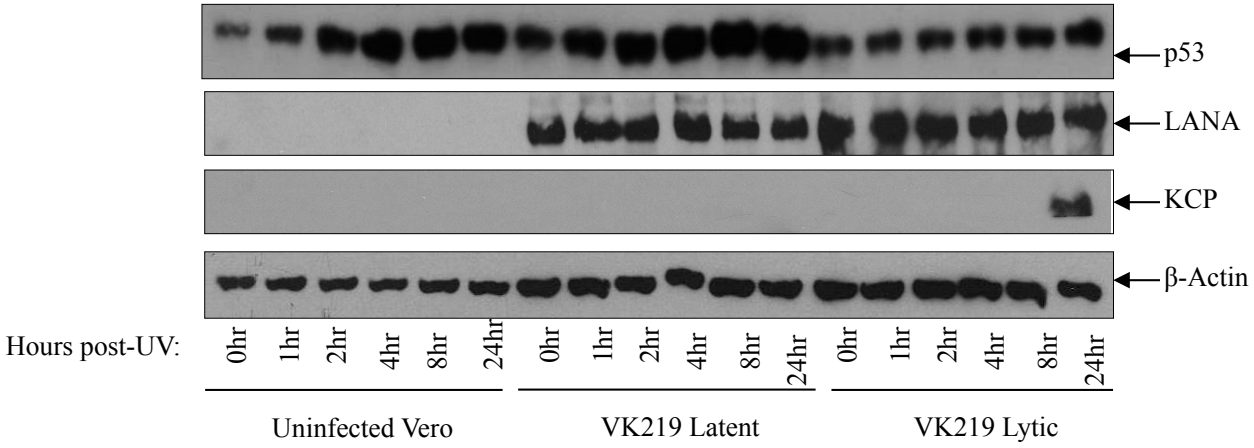

Figure 3.6: Lytic KSHV Replication Inhibits the DNA Damage Response in Response to Ultra-Violet Radiation. Uninfected Vero cells, VK219 cells latently infected with KSHV and reactivated VK219 cells were exposed to $20JM^{-2}$ UV radiation. Cells were harvested at 0, 1, 2, 4, 8 and 24 hours post-UV exposure and analysed by Western blotting for p53, LANA, KCP and β-Actin. These data are representative of one experiment performed twice.

3.6 Latent KSHV Infection Induces the DNA Damage Response in Response to Ionising Radiation

To determine whether cells infected with KSHV respond differently to different forms of DNA damage, the response to IR inducing double-strand breaks of uninfected Vero cells, VK219 cells (latently infected with KSHV) infected cells, and VK219 cells which had been reactivated to induce lytic KSHV replication 24 hours previously were examined. Cells were exposed to IR and harvested at 0, 1, 2, 4, 8 and 24 hours post-IR and subjected to Western blotting for p53, LANA (infection control), KCP (lytic infection control) and β-Actin (loading control). In response to IR, VK219 cells (latently infected with KSHV) induce p53 protein levels to a greater extent than uninfected control Vero cells. Reactivated VK219 cells had a similar response to IR as uninfected control Vero cells (Figure 3.7).

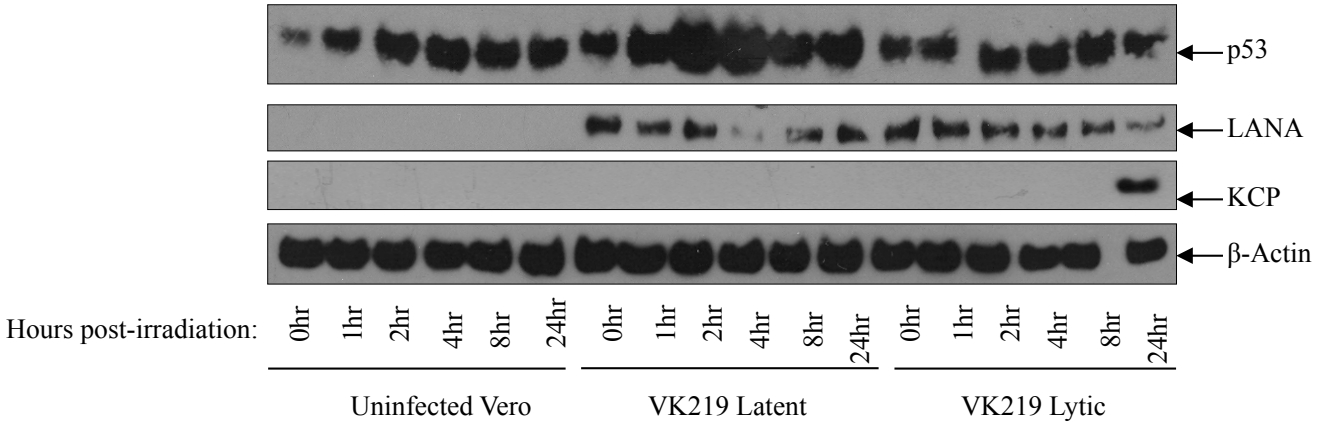

Figure 3.7: Latent KSHV infection Induces the DNA Damage Response in Response to Ionising Radiation. Uninfected Vero cells, VK219 cells latently infected with KSHV and reactivated VK219 cells were exposed to IR. Cells were harvested at 0, 1, 2, 4, 8 and 24 hours post-IR exposure and analysed by Western blotting for p53, LANA, KCP and β-Actin. These data are representative of one experiment performed twice.

Chapter Four:

Discussion

4. Discussion

At the beginning of this study, the relationship of KSHV infection with the DNA damage response was incompletely understood. A number of publications had suggested that KSHV proteins are able to interact (although not necessarily physically), with components of the DNA damage responses. For example, vIRF1 was shown to inhibit ATM and p53 activity in order to promote viral replication in infected cells, whilst vCyclin was shown to activate ATM, H2AX and Chk2 (Shin et al., 2006; Koopal et al., 2007). Further evidence for a role of KSHV and the DNA damage response came from studies of the related murine gamma-herpesvirus, MHV68. Studies on this virus showed that the viral protein, orf36, was able to directly phosphorylate H2AX, and interestingly the effect was to promote viral replication (Tarakanova et al., 2007). Other related herpesviruses, including HSV1, CMV and EBV have all been previously shown to interact with cellular DNA damage response proteins, another indication that KSHV may have a close relationship with components of the DNA damage response (Section 1.5).

The principle aim of this study was elucidate the relationship between KSHV infection and the cellular DNA damage response. Therefore the first objective of this study was to determine the effects of *de novo* KSHV infection on components of the cellular DNA damage response (Objective 1, Section 1.6). Generally it is believed that oncogenic viruses are able to either inhibit or activate the cellular DNA damage response. In some cases, viral genomes are recognised as 'broken cellular DNA' and as a result, are targeted by the cellular DNA damage response. In order to prevent this, some viruses have evolved complex mechanisms to circumvent, or inhibit, the DNA damage response (Lilley et al., 2007). Mechanisms of inhibition usually include mislocalisation of DNA damage proteins away from sites of

damage, or degradation of the damage proteins themselves. This is certainly the case for adenovirus, where the adenoviral E4orf3 protein is able to mislocalise Mre11 away from viral replication centres, and the adenoviral E4orf6/E1B55K complex targets a number of DNA damage proteins for degradation (Weitzman and Ornelles, 2005). In other cases, viruses, such as EBV, exploit the cellular DNA damage response. A number of mismatch repair proteins including MSH-2, MSH-6 and MLH1 are assembled into viral replication centres during EBV infection, presumably to correct any mismatches in replicated viral DNA (Daikoku et al., 2006). Work presented in this study shows that *de novo* KSHV infection of Ad5E1HEK293 cells is able to activate components of the DNA damage response. We observed an increase in phosphorylation of ATM, NBS1, Chk1, RPA and H2AX in KSHV infected Ad5E1HEK293 cells when compared to uninfected controls (Figure 3.2). To our knowledge, this is the first report to suggest that *de novo* KSHV infection is able to activate components of the DNA damage response. The work presented here is consistent with the study by Koopal et al who suggested that the KSHV viral protein vCyclin can activate the phosphorylation of ATM, H2AX and Chk2 (Koopal et al., 2007). Reactivation of cells latently infected with KSHV also activated the cellular DNA damage response as determined by phosphorylation of ATM, Chk2, RPA and H2AX (Figure 3.3) (Objective 2, Section 1.6). Interestingly, activation of ATM, Chk2 and H2AX was also observed during lytic replication of the related EBV (Nikitin et al., 2010). The reason why the cellular DNA damage response is induced post-KSHV infection is unclear at present. The possibility that the viral genome is recognised as 'broken DNA ends' (as in adenovirus infection) is unlikely since the KSHV genome is circularised almost immediately upon infection, and DNA damage responses were not activated until approximately 72 hours post-KSHV infection (Figure 3.2). Instead, we speculate that the host

cell may respond to the production of viral protein, and responding to cellular stress, induce a cellular DNA damage response.

The next objective of this study was to establish whether KSHV uses the cellular DNA damage response to aid infection of the host cell (Objective 3, Section 1.6). In response to treatment with the broad-spectrum ATM/ATR inhibitor caffeine, we observed a statistically significant increase in KSHV infectivity during the early stages of infection (24-48 hours post-infection) when compared to untreated controls (Figure 3.4). In contrast to the previous result suggesting that activation of the cellular DNA damage response may be important during KSHV infection, this suggests that abrogated ATM/ATR signalling pathways are beneficial for KSHV infectivity. Curiously, there was a statistically significant decrease in the percentage of lytically replicating KSHV infected cells when compared to untreated controls, suggesting that KSHV requires the cellular DNA damage pathways intact during lytic replication (Figure 3.5).

Recently, it has become apparent that a single virus is able to both activate and inhibit components of the DNA damage response, revealing a more complex relationship between viruses and the cellular response to DNA damage. In the context of herpesviruses, HSV1 is an example of a virus which is able to both activate and inhibit components of the response pathway. HSV1 infection induces a DNA damage response, activating ATM and downstream targets such as Nbs1, Chk2 and p53 (Shirata et al., 2005). In addition, HSV1 infection induces the cellular activation of RPA (Wilkinson and Weller, 2004). Interestingly, HSV1 appears to be able to inhibit ATR activity through its association with, and sequestering of, phosphorylated RPA and ATRIP. It is thought that the viral protein ICP0 is responsible for

sequestering ATRIP, preventing downstream activation of ATR targets (Wilkinson and Weller, 2006). In addition, the HSV-1 protein, Vmw100, is thought to induce proteasomal degradation of the NHEJ repair protein DNA-PK_{CS} (Parkinson et al., 1999). In the case of the murine herpesvirus, MHV68, the M2 protein is able to activate ATM and induce the localisation of the DDB1/COP9/cullin DNA repair complex to the nucleus in the absence of DNA damage. In response to DNA damage, the MRN complex is not recruited to the sites of damage, and H2AX remains unphosphorylated, preventing apoptosis of the infected cell (Liang et al., 2006). HCMV infection induces cellular activation of ATM, H2AX, Chk2 and p53. However, a number of DNA damage proteins, including ATM, Chk2 and Ku proteins (involved in NHEJ repair), are sequestered away from viral replication centres, suggesting that some components of the DNA damage response are required to be inhibited for the virus to replicate effectively (Luo et al., 2007; Gaspar and Shenk., 2005).

The relatively novel idea that oncogenic viruses are able to both inhibit and activate the cellular DNA damage response is interesting in light of the results obtained in this study. In the case of KSHV infection, it is already known that the vCyclin can induce the cellular DNA damage response, causing activation and phosphorylation of ATM, H2AX and Chk2. In addition, vIRF1 is believed to inhibit the activity of ATM and p53 (Shin et al., 2006). Taken together, these data suggests that KSHV has a dual role as both an activator and inhibitor of the cellular DNA damage response. Indeed, data presented in this study supports this concept, since *de novo* KSHV infection is able to induce the activation of the damage response and yet, inhibition of ATM activity appears to increase KSHV infectivity (Figure 3.2 and Figure 3.4). Following initial activation of the damage response, possibly by detection of viral RNA or protein, KSHV proteins (such as vIRF1) may then inhibit certain components of the DNA

damage pathways, whether by direct interaction (vIRF1 and ATM), proteasome-mediated degradation (vIRF1 and p53), or by mislocalisation away from the sites of DNA damage (as is the case with other herpesviruses such as HSV1, MVH68 and HCMV). Elimination of components of the cellular DNA damage response, in this context, may be beneficial for KSHV in order to effectively replicate and avoid host cell surveillance and subsequent apoptosis.

The final objective of this study was to determine the capacity of KSHV to modulate the DNA damage response to mutagenic treatments (Objective 4, Section 1.6). In response to UV radiation, lytically-replicating KSHV-infected cells inhibited the normal DNA damage response observed in uninfected control cells (Figure 3.6). Since this was observed after UV radiation, we speculate that KSHV targets components of the ATR signalling pathway, possibly by direct targeting, degradation or mislocalisation, thereby inhibiting the cellular DNA damage response and in turn preventing apoptosis of the infected cell. Indeed, during MHV68 infection, the MRN complex is not relocalised to sites of DNA damage in response to DNA damaging agents (Liang et al., 2006). Further investigation will determine whether the same can be said for KSHV infection. In addition, in response to IR, cells latently infected with KSHV induced the cellular DNA damage response to a greater extent than observed in control, uninfected cells (Figure 3.7). This perhaps suggesting that KSHV may use the cellular DNA damage response, or more specifically components of the ATM pathway, to effectively replicate in the host.

4.1 Limitations

One issue throughout the duration of this project was the use of the Ad5E1HEK293 cell line as a target for infection with KSHV. Since the Ad5E1HEK293 cell line is virally transformed using the Adenovirus E1 proteins, it is not surprising we observed a small degree of phosphorylation of DNA damage proteins in the uninfected, control cells. Unfortunately the Ad5E1HEK293 cell line is the most readily infectable with KSHV; our laboratory has previously attempted to infect HeLas (this proved difficult without using high titres of virus) and primary human umbilical vein endothelial cells (HUVECs), which are notoriously difficult to infect. Another limitation in this study was in obtaining sufficient recombinant KSHV. Each virus preparation produced a relatively low virus titre, meaning that it was difficult to repeat the caffeine infectivity assay in triplicate. As a result, different virus preparations were used to repeat the experiment, resulting in large variations between experiments which masked statistical significance (Figure 3.4 and 3.5). Finally, the use of the ATM/ATR inhibitor caffeine is relatively non-specific and is known to inhibit other kinases, therefore the results obtained in this study may not only be due to the inhibition of ATM and ATR.

4.2 Future Work

To circumvent the limitations of this study, it would be beneficial to infect with recombinant KSHV in a number of different cells lines in order to confirm the activation of the cellular DNA damage response in response to KSHV infection. In addition, we would like to prepare larger virus preparations, to produce enough virus so that the caffeine infectivity assay could be run in triplicate. Furthermore, it would be advantageous to use specific inhibitors of ATM

and ATR to assess whether the results obtained in this study are due to the inhibition of these kinases or due to caffeine's non-specific inhibition of other kinases.

To follow on from this project, it would be interesting to assess, via immuno-fluorescence microscopy, whether DNA damage proteins localise to viral replication centres during *de novo* infection and reactivation, and whether any damage proteins are mislocalised away from these centres (such is the case for other herpesviruses). These results would give a clearer indication of the role of the cellular DNA damage response during KSHV infection and reactivation. In addition, it would be interesting to determine by siRNA interference against viral proteins such as vIRF1 and vCyclin, whether activation of the cellular DNA damage response remains the same in the absence of these viral proteins.

Chapter Five:

References

Aoki, Y., Jaffe, E. S., Chang, Y. et al (1999). Angiogenesis and Hematopoiesis Induced by Kaposi's Sarcoma-Associated Herpesvirus-Encoded Interleukin-6. **Blood** 93: 4034-4043.

Araujo, F. D., Stracker, T. H., Carson, C. T. et al (2005). Adenovirus Type 5 E4orf3 Protein Targets the Mre11 Complex to Cytoplasmic Aggresomes. **J Virol.** 79: 11382-11391.

Baker, A., Rohleder, K. J., Hanakahi, L. A. et al (2007). Adenovirus E4 34k and E1b 55k Oncoproteins Target Host DNA Ligase IV for Proteasomal Degradation. **J Virol.** 81: 7034-7040.

Barton, E., Mandal, P., Speck, S. H. (2011). Pathogenesis and Host Control of Gammaherpesviruses: Lessons from the Mouse. **Annu Rev Immunol.** 29: 351-397.

Berkova, Z., Wang, S., Wise, J. F. (2009). Mechanism of Fas Signaling Regulation by Human Herpesvirus 8 K1 oncoprotein. **J Natl Cancer Inst.** 101: 399-411.

Blackford, A. N., Bruton, R. K., Dirlik, O. et al (2008). A Role for E1B-AP5 in ATR Signaling Pathways during Adenovirus Infection. **J Virol.** 82: 7640-7652.

Blackford, A. N., Patel, R. N., Forrester, N. A. et al (2010). Adenovirus 12 E4orf6 inhibits ATR activation by promoting TOPBP1 degradation. **Proc Natl Acad Sci U S A.**107: 12251-12256.

Boshoff, C., Endo, Y., Collins, P. D. et al (1997). Angiogenic and HIV-inhibitory Functions of KSHV-Encoded Chemokines. **Science** 278: 290-294.

Boyer, J., Rohleder, K., Ketner, G. (1999). Adenovirus E4 34k and E4 11k Inhibit Double Strand Break Repair and Are Physically Associated with the Cellular DNA-Dependent Protein Kinase. **Virology** 263: 307-312.

Bouvard, V., Baan, R., Straif, K. et al (2009). A review of human carcinogens—Part B: biological agents. **Lancet Oncol.** 10: 321-322.

Bugreev, D. V., Yu, X., Egelman, E. H., Mazin, A. V. (2007). Novel pro- and anti-recombination activities of the Bloom's syndrome helicase. **Genes Dev.** 21: 3085-3094.

Cai, Q. L., Knight, J. S., Verma, S. C. et al (2006). EC5S ubiquitin complex is recruited by KSHV latent antigen LANA for degradation of the VHL and p53 tumour suppressors. **PLoS Pathog.** 2: 1002-1012.

Carson, C. T., Schwartz, R. A., Stracker, T. H. et al (2003). The Mre11 complex is required for ATM activation and the G2/M checkpoint. **EMBO J.** 22: 6610-6620.

Cesarman, E., Nador, R. G., Bai, F. et al (1996). Kaposi's sarcoma-associated herpesvirus contains G protein-coupled receptor and cyclin D homologs which are expressed in Kaposi's sarcoma and malignant lymphoma. **J Virol.** 7: 8218-8123.

Chang, Y., Cesarman, E., Pessin. M. S. et al (1994). Identification of herpesvirus-like DNA sequences in AIDs-associated Kaposi's sarcoma. **Science** 266: 1865-1869.

Chu, W. T. and Hickson, I. D. (2009). RecQ helicases: multifunctional genome caretakers. **Nat Rev Cancer.** 9: 644-654.

Cimprich, K. A. and Cortez, D. (2008). ATR: an essential regulator of genome integrity. **Nat Rev Mol Cell Biol.** 9: 616-627.

Coscoy, L. (2007). Immune Evasion by Kaposi's sarcoma-associated herpesvirus. **Nat Rev Immunol.** 7: 391-401.

Daikoku, T., Kudoh, A., Sugaya, Y. et al (2006). Postreplicative Mismatch Repair Factors Are Recruited to Epstein-barr virus Replication Compartments. **J Biol Chem.** 281; 11422-11430.

Dobbelstein, M., Roth, J., Kimberly, W. T. et al (1997). Nuclear export of the E1B 55-kDa and E4 34-kDa adenoviral oncoproteins mediated by a rev-like signal sequence. **EMBO J.**16: 4276-4284.

Evans, J. D. and Hearing, P. (2005). Relocalisation of the Mre11-Rad50-Nbs1 Complex by the Adenovirus E4 ORF3 Protein Is Required for Viral Replication. **J Virol.** 79: 6207-6215.

Forrest, J. C. and Speck, S. H. (2008). Establishment of B-Cell Lines Latently Infected with Reactivation-Competent Murine Gammaherpesvirus 68 Provides Evidence for Viral Alteration of a DNA Damage-Signaling Cascade. **J Virol.** 82: 7688-7699.

Forrester, N. A., Sedgwick, G. G., Thomas, A. et al (2011). Serotype-Specific Inactivation of the Cellular DNA Damage Response during Adenovirus Infection. **J Virol.** 85: 2201-2211.

Freeman, A. E., Black, P. H., Vanderpool, E. A. et al (1967). Transformation of primary rat embryo cells by adenovirus type 2. **Proc Natl Acad Sci U S A.** 58: 1205-1212.

Frisch, S. M. and Mymryk, J. S. (2002). Adenovirus-5 E1A: paradox and paradigm. **Nat Rev Mol Cell Biol.** 3: 441-452.

Fujimuro, M., Wu, F. Y., apRhys, C. et al (2003). A novel viral mechanism for dysregulation of β-catenin in Kaposi's sarcoma-associated herpevirus. **Nat Med.** 9: 300-306.

Gaspar, M. and Shenk, T. (2005). Human cytomegalovirus inhibits a DNA damage response by mislocalizing checkpoint proteins. **Proc Natl Acad Sci U S A** 103: 2821-2826.

German, J., Sanz, M. M., Ciocci, S. et al (2007). Syndrome-causing mutations of the BLM gene in persons in the Bloom's syndrome registry. **Hum Mutat.** 28: 743-753.

Godden-Kent, D., Talbot, S. J., Boshoff, C. et al (1997). The Cyclin Encoded by Kaposi's Sarcoma-Associated Herpesvirus Stimulates cdk6 To Phosphorylate the Retinoblastoma Protein and Histone H1. **J Virol.** 71: 4193-4198.

Gravel, S., Chapman, J. R., Magill, C. et al (2008). DNA helicases Sgs1 and BLM promote DNA double-strand break resection. **Genes Dev.** 22: 2767-2772.

Guasparri, I., Keller, S. A., Cesarman, E. (2004). KSHV vFLIP is essential for the survival of infected lymphoma cells. **J Exp Med.** 199: 993-1003.

Hartl, B., Zeller, T., Blanchette, P. et al (2008). Adenovirus type 5 early region 1B 55-kDa oncoprotein can promote cell transformation by a mechanism independent from blocking p53-activated transcription. **Oncogene** 27: 3673-3684.

Khanna, K. K. and Jackson, S. P. (2001). DNA double-strand breaks: signalling, repair and the cancer connection. **Nat Genet.** 27: 247-254.

Kumagai, A., Lee, J., Yoo, H. Y. et al (2006). TopBP1 activates the ATR-ATRIP complex. **Cell** 124: 943-955.

Koopal, S., Furuhjelm, J. H., Jarviluoma, A. et al (2007). Viral Oncogene-Induced DNA Damage Response Is Activated in Kaposi Sarcoma Tumorigenesis. **PLoS Pathog.** 3: 1346-1360.

Kudoh, A., Fujita, M., Zhang, L. et al (2005). Epstein-Barr Virus Lytic Replication Elicits ATM checkpoint Signal Transduction While Providing an S-phase-like Cellular Environment. **J Biol Chem.** 280: 8156-8163.

Jham, B. C. and Montaner, S. (2010). The Kaposi's Sarcoma-Associated Herpesvirus G Protein-Coupled Receptor: Lessons on Dysregulated Angiogenesis from a Viral Oncogene. **J Cell Biochem.** 110: 1-9.

Lee, J. H. and Paul, T. T. (2005). ATM activation by DNA double-strand breaks through the Mre11-Rad50-Nbs1 complex. **Science** 308: 551-554.

Liang, X., Pickering, M. T., Cho, N. et al (2006). Deregulation of DNA Damage Signal Transduction by Herpesvirus Latency-Associated M2. **J Virol.** 80: 5862-5874.

Lilley, C. E., Schwartz, R. A., Weitzman, M. D. (2007). Using or abusing: viruses and the cellular DNA damage response. **Trends Microbiol.** 15: 119-126.

Lin, J., Chen, J., Elenbaas, B. et al (1994). Several hydrophobic amino acids in the p53 amino-terminal domain are required for transcriptional activation, binding to mdm-2 and the adenovirus 5 E1B 55K protein. **Genes Dev.** 8: 1235-1246.

Liu, L., Eby, M. T., Rathore, N. et al (2002). The Human Herpes Virus 8-encoded Viral FLICE Inhibitory Protein Physically Associates with and Persistently Activates the IkB Kinase Complex. **J Biol Chem.** 277: 13745-13751.

Liu, Y., Shevchenko, A., Shevchenko, A., Berk, A. J. (2005). Adenovirus Exploits the Cellular Aggresome Response To Accelerate Inactivation of the MRN complex. **J Virol.** 79: 14004-14016.

Luo, M. H., Rosenke, K., Czornak, K. et al (2007). HCMV disrupts both ATM and ATR-mediated DNA damage responses during lytic infection. **J Virol.** 81: 1934-1950.

McBride, W. D. and Weiner, A. (1964). In vitro transformation of hamster kidney cells by human adenovirus type 12. **Proc Soc Exp Biol Med.** 115: 870-874.

McCormick, C. and Ganem, D. (2005). The Kaposin B Protein of KSHV Activates the p38/MAPK Pathway and Stabilizes Cytokine mRNAs. **Science** 307: 739-741.

Mesri, E. A., Cesarman, E., Boshoff, C. (2010). Kaposi's sarcoma and its associated herpesvirus. **Nat Rev Cancer.** 10: 707-719.

Miller, G., Heston, L., Grogan, E. et al (1997). Selective Switch between Latency and Lytic Replication of Kaposi's Sarcoma Herpesvirus and Epstein-Barr Virus in Dually Infected Body Cavity Lymphoma Cells. **J Virol.** 71: 314-324.

Muralidhar, S., Pumfery, A. M., Hassani, M. et al (1998). Identification of Kaposin (Open Reading Frame K12) as a Human Herpesvirus 8 (Kaposi's Sarcoma-Associated Herpesvirus) Transforming Gene. **J Virol.** 72: 4980-4988.

Neff, N. F., Ellis, N. A., Ye, T. Z. et al (1999). The DNA helicase activity of BLM is necessary for the correction of the genomic instability of bloom syndrome cells. **Mol Biol Cell** 10: 665-676.

Nikitin, P. A., Yan, C. M., Forte, E. et al (2010). An ATM/Chk2-Mediated DNA Damage-Responsive Signaling Pathway Suppresses Epstein-Barr virus Transformation of Primary Human B Cells. **Cell Host Microbe.** 8: 510-522.

Nimonkar, A. V., Ozsoy, A. Z., Genschel, J. et al (2008). Human exonuclease 1 and BLM helicase interact to resect DNA and initiate DNA repair**. Proc Natl Acad Sci U S A** 105: 16906-16911.

Orazio, N. I., Naeger, C. M., Karlseder, J. et al (2011). The Adenovirus E1b55K/E4orf6 Complex Induces Degradation of the Bloom Helicase during Infection. **J Virol.** 85: 1887-1892.

Ornelles, D. A. and Shenk, T. (1991). Localization of the Adenovirus Early Region 1B 55-Kilodalton Protein during Lytic Infection: Association with Nuclear Viral Inclusions Requires the Early Region 4 34-Kilodalton Protein. **J Virol.** 65: 424-439.

Ouyang, K. J., Woo, L. L., Ellis, N. A. (2008). Homologoud recombination and maintenance of genome integrity: Cancer and aging through the prism of human RecQ helicases. **Mech Ageing Dev.** 129: 425-440.

Parkinson, J., Lees-Miller, S. P., Everett, R. D. (1999). Herpes Simplex Virus Type 1 Immediate-Early Protein Vmw110 Induces the Proteasome-Dependent Degradation of the Catalytic Subunit of DNA-Dependent Protein Kinase. **J Virol.** 73: 650-657.

Payne, M. and Hickson, I. D. (2009). Genomic instability and cancer: lessons from analysis of Bloom's syndrome. **Biochem Soc Trans.** 37: 553-559.

Pelka, P., Ablack, J. N. G., Fonseca, G. J. (2008). Intrinsic Structural Disorder in Adenovirus E1A: a Viral Molecular Hub Linking Multiple Diverse Processes. **J Virol.** 82: 7252-7263.

Querido, E., Blanchette, P., Yan, Q. et al. (2001). Degradation of p53 by adenovirus E4orf6 and E1B55K proteins occurs via a novel mechanism involving a Cullin-containing complex. **Genes Dev.** 15: 3104-3117.

Radkov, S. A., Kellam, P., Boshoff, C. (2000). The latent nuclear antigen of Kaposi sarcoma-associated herpesvirus targets the retinoblastoma-E2F pathway and with oncogene Hras transforms primary rat cells. **Nat Med.** 6: 1121-1127.

Ralf, C., Hickson, I. D., Wu, L. (2006). The Bloom's Syndrome Helicase Can Promote the Regression of a Model Replication Fork. **J Biol Chem.** 281: 22839-22846.

Raynard, S., Bussen, W., Sung, P. (2006). A Double Holliday Junction Dissolvasome Comprising BLM, Topoisomerase IIIa, and BLAP75. **J Biol Chem.** 281: 13861-13864.

Rogakou, E. P., Pilch, D. R., Orr, A. H. et al (1998). DNA double-stranded breaks induce histone H2AX phosphorylation on serine 139. **J Biol Chem.** 273: 5858-5868.

Russell, W. C. (2000) Update on adenovirus and its vectors. **J Gen Virol.** 81: 2573-2604.

Sakakibara, S., Pise-Masison, C. A., Brady, J. N. et al (2009). Gene regulation and functional alterations induced by Kaposi's sarcoma-associated herpesvirus-encoded ORFK13/vFLIP in endothelial cells. **J Virol.** 83: 2140-2153.

Sarkaria, J. N., Busby, E. C., Tibbetts, R. S. et al (1999). Inhibition of ATM and ATR Kinase Activities by the Radiosensitizing Agent, Caffeine. **Cancer Res.** 59: 4375-4382.

Shin, Y. C., Nakamura, H., Liang, X. et al (2006). Inhibition of the ATM/p53 Signal Transduction Pathway by Kaposi's Sarcoma-Associated Herpesvirus Interferon Regulatory Factor 1. **J Virol.** 80: 2257-2266.

Shirata, N., Kudoh, A., Daikoku, T. et al (2005). Activation of Ataxia Telangiectasia-mutated DNA damage Checkpoint Signal Transduction Elicited by Herpes Simplex Virus Infection. **J Biol Chem.** 280: 30336-30341.

Shrivastav, M., De Haro, L. P., Nickoloff, J. A. (2008). Regulation of DNA Double-strand break repair pathway choice. **Cell Res.** 18: 134-147.

Soulier, J., Grollet, L., Oksenhendler, E. et al (1995). Kaposi's sarcoma –associated herpesvirus-like DNA sequences in multicentric Castleman's disease. **Blood** 86: 1276-1280.

Srivastava, V., Modi, P., Tripathi, V. et al (2009). BLM helicase stimulates the ATPase and chromatin-remodelling activities of RAD54. **J Cell Sci.** 122: 3093-3103.

Stine, J. T., Wood, C., Hill, M. et al (2000). KSHV-encoded CC chemokine vMIP-III is a CCR4 agonist, stimulates angiogenesis, and selectively chemoattracts TH2 cells. **Blood** 95: 1151-1157.

Stracker, T. H., Carson, C. T., Weitzman, M. D. (2002). Adenovirus oncoproteins inactivate the Mre11-Rad50-NBS1 DNA repair complex. **Nature** 418: 348-352.

Stucki, M., Jackson, S. P. (2006). gammaH2AX and MDC1: anchoring the DNA-damage-response machinery to broken chromosomes. **DNA Repair** 5: 534-543.

Sung, P and Klein, H. (2006). Mechanism of homologous recombination: mediators and helicases take on regulatory functions. **Nat Rev Mol Cell Biol.** 7: 739-750.

Tarakanova, V. L., Leung-Pineda, V., Hwang, S. et al (2007). Gamma-Herpesvirus Kinase Actively Initiates a DNA Damage Response by Inducing Phosphorylation of H2AX to Foster Viral Replication. **Cell Host Microbe.** 1: 275-286.

Tomlinson, C. C., Damania, B. (2004). The K1 Protein of Kaposi's Sarcoma-Associated Herpesvirus Activates the Akt Signaling Pathway. **J Virol.** 78: 1918-1927.

Trentin, J. J., Yabe, Y., Taylor, G. (1962). The Quest for Human Cancer Viruses. **Science** 137: 835-841.

Van den Elsen, P. J., A. Houweling., A. van der Eb. (1983). Expression of region E1B of human adenoviruses in the absence of region E1A is not sufficient for complete transformation. **Virology** 128: 377-390.

Verma, S. C., Borah, S., Robertson, E. S. (2004). Latency-associated nuclear antigen of Kaposi's sarcoma-associated herpesvirus up-regulates transcription of human telomerase reverse transcriptase promoter through interaction with transcription factor Sp1. **J Virol.** 78: 10348-10359.

Vieira, J. and O'Hearn, P. M. (2004). Use of the red fluorescent protein as a marker of Kaposi's sarcoma-associated herpesvirus lytic gene expression. **Virology** 325: 225-240.

Weiden, M. D. and Ginsberg, H. S. (1994). Deletion of the E4 region of the genome produces adenovirus genome concatemers. **Proc Natl Acad Sci U S A.** 91: 153-157.

Weitzman, M. D. and Ornelles, D. A. (2005). Inactivating intracellular antiviral responses during adenovirus infection. **Oncogene** 24: 7686-7696.

Weitzman, M. D., Lilley, C. E., Chaurushiya, M. S. (2010). Genomes in Conflict: Maintaining Genome Integrity During Virus Infection. **Annu Rev Microbiol.** 64: 61-81.

Wilkinson, D. E. and Weller, S. K. (2004). Recruitment of Cellular Recombination and Repair Proteins to Sites of Herpes Simplex Virus Type 1 DNA Replication is Dependent on the Composition of Viral Proteins within Prereplicative Sites and Correlates with the Induction of the DNA Damage Response. **J Virol.** 78: 4783-4796.

Wilkinson, D. E. and Weller, S. K. (2006). Herpes simplex virus type 1 disrupts the ATR-dependent DNA-damage response during lytic infection. **J Cell Sci.** 119: 2695-2703.

Woo, J. L. and Berk, A. J. (2007). Adenovirus Ubiquitin-Protein Ligase Stimulates Viral Late mRNA Nuclear Export. **J Virol.** 81: 575-587.

Wu, L., Bachrati, C. Z., Ou, J. et al (2006). BLAP75/RMI1 promotes the BLM-dependent dissolution of homologous recombination intermediates. **Proc Natl Acad Sci U S A.**103: 4068-4073.

Yang, X. H. and Zou, L. (2006). Checkpoint and coordinated cellular responses to DNA damage. **Results Probl Cell Differ.** 42: 65-92.

Zhou, B. S. and Bartek, J. (2004). Targeting the Checkpoint Kinases: Chemosensitization versus Chemoprotection. **Nat Rev Cancer.** 4: 1-10.

Zou, L. and Elledge, S. J. (2003). Sensing DNA damage through ATRIP recognition of RPA-ssDNA complexes. **Science** 300: 1542-1548.